The response of the outer slope stability to drawdown conditions in the regional flood defenses of Hoogheemraadschap Hollands Noorderkwartier

Bachelor Thesis

Fernando Paul Guanoluisa Vela
S2031272

August 25th, 2021

Bachelor thesis Civil Engineering

The response of the outer slope stability to drawdown conditions in the regional flood defenses of Hoogheemraadschap Hollands Noorderkwartier

by

Fernando Paul Guanoluisa Vela

Student number: S2031272

to obtain the degree of

Bachelor of Civil Engineering

at the University of Twente

Project duration:	February 2021 till August 2021
Host company:	Hoogheemraadschap Hollands Noorderkwartier
Supervisors:	dr. ir. J.H. Damveld, University of Twente
	ing. T. Zonneveld, HHNK
	ir. J-W. Evers, HHNK
Thesis committee:	dr. A. Hartmann, University of Twente
Version:	Final
Date	August 25th, 2021

UNIVERSITY OF TWENTE.

hoogheemraadschap Hollands Noorderkwartier

Preface

I present to you the final report of my bachelor thesis: "The response of the outer slope stability to drawdown conditions in the regional flood defenses of Hoogheemraadschap Hollands Noorderkwartier." With this research, I end my civil engineering bachelor's degree at the University of Twente. This research has been done in collaboration with Hoogheemraadschap Hollands Noorderkwartier.

Firstly, I would like to thank the University of Twente and all the staff of the civil engineering department for allowing me to be part of their community and carry out my bachelor's degree program. In the same way, I would like to thank Johan Damveld for his engagement and critical mindset, which positively impacted this work. I appreciated your constructive feedbacks and the guidance provided for the correct development of my thesis.

Besides the members of UT, I am very thankful to Hoogheemraadschap Hollands Noorderkwartier for the opportunity to develop my thesis assignment with them. Similarly, I would like to thank Thijs Zonneveld and Jan-Willem Evers, my assessors on Hoogheemraadschap Hollands Noorderkwartier. Due to current global circumstances, Covid-19, my internship period had to be carried out online. However, I was warmly welcomed by them. I am grateful for the supervision and the proactivity to provide me with all the information that I have required through this process. Their ability to share their knowledge through feedback was vital for this thesis. Undoubtedly, this project could never have been realized without your help.

Another importantly knowledgeable professional that I would like to thank is dr. Vanessa Magnanimo. From the moment I asked for a professional consultancy with you, I realized your enthusiasm to answer all my questions and provide new academic knowledge for this research. I also would like to thank my sponsorships, SENESCYT and the Government of Ecuador, for their financial help in my bachelor program.

Finally, I will always be grateful to my girlfriend, family, friends, and those that are not here anymore for their unconditional support during the critical moments I have encountered throughout my thesis and bachelor's program.

Abstract

Hoogheemraadschap Hollands Noorderkwartier (HHNK) is the water authority in the area of North Holland. Their responsibilities include the supervision, maintenance, and management of the regional flood defenses in the area. This way, HHNK carries out a mandatory safety assessment in all the regional defenses every 12 years. One failure mechanism to assess the flood defense in the Netherlands is the outer slope stability under drawdown conditions. The rapid drawdown condition occurs when a submerged slope experiences a decrease in the external water level. Due to the external water level serves as a stabilizing force to support the slope, the stability of the structure is affected by this event. Furthermore, the other effect is the modification of the internal pore pressure inside the slope, which also threatens stabilization.

Traditionally, this failure mechanism has been studied from different perspectives such as laboratory tests, limit equilibrium, and numerical solutions due to the difficulty of analyzing all the processes and their effects during the drawdown event, such as the seepage-induce pore pressure calculation, the dissipation process, and others. The methods used to analyze this failure mechanism have focused on specific characteristics without considering the reality during this condition. In the last decades, technology has provided new alternatives to conduct more complex analyses. Therefore, the assessment methods also have improved their approaches.

This is the case of HHNK that finds to improve the methodology employed in assessing this failure mechanism and gain knowledge in the topic. In this way, the thesis aims to provide state-of-the-art knowledge of this failure mechanism. To gain a better understanding, a literature review was conducted, determining that finite element analysis is the approach that shows the more realistic results. Furthermore, it can also be determined the factors influencing these failure mechanics and the relationship between them and their effects. Finally, an stability analysis was performed on 15 regional flood defenses under the control of HHNK in order to obtain a better insight into this topic on these specific infrastructures.

Contents

1

Introduction

The Netherlands is a country that lies in the delta of several rivers such as Rhine, Meuse, Scheldt, and bordering the North Sea. Large flooding disasters have marked its history, mainly because 60% of its land is vulnerable to flooding. In this way, in its aim to protect its citizens, the Dutch government has put special effort into developing policies for the correct management and prevention of flooding. One of the measures that the government and the water authorities took many decades ago was improving flood protection structures alongside the water bodies in the country. These structures consist of dykes, embankments, dams, locks, pumping stations, storm surge barriers, and dunes, which sum up around 22.500 kilometers length of defense structures (Jorissen & Kraaij, 2016).

The flood defenses are classified into two categories, the national flood defenses that protect from the sea and significant rivers water levels, while the regional flood defenses surround the polders in the country and protect from large storage canals. Both types are in charge of regional water authorities, known as waterschap of Hoogheemraadschap. These waterboards are supervised by the national water authority, Rijkswaterstaat, and the provincial governments. In this way, the regional water authorities are responsible for protecting the hinterland from flooding events (Dutch Water Authorities, 2017).

In general terms, water management in the country has succeeded in the last decades due to its policies regarding safety standards, forms of governance, and safety assessment. However, its success has been challenged in the last years due to the rising sea level, climate change, land subsidence, and urbanization. Although the current infrastructure provides high safety standards against the initial effects of these threats, a disaster is always possible. Therefore, water authorities are in constant improvement of the water flood risk policies.

A measure that the Dutch government has considered to deal with the new treats was the periodic assessment of all the flood defenses in the country. The assessment is guided by a mandatory safety assessment manual (OECD, 2014). In the case of national defuses the manuel is developed by the national government. On the other hand, the manual for regional defences is developed by the provincial government and the assessment is performed every 12 years (Slomp, 2012). A centralized manual is employed by all the waterboards, which contains approaches for evaluating several failure mechanisms.

Although this manual provides the most relevant approaches to conduct the assessment, one of the most common problems arises due to the gaps in knowledge in specific topics. In some cases, the provided information is insufficient or outdated, leading to an unrealistic performance in evaluating flood defenses.

This is the case of the Hoogheemraadschap Hollands Noorderkwartier, the water authority responsible for the flood defenses in a part of North Holland. This waterboard evaluates the different structures based on the safety assessment manual "Leidraad Toetsen op Veiligheid Regionale Waterkeringen," whose last version was published in 2015 by the provincial government of Noord-Holland.

In this way, HHNK needs to gain a better understanding of this failure mechanism, that enable HHNK to perform the safety assessment efficiently and correctly in regional flood defenses with different dimension. Moreover, the gaining insight will also help to determine when the instability of the outer slope is a safety risk.

1.1. Problem statement

HHNK has to assess the safety of 1065 km regional flood defenses, which protect against flooding from the inland canals. One of the failure mechanisms to be assessed is (in)stability of the outer slope. The instability of the outer slope is usually caused by a rapid drop in the canal's water level (rapid drawdown). The water level drop leads to reduced pore hydrostatic pressure against the outer slope, affecting the slope's equilibrium. Wind (during storms), pumping stations, or a breach of a dyke causing flooding of a polder can cause water level drop in the inland canal. The instability could also be caused by increased phreatic water table in the dyke due to excessive rain.

The mandatory assessment manual (Leidraad Toetsen op Veiligheid Regionale Waterkeringen) gives guidelines for assessing the instability of the outer slope. However, HHNK still has some questions. E.g., the manual offers two assessment methods based on the dimensions of a damaged dyke, sometimes leading to different conclusions. Also, it is unclear which load situation should be considered.

At the moment, HHNK cannot assess correctly when the instability of the outer slope is considered a significant safety risk. Therefore, HHNK needs to gain a better understanding of this failure mechanism. Better understanding will enable HHNK to perform the safety assessment efficiently and correctly and determine when the instability of the outer slope is a significant safety risk.

1.2. Research objective

The research objective is to understand the failure mechanism outer slope instability under drawdown conditions and improve the methodology employed in assessing this mechanism conducted by Hoogheemraadschap Hollands Noorderkwartier in the regional flood defenses in North Holland. By understanding the current methods employed to analyze this failure mechanism, the factors influencing the slope stability, and their influence, the safety assessment process can be done more efficiently and confidently. For this, a summary of the state-of-the-art knowledge in slope stability under rapid drawdown conditions and an analysis of the relationship between the amount of drawdown and the size of the slip plane will be presented.

1.3.Research questions

1.3.1. Main research question

The main research question to achieve the objective of the research has been formulated as follows:

When does a rapid drawdown condition in the canal affect the stability of the outer slope in such a manner that it has to be considered a significant safety risk?

1.3.2. Sub questions

The main research questions require the answering of different aspects involved during the rapid drawdown failure mechanism. Therefore, three sub-questions have been formulated to support each of these aspects.

First of all, the topic requires knowing the current methods used to analyse this failure mechanism. In this way, other parameters and factors can be determined according to the assumptions and limitations of these methods. Therefore, the first sub-question is formulated as follows:

1. **Which approaches are currently used to analyse the outer slope response under drawdown conditions?**

The second aspect is related to the factors and their influence. Sub question two seeks to determine the influence of the factors in the slope stability according to the limitations and characteristics of the used methods to analyze.

2. **What factors determine if a slope becomes unstable during rapid drawdown conditions?**

The third aspects focus on determining the time to response of the slope. Therefore, sub-question three has been formulated as follows:

3. **What factors determine how fast a slope becomes unstable during rapid drawdown conditions?**

Finally, the relation between the water drawdown and the size of the slip surface is intended to figure out. This way, the sub-question has been formulated as follows:

4. **What correlation is there between the amount of water-level drawdown and the size of the slip plane?**

1.4.Methodology

This section describes the methods employed in answering the sub-questions and a general overview of the structure of the remaining part of the report. Two methods were used, namely literature review and modeling study. The methodology to answer each sub-question is briefly described below. However, Methodology of the scenario analysis describes a more detailed overview of the modeling part. A common pattern alongside the whole research process is that the information gathering in the previous sub-question serves as the initial point for the following sub-questions. In this way, the literature review output will be employed as background information for the modeling part.

Sub-question 1 and 3

A systematic literature review will be conducted to answer this sub-question. This approach focuses on determining the core of the research question and then sets a research strategy according to pre-specific criteria on this subject. In this case, the main subject is the approaches to analyze the slope stability under drawdown conditions.

The criteria focus on determining the following subjects:

- Traditional and modern approaches
- Advantages and limitations of these approaches
- Applicability to real cases
- Reliability and difficultness of the process

The research will use as primary sources virtual libraries and academic web pages. Furthermore, an expert consultation will be conducted with Dr. Vanessa Magnanimo, professor of soil micromechanics at the University of Twente. The literature review results in this part are presented in 2 Theoretical Framework and aim to contribute to sub-question 2 and 3 by defining the methods and the factors used in this analysis.

Sub-question 2 and 4

For answering these sub-questions, a literature review and modeling study will be employed.

In the case of literature review, the research will extend the knowledge acquired in the previous sub-question. The review will focus on determining:

- Factors influencing the slope stability according to each method
- The range of influence of these factors
- Under which conditions do these factors influence the most
- Real examples cases that show the influence of these factors
- The relationship between the size of the slip plane and the size of the drawdown

As in the previous question, the primary sources are virtual libraries, academic web pages, and expert consultation, and 5 Model Results shows the results of this part. Moreover, the result of this part will be used as background information for the modeling.

The modeling will focus on two aspects, the influence of the factors in the slope stability under drawdown conditions and the influence of drawdown size on the size of the slip circle. The modeling will be conducted in the Software “D-Geo Stability,” which allows the numerical analysis of the slope stability in two-dimensional geometry. In this case, the Bishop method will be employed because HHNK also uses it to assess some regional flood defenses under their control.

Scenario analysis will guide the modeling part to provide a general overview of the possible outcomes of the two particular aspects previously mentioned. For this, different scenarios have been set, where parameters such as hydraulic boundary conditions, permeability, strength soil parameters, phreatic line, coordinates of slip plane, and more factors will be modified according to the findings in the literature review.

The different scenarios will be applied to the most common regional flood defenses under the control of HHNK. Moreover, HHNK has provided the soil parameter values and cross-sections dimensions of these infrastructures. The software description can be found in 3
D-Geo Stability model, the settings for the scenario analysis of each structure are described in 4
Model set-up, and 5
Model Results depicts the modeling results.

1.5.Thesis outline

This thesis is divided into eight chapters.

- Chapter 2 presents a brief literature review about the failure mechanism slope stability under drawdown conditions, where the analysis methods, factors that influence, and their relationships are described. Afterward, an example solving with the finite element method is presented.
- Chapter 3 describes the software D-Geo stability and its features. Moreover, the Bishop method, the method for the slope stability analysis, is outlined.
- Chapter 4 shows the set-up for the modeling part. This way, this part presents the scenario analysis methodology and the set-up of the different scenarios applied to 15 regional flood defenses controlled by HHNK.
- Chapter 5 shows the results from the modeling part. Here the stability assessment describes the factors of safety provided by D-Geo stability. The results are divided into three groups according to the soil configuration of the flood defense infrastructures.
- Chapter 6 presents the discussion section. The results and limitations of the modeling part will be argued in this section.
- Chapters 7 and 8 show the conclusion of the research. Each sub-question is answering according to the findings in the modeling and literature review. Finally, some recommendations for future research on the topic are provided.

2

Theoretical Framework

This section provides the theory regarding the failure mechanism, slope stability under drawdown conditions, and the numerical method, finite element method (FEM), employed in the analysis of water drawdown. Firstly, the concept of slope stability and the failure mechanism rapid drawdown is defined. Then, the employment of FEM in the analysis of the drawdown failure mechanism is described. Finally, an example using FEM is presented that outlines the factors influencing the slope stability and the different outputs that this method provides.

2.1. Slope stability

Slope stability refers to the capability of the soil mass in an inclined slope to withstand its gravitational forces, the additional loads acting on the slope and potential dynamic loads without experiencing displacement. However, when the stability conditions are not met, the soil mass experiences the downward movement of soil from high points to low points. This movement could be either rapid or progress gradually at fixed rates. This phenomenon is known as slope failure or landslide (Murthy, 2002). Therefore, the analysis of slope stability in structures such as dykes, dams, levees, and embankments is of the utmost importance for the prevention of substantial economic and social damages.

The slope stability analysis focuses on determine causes and trigger factors in a slope failure phenomenon. In this way, the analysis concentrates on three main aspects: geometry, soil properties, and forces acting on the infrastructure. For this, static or dynamic, analytical or empirical methods are employed to evaluate the stability of the structure (Murthy, 2002). The foremost causes to develop slope instability are rainfalls, erosion, forces due to earthquakes, and the rapid drawdown of water adjacent to the slope. Furthermore, the factor of safety (FOS) is the most common metric to assess slope stability performance. Similarly, the most critical slip surface is also an essential aspect in the analysis (Verruijt, 2001; Hammouri et al., 2008; Murthy, 2002).

2.2. Failure mechanism during rapid drawdown

A dyke experiences a drawdown condition when its outer slope is partly or totally submerged, and a sudden decrease of the free water level occurs after a long period of average water level, as shown in Figure 1. At standard conditions, the water level helps to stabilize the forces acting on the slope. However, when a sudden drawdown occurs, the slope experiences two main effects. First, a reduction of the stabilizing external hydrostatic pressure, and second, a modification of the internal water pressure (Alonso & Pinyol, 2016; Pinyol et al., 2008). These effects strongly correlate with reducing the factor of safety in the stability of the dyke. (Alonso Pérez de Agreda and Pinyol Puigmartí, 2009).

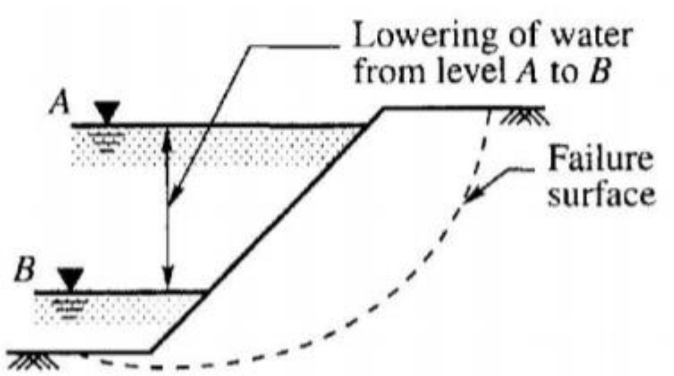

Figure 1 A simple slope under drawdown condition.

When a slope is subjected to a rapid drawdown, it experiences a decrease in soil buoyancy. This reduction means an increase in weight. Moreover, the extra weight also triggers growth in the shearing stress. This shearing stress needs to be counteracted by the shear resistance of the upper slope. However, the shearing strength depends on the compression that soil could undergo. If the compression is insufficient, the weight will overpass the shearing strength, causing the slope to slide. For instance, in the case of saturated soil with low permeability, the soil volume will not change, or if it happens, the change will be slow. This way, the increase of strength will be insufficient to counteract the shearing stress-causing by the extra weight (Murthy, 2002).

To sum up, a slope under drawdown conditions fails when the driving force (gravity) overcomes the resistance derived from the shear strength of the soil along the rupture surface (Pinyol et al., 2008; Johansson, 2014). The description of the failure mechanism states clearly that the decrease in buoyancy triggers the slope failure. According to Alonso & Pinyol (2016) and Zhang et al. (2019), the modification of internal pore water pressure is the drawdown effect that needs the most attention since the pore water pressure is the factor that controls the magnitude of the buoyancy forces acting on the structure.

2.3. Analysis of slope stability under drawdown conditions

The impact of water drawdown on slope stability has been studied from different perspectives based on laboratory tests, numerical solutions, and limit equilibrium. The limit equilibrium approach usually employs the method of slices. Meanwhile, numerical solutions use finite element methods. These approaches can be applied alone or combined according to the soil state behavior and analysis period (Alonso & Puigmartí, 2009). In the case of long-term stability analysis employs the drained parameters (effective stress analysis). While in the case of short-term stability analysis uses the undrained parameters (total stress analysis) (Berilgen, 2007).

The total stress analysis had been commonly used because this analysis does not require the estimation of pore pressure inside the slope, facilitating the procedure to obtain the stability factor of the slope. The main methods developed for the total stress analysis are Corps of Engineers, Lowe and Karafiath, Ducan, Wring and Wong methods. Currently, effective stress analysis is more frequently used because it provides a more realistic slope stability analysis. This analysis requires determining pore water pressure. For this, numerical techniques are employed to define the effects of seepage-induced pore pressure. Furthermore, the numerical results are also used in the limit equilibrium analysis. The methods to conduct the effective stress analysis have been developed by

Svano and Nordal and Wringht and Duncan (Berilgen, 2007; Hammouri et al., 2008; see also Rocscience Inc., 2001).

Berilgen (2007) uses the numerical method known as the finite element method (FEM) to conduct the slope stability analysis under drawdown conditions. This method considers the effective stress analysis that requires evaluating pore pressures during and after the drawdown event. Therefore, before describing the different aspects of this method, the mechanism influencing the pore pressure under drawdown conditions and the approaches to calculate pore pressure modifications are described.

2.3.1. Mechanisms influencing pore water pressure

Pore water pressure inside a slope suffers modifications during and after a drawdown event. In this way, two fundamental mechanisms control the resulting pore water pressure: Firstly, the change in the initial hydrostatic pressures impacts the total stress conditions inside the slope, resulting in stress-induced excess pore pressure. Secondly, the transient flow regime also generates seepage-induced pore pressure. The resulting pore pressure inside the slope combined with the decrease of water load represents a reduction of slope stability (Alonso & Pinyol, 2016; Pinyol et al., 2008).

During the drawdown event, the excess pore pressure starts to be dissipated. At the same time, a consolidation process also occurs. Two factors influence the dissipation rate of excess pore pressure and the decrease of the seepage-induced pore pressure: the hydraulic conductivity and compressibility of the slope materials and the drawdown rate. For instance, in slopes with high permeable soils, the dissipation of stress-induced pore pressure occurs fast, and the period of dissipation is similar to the time taken by the modification of boundary conditions. In this way, the changes suffered by the factor of safety are minimal. This state is known as a drained soil behavior.

On the other hand, in soils with low permeability, the seepage-induced and the stress-induced pore pressures dissipate at slower rates than the change of boundary condition. Due to the low drainage rate in the slope, the excess pore pressure creates slope instability reducing the factor of safety of the infrastructure. In this way, the state of soil under these circumstances is known as undrained soil behavior (Berilgen, 2007).

2.3.2. Modelling pore water pressure under drawdown conditions

There are two traditional procedures to predict the pore pressure regime during and after water drawdown, the "stress-based" undrained approach and the "flow" approach. These approaches calculate the stress-induced excess pore pressure and the seepage-induced pore pressure, respectively.

2.3.2.1. Undrained approach

This approach seeks to determine the pore pressure regime inside the slope resulting from a sudden drawdown condition. For this, the undrained methods consider the effects of changing boundary stresses against the slope by employing a soil mechanical constitutive equation. In this way, the intensity of stress-induced excess pore pressure can be determined in impervious soil slopes. The soil is assumed to be impervious because drawdown occurs instantaneously, and seepage-pore pressure does not dissipate during drawdown events. Although the results of this approach are conservative, in most cases, its applicability in real cases provides unrealistic results (Alonso & Pinyol, 2016; Pinyol et al., 2008).

2.3.2.2. Flow approach

Flow methods focus on determining the seepage-induced pore pressure by resolving the flow problem caused by the seepage in the flow domain, which involves changes in boundary conditions and modification of the initial free surface. Moreover, its application is focused on relative pervious slopes (granular soils). Due to the approach considers a rigid soil skeleton, the methods implicitly assume that no stress-related changes in pore pressure are produced. Nevertheless, dilatancy generates effects in shear stress, which leads to a generation of extra pore pressure. Thus, the estimation of the stress-induced extra pore pressure generated by soil deformation is underestimated by this approach (Alonso & Pinyol, 2016; Pinyol et al., 2008).

Both methods concentrate on specific soil characteristics. However, field conditions do not behave rigid or pure undrained; materials of different permeability and compressibility are often arranged in complex geometries. Therefore, these methods' employment is limited to specific situations (Alonso & Pinyol, 2016; Pinyol et al., 2008). In the case of FEM, this method seeks to analyze the slope stability considering the coupled effects of changing boundary stresses and the seepage forces due to the transient flow of water together. This is because the principle of effective stress employed on the FEM analysis states that in a two-phase medium composed of soil skeleton and pores saturated with pore fluid, the total stress vector can be expressed as follow:

$$\{\Delta\sigma\} = [D'] \{\varepsilon\} + \left\{\Delta p_f, \Delta p_f, \Delta p_f, 0,0,0\right\}$$

Where

$\Delta\sigma = total\ stress\ vector$
$D' = effective\ constitutive\ matrix$
$\Delta\varepsilon = strain\ increment\ vector$
$\Delta p_f = the\ change\ in\ pore\ fluid\ pressure$
Due to the change in pore fluid pressure is composed in the following way.

$$\Delta p_f = \Delta p_{seepage} + \Delta p_{excess}$$

Where

$\Delta p_{seepage} = pore\ pressure\ increase\ due\ to\ seepage\ in\ the\ flow\ domain$
$\Delta p_{excess} = excess\ pore\ pressure\ due\ to\ stress\ change$

Neither of the traditional approaches covers the actual change of pore pressure produced in real drawdown conditions. Therefore, FEM employs a coupled analysis that considers the transient seepage and the deformation due to stress included consolidation (Berilgen, 2007). Once the importance of pore pressure in this failure mechanism has been outlined, the different aspects of the slope stability analysis using in the FEM are explained below.

2.3.3. Finite element method

The finite element method (FEM) is a numerical method employed to estimate the stability factor of the slope. Since FEM uses effective stress analysis, which considers the undrained parameters for the short-term stability analysis, this method employs the coupled transient seepage and deformation analysis including consolidation to estimate the resulting pore water pressure during the drawdown, together with the stability analysis to determine in a comprehensive form the stability factor of the slope. Furthermore, it also considers the nonlinear material behavior, complex boundary, and loading conditions during the analysis.

The main advantages of FEM are the possibility of analyzing traditional drawdown scenarios such as slow drawdown and fully rapid drawdown. Since FEM employs the coupled analysis, this allows the study of transient drawdown corresponding to different drawdown rates. In this way, FEM allows the setting of different drawdown ratios and drawdown rates to analyze the slope stability without discarding the transient process between undrained and drained soil states. Furthermore, the possibility of modeling different drawdown categories also allows identifying the influence of factors such as soil permeability, the drawdown rates, and drawdown ratios in the slope stability.

The finite element method and its features have been explained above. Berilgen (2007) presented an example that employs this method. The example seeks to determine the slope stability during drawdown conditions depending on the soil permeability, drawdown rate, and drawdown ratio, considering the nonlinear material behavior and loading conditions. For this:

1. The scenarios of analysis are described.
2. The different analyses employed on the numerical method are briefly explained.
3. The material parameters used during the analysis are shown.
4. The results and conclusion of the example are delivered.

2.3.3.1. Scenarios and cases description

In the example, three categories of drawdown will be evaluated in two dykes with a 3:1 slope. Furthermore, a scenario analysis will evaluate the three drawdown categories. The scenarios will be customized based on four factors, the height of the dyke H (7 m and 14 m), drawdown rate R (1 m/day and 0.1 m/day), soil hydraulic conductivity (10^{-4} $\mathrm{cm/s}$ and 10^{-6} $\mathrm{cm/s}$), and drawdown ratio, L/H (where L indicates the height between the initial and the final drop of external water level).

Figure 2 shows the drawdown categories. Case A represents the "fully slow drawdown"; this case considers the soil totally drained during drawdown. This is because the drawdown rate is slow enough to allow the dissipation of excess pore water pressure from the inside of the slope. Case C shows the "fully rapid drawdown," which assumes undrained soil behavior during drawdown. Case A and C represent the two extreme cases where phreatic level after drawdown either drop at the same rate as drawdown ratio or maintain at the initial external water level, respectively. In reality, these cases are not likely to occur as mentioned in Mechanisms influencing pore water pressure. Therefore, Case B is the best approach to model the real behavior of slope response during a drawdown event because it considers the transient drawdown.

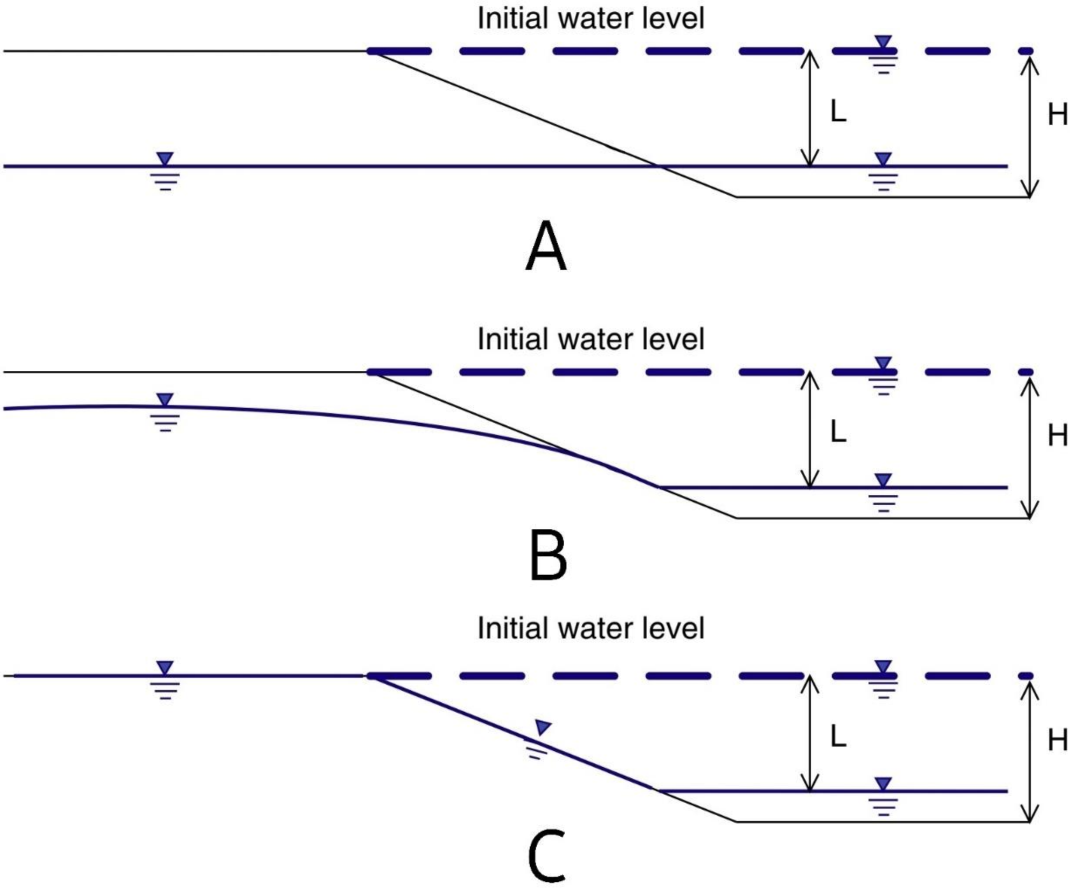

Figure 2 Phreatic level after drawdown; (a) fully slow drawdown; (b) transient drawdown; (c) fully rapid drawdown rate (Berilgen, 2007).

2.3.3.2. Description conducted analysis

Each of the described cases requires specific types of analysis, Table 1 states the required analyses for each drawdown case. For instance, Case A and Case C only requires the deformation analysis that seeks to calculate the stress-induced pore pressure, together with the stability analysis. On the other hand, Case B requires the performance of transient seepage and consolidation analysis concurrently with the stability analysis, in this case, both stress-induced and seepage-induce pore pressure are calculated at the same time. All these analysis are explained below.

Table 1 Types of analysis for different categories of drawdowns (Berilgen, 2007).

Case	Analysis	Material behaviour	Transient seepage	Deformation	Consolidation	Stability
A	Fully slow drawdown	Drained	NA	✓	NA	✓
B	Coupled analysis	Undrained	✓	✓	✓	✓
C	Fully rapid drawdown	Undrained	NA	✓	NA	✓

NA= not applicable

Moreover, the analyses employ 2D plane-strain models. In the case of transient seepage is performed on PLAXFLOW program, while, the deformation and stability analysis are performed on PLAXIS program. All the analysis uses a plane strain of fifteen-node triangular elements for the finite element mesh.

Transient seepage analysis

FEM analysis starts by employing the transient seepage analysis to determine the seepage-induced pore pressure and the free groundwater-surface at different drawdown ratios and drawdown rates. Moreover, other groundwater flow parameters are also calculated, such as the hydraulic heads and flow rates, parameters used in the deformation analysis. For the transient analysis, two different slope heights and two permeabilities were considered.

Deformation analysis

This analysis is employed to calculate the stress-induced pore pressure and the resulting stresses and strains. The analysis models the undrained soil behavior as a fully saturated and two-phased continuous medium that consists of soil skeleton and pore water. Since the impervious assumption employed to calculate the induced pore pressure provides conservative but not realistic results, this analysis uses a nonlinear elastoplastic material model, called the "hardening soil model" (HSM), to calculate the induced pore pressure as realistic as possible.

Consolidation analysis

FEM uses a fully coupled consolidation analysis to determine the dissipated stress-induced pore pressure. Due to the generation of the induced pore pressure occurs at the exact moment of its dissipation, this analysis allows to estimate the pore pressure dissipated at any stage of the drawdown event. The analysis employs Biot´s consolidation theory. During the analysis, two permeability were used.

Stability analysis

The stability analysis uses the phi-ci reduction method to find the factor of safety. The strength parameters obtained in the Mohr-Coulomb material model, such as cohesion ($c´$) and friction angle ($\emptyset´$), are reduced at a specific rate until failure of the structure occurs.

$$\Sigma\mathrm{Msf} = \frac{\tan \emptyset´_{input}}{\tan \emptyset´_{reduced}} = \frac{c´_{input}}{c´_{reduced}}$$

As a result, the factor of safety in this model is defined as the ratio of the resisting shear strength of the material to the driving shear stress. Therefore, the minimum safety factor (ΣMsf) that provides equilibrium is called the factor of safety (FoS).

2.3.3.3. Material parameters

Figure 3 shows the material used in the different sections of the FEM analysis. Factors such as permeability, dilatancy, and unit weight soil have been employed on the obtention of global equations, e.g., equations of equilibrium and equation of continuity employed in the finite element formulation. The elasto-plastic material model HSM uses the secant reference stiffness modulus and oedometer modulus, unloading-reloading reference stiffness modulus, poison ratio, reference stress for stiffness, and power for stress level dependency to capture the soil behavior. Berilgen (2007) presents the extended calculations of these procedures.

Material properties	Symbol	Unit	Value
Unit weight of soil	γ	kN/m^3	20
Permeability	k	cm/s	10^{-4} and 10^{-6}
Cohesion intercept	c'	kN/m^2	10
Internal friction angle	ϕ'	°	20
Dilatancy angle	Ψ	°	0
Secant reference stiffness modulus	E_{50}^{ref}	kN/m^2	1000
Secant reference oedometer modulus	E_{oed}^{ref}	kN/m^2	1000
Unloading–reloading reference stiffness modulus	E_{ur}^{ref}	kN/m^2	3000
Poisson ratio	n	–	0.2
Reference stress for stiffness	p^{ref}	kN/m^2	100
Power for stress level dependency	m	–	0.7

Figure 3 Soil parameters used in the FEM analysis (Berilgen, 2007)

2.3.3.4. FEM performance

<u>Groundwater flow and deformation</u>

The first aspects to analyze were the groundwater and deformation resulting from the drawdown condition. Figure 4 shows the different scenarios analyzed where the displacement contours are depicted in the soil mass and the final phreatic surface. It can be seen that both the drawdown rate and hydraulic conductivity influence the level of displacement on the soil mass. The more significant displacement occurs with a high drawdown rate and low hydraulic conductivity, as shown in scenario C. Furthermore, the yield deformation patterns seem to provide an idea of the sliding surface.

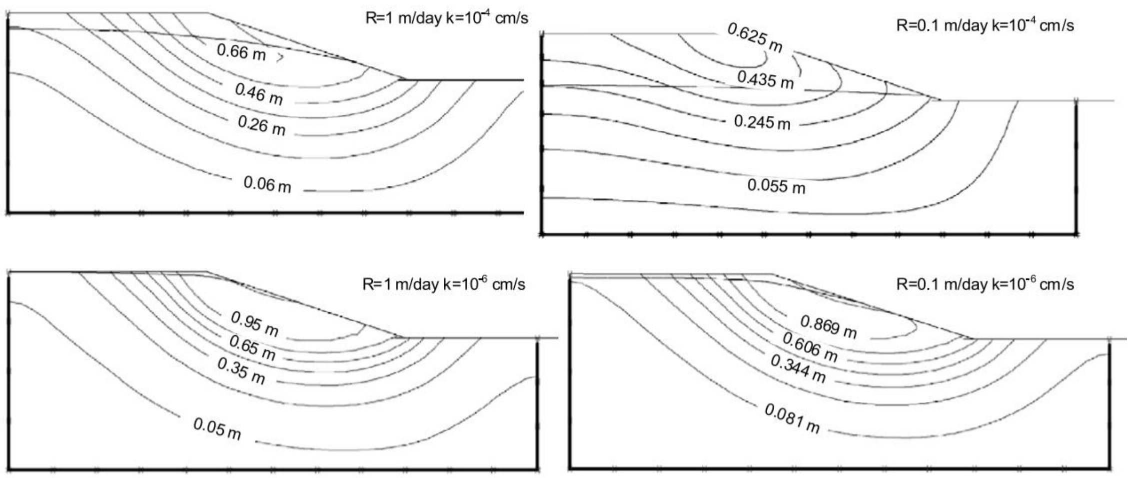

Figure 4 Displacement contour for different hydraulic conductivity k and drawdown rates at drawdown ratio L/H=1 (Berilgen, 2007).

The analysis also provides the relationship between the soil displacement horizontally and vertically and the drawdown rate. Figure 5 shows the development of this relationship for different drawdown ratios in the crow and toe of the slope. At looking at this relationship, it can be seen that the soil displacement is minimum at a low drawdown ratio.

Figure 5 shows that at low drawdown ratios (until L/H=0.2 approximately), the drawdown rate and hydraulic conductivity values are not relevant due to the minimum soil displacement. However, at higher drawdown ratios, the dominant factor was the hydraulic conductivity, leading to larger displacements at lower permeability values. Although negative vertical displacements were identified in the slope crown, the displacement patterns concerning the drawdown ratio were similar in both study areas, crown and toe of the slope. Moreover, a more significant displacement is detected at slope crown, which presents a 10% higher displacement than the toe of the slope.

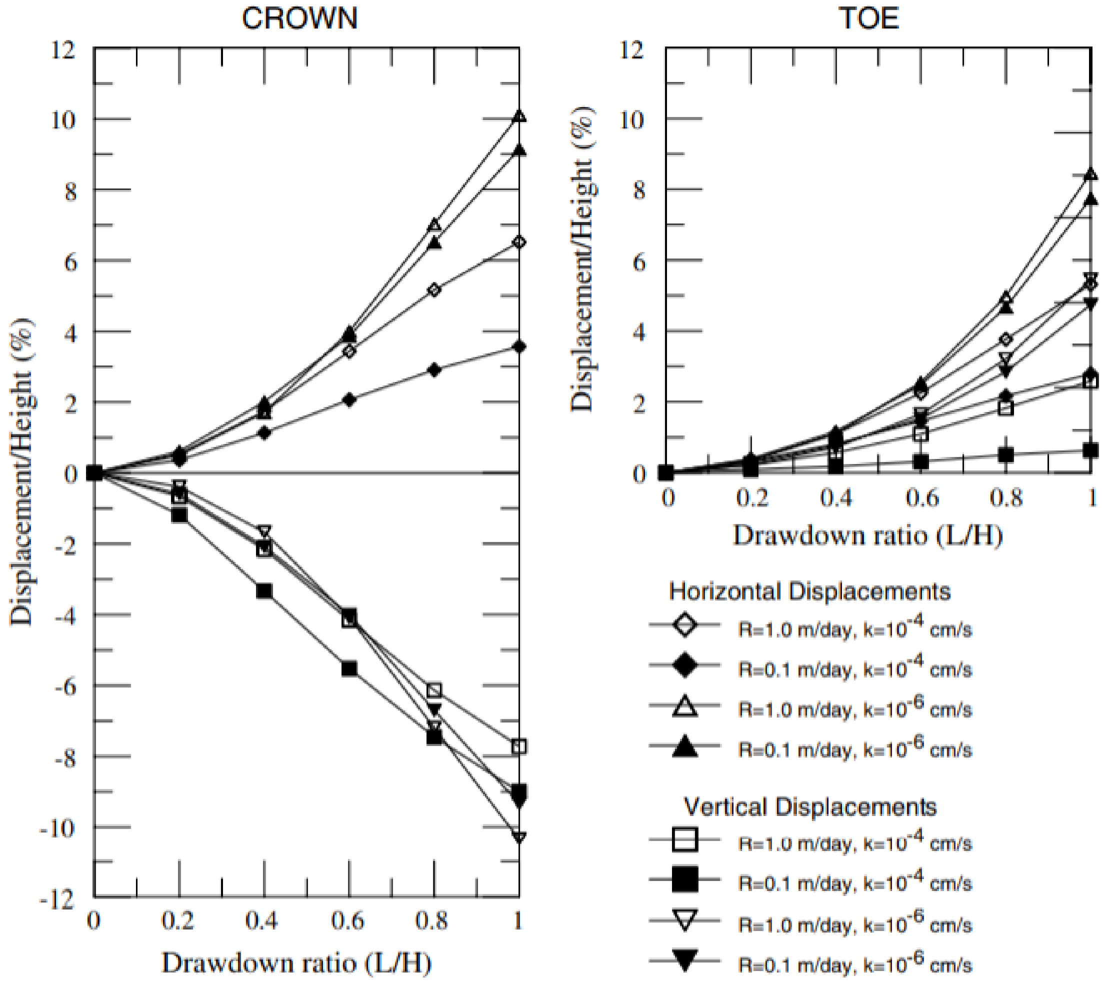

Figure 5 Displacement versus drawdown ratio for different drawdown rate R and hydraulic conductivity k on crown and toe of the slope (Berilgen, 2007).

Factor of safety

Another output of the FEM analysis is the factor of safety. In this analysis, the same factors used in the previous section are employed for two dykes of different heights. Figure 6 and Figure 7 show the development of the safety factor under different drawdown rates and hydraulic conductivities at different drawdown ratios for the two dykes, respectively.

It can be seen that in both dykes, two scenarios follow similar patterns. On one side, the soil with low hydraulic conductivity (under a fast drawdown rate (R=1.0 m/day) presents a slope behavior similar to the fully rapid drawdown condition. On the other hand, the soil with the same hydraulic conductivity but a slower drawdown rate (R=0.1 m/day) also provides almost the same pattern as the fully rapid drawdown condition. This way, the analysis on these dykes shows that the drawdown rate has no significant influence in soils with very low permeability due to minimal drainage. Therefore, the fully rapid drawdown assumption can be employed for the stability analysis, implying the omission of analysis such as transient seepage and consolidation.

The remaining scenarios show that even soil with high hydraulic conductivity ($k = 10^{-4}$ cm/s), also tends to behave in a fully rapid drawdown pattern if its drawdown rate (R=1.0 m/day) is high. An opposite pattern is shown with high hydraulic conductivity and a slow drawdown rate. In this last case, a good drainage process is possible. Since the patterns present considerable differences regarding the extreme cases, these scenarios require a coupled analysis.

Finally, the last factor analyzed was the strength/stress ratio defined by $c'/\gamma H$ (Lane & Griffiths, 2000). If the two dykes are compared, it is visible that although both dykes have been evaluated under the same scenarios and present the same soil parameters, the development of safety factors is different alongside the drawdown ratio increment. In the case of dyke with height H=7 m, starts with a FoS=2.67 when it is totally submerged (H/L=1) and finished the analysis with a FoS=1.1 when the reservoir is totally empty.

On the other hand, dyke with H=14 m starts with a FoS=2.02 at a fully submerged slope. However, this dyke reached a critical safety factor at L/H=0.6, which means that the slope stability failures at this water level if the slope has been evaluated with the fully rapid drawdown analysis. This highlights the influence of height and the drainage conditions during the drawdown event. If the dyke with H=14 m presents a slow drawdown rate and high hydraulic conductivity, a factor of safety lower than one cannot be possible.

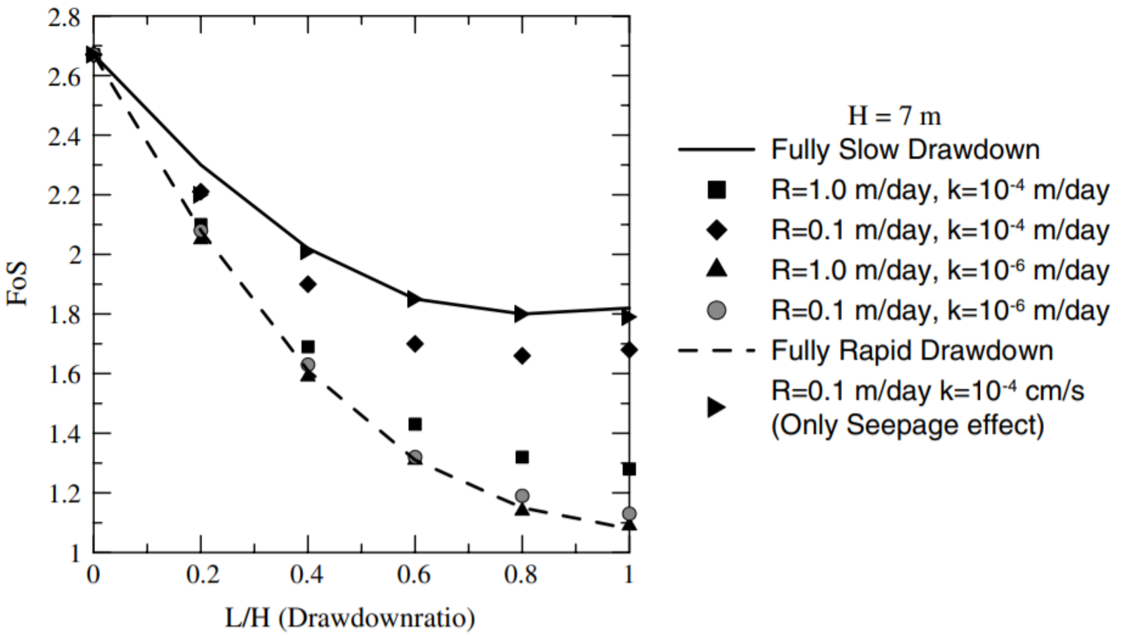

Figure 6 Variation of FoS with drawdown ratio for H = 7 m slope (Berilgen, 2007).

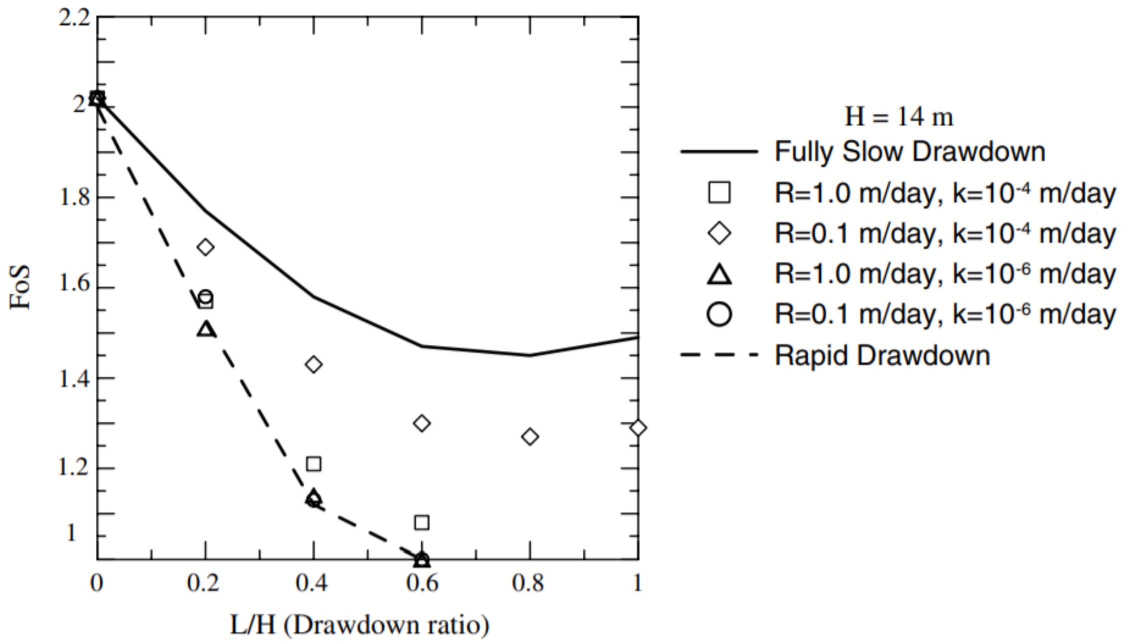

Figure 7 Variation of FoS with drawdown ratio for H = 14 m slope (Berilgen, 2007).

Variation of FoS with drawdown time

The final output from the FEM analysis is the development of the safety factor along the drawdown time, as shown in Figure 8. The analysis employs two drawdown rates, two hydraulic conductivities, and two dykes with different heights. The analysis allows identifying the influence of hydraulic conductivity and the drawdown rate regarding the drawdown time in slopes under drawdown conditions.

In the case of dykes with equal low hydraulic conductivity and different drawdown rates, the factor of safety in slopes experiencing fast drawdown rates (R=1.0 m/day) decreases in the first days. On the other hand, reducing the factor of safety starts after some days in the slope experiencing a slow drawdown rate. Furthermore, the delay in the decrement of the safety factor is also affected by the height of the dyke. Dykes with considerable heights suffer some delay in comparison with dykes with low heights until the factor of safety starts to drop.

The influence of hydraulic conductivity regarding the drawdown time can be described as follow. In the case of the same high drawdown rate and different hydraulic conductivity, the slope with lower conductivity will experience a higher decrease in its safety factor.

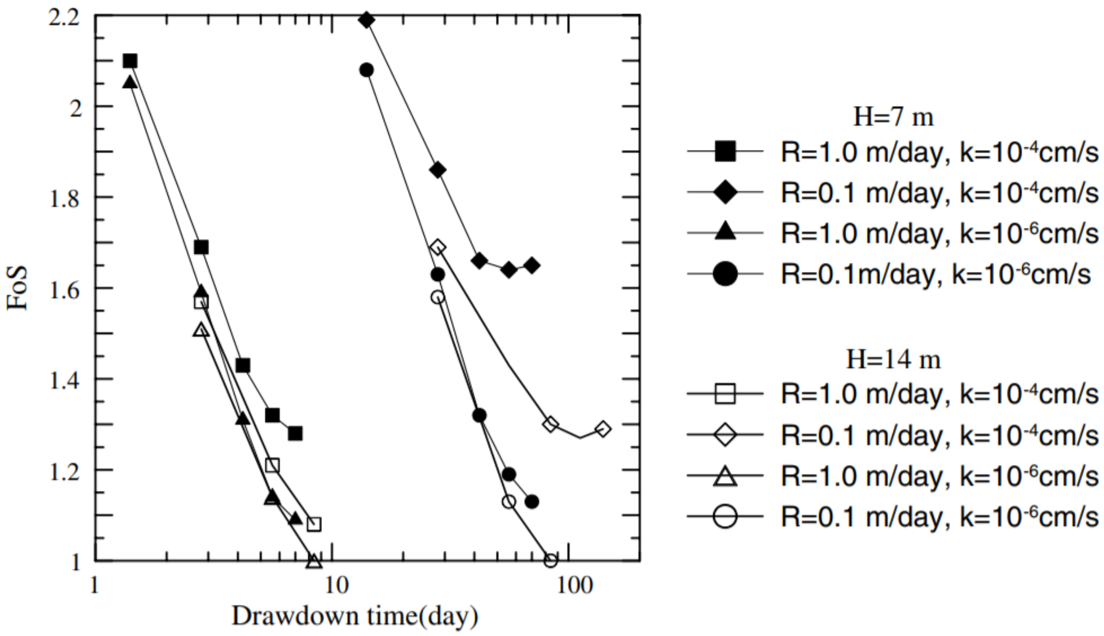

Figure 8 Variation of FoS with drawdown time for different slope heights, hydraulic conductivities and drawdown rates (Berilgen, 2007).

2.4. Theoretical answers research sub-questions

The literature review conducted in this section provides a clear insight to answer sub-question 1, 2 and 3. The slope stability analysis have traditionally used three approaches to analyse the homogeneous and inhomogeneous slopes by considering the rapid drawdown condition. These are laboratory tests, limit equilibrium with the limit equilibrium method and numerical solutions with finite element analysis (Alonso & Pinyol, 2016). Lane & Griffiths (2000) and Rocscience Inc. (2001) have explained the advantages and disadvantages of both approaches concluding that finite element method presents a more practical use. This mainly because the limitations regarding the computational difficulties and numerical inconsistency at locating the critical slip surface and establishing the factor of safety encountered in the limit equilibrium method put in disadvantage in comparison with finite element method, which allows to find the critical slope surface without assume any shape. Furthermore, FEM also provides to monitor the progressive failure and to evaluate the stresses, deformation and pore pressures in the studied embankments.

Berilgen (2007) described an example where the stability analysis of a slope under drawdown condition is analyszed by applying the FEM. The example highlights the factor influencing the slope stability, In this way, it could be determined that one of the main factors are the resulting pore pressure induced by the water drawdown, specifically the seepage-induced pore pressure and stress-induced pore pressure. If these factors are not properly evaluated, the factor of safety can be either overestimated or underestimated (Alonso and Pinyol, 2016). Furthermore, other factors that also present an influence in the development of the factor of safety are the hydraulic conductivity, the drawdown rate and the drawdown ratios. The influence of these factors under different scenarios has been described and evaluated above.

3

D-Geo Stability model

This section provides general information about the software D-Geo Stability. This software was employed to conduct the scenario analysis for the regional flood defenses under the control of HHNK. The stability analysis on the different scenarios will provide more insight into the factors influencing the studied failure mechanism. Moreover, the relevant technical details used in the software are described. Finally, a brief description of the Bishop method, the approach employed to analyze the slope stability at different water, is presented.

3.1. General information

The theoretical section identifies that hydraulic conductivity, drawdown rate, compressibility, and slope geometry are the main factors influencing the pore water pressure regime inside the slope, which means an affection on the slope stability. The influence of these factors was shown in the results presented by the example in the previous section. Although, great insight obtaining in the literature review section. These findings will be supported by analyzing the slope stability of the regional flood defenses under the control of HHNK in front of drawdown conditions. For this, the software D-Geo stability has been selected.

D-Geo Stability is basic software that allows the numerical analysis of slope stability in two-dimensional geometry. The software is part of the Deltares systems. The software has been developed according to some standards of the Netherlands. Therefore, it provides unique benefits for this research. In this way, some of its predefined standards and factors are based on Dutch reality. Moreover, the software provides different approaches for analyzing the slope stability, within the most used are Bishop, Spencer, and Uplift Van model.

3.2. Technical details

D-Geo Stability allows the set-up of different features regarding the structure's geometry, the materials employed, and the internal and external loads acting in the infrastructure. A brief description of these features is provided below (D-Geo Stability: Slope Stability Software for Soil Engineering, 2016). Furthermore, Set-up for the scenario analysis describes the settings employed in the modeling of the regional flood defenses.

3.2.1. Soil modelling

The software allows the employment of different soil layers in the soil configuration. Therefore, each layer is assigned a soil material. The characteristics of the materials can be modified according to field tests results, or they can take standard values provided by the software. Besides, the modeling of geotextile and nails are also possible.

3.2.2. Loads

The software allows determining the internal and external loads acting on the given infrastructure, such as the hydrostatic pore pressure distribution, the phreatic level, the volumetric weight of water, and the suction pore pressure. Furthermore, external loads such as line or uniform loads produced by roads or construction above the analyzed infrastructures can also be considered.

3.2.3. Slip plane determination

D-Geo Stability uses the method of slices to estimate the slope stability. The method considers a circular slip plane with radius "r" and divides the mass above this plane into an "n" number of vertical slices, as shown in Figure 9.

In order to determine the critical slip surface, the software employs a search algorithm knows as the grid method. The method uses tangent lines and a grid composed of many center points. The method starts by connecting the center points with the tangent lines creating a circular plane that cuts the boundaries of the infrastructure, as shown in Figure 9. In this way, many combinations proposing slip surfaces are created until the slip surface with the minimum factor of infrastructure safety is considered the critical slip surface.

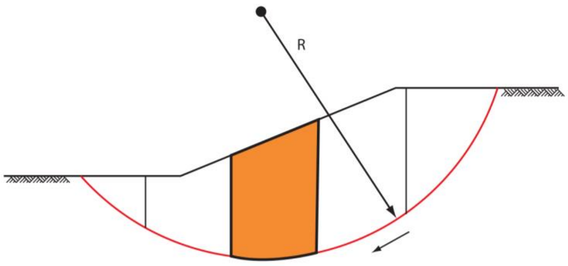

Figure 9 Slip plane including method of slices (D-Geo Stability: Slope Stability Software for Soil Engineering, 2016).

3.2.4. Results

The model calculates the different acting stresses on the slices and the pore pressure, assuming these values as valid for the entire soil within the circular surface. Furthermore, a detailed report about the different slip surfaces is provided, which details the safety factor in each slip plane. Additionally, it is possible to obtain a graphical result of the regions with the safety values between the range bounds.

3.2.5. Limitations

- The main limitation of the program is that specific approaches such as the couple-flow analysis are not available in the package. Therefore, the dissipation process of the pore water pressure inside the slope cannot be properly simulated.
- The Bishop method discards the horizontal stress components at the vertical slices. In this way, limit equilibrium analysis is only performed considering the vertical stress components.
- The program uses the grid method to determine the critical slip circle. However, the user needs to predefined the location of the grid and tangent lines before the analysis. In this way, if the location of these parameters is not reasonably

located, the analysis can provide unrealistic critical slip surfaces or any at the worst situation.

- The software can be employed only for two-dimensional geometries.

3.3. Bishop method

As mentioned before, the software provides different methods to analyze slope stability. In this case, the Bishop method will be used for the slope stability analysis of the flood defenses under the control of HHNK. This method is used in cases where the slope consists of several types of soil with different values of cohesion and friction angle, and the pore pressure in the slope is known or can be estimated. Furthermore, the analysis of the free body, the soil above the failure surface, is divided into vertical parallel slides and considers a normal stress variation along the potential failure surface and the equilibrium on each of the slides.

Figure 10 shows a given section of a dyke that presents the simplified bishop analysis method with a sloping surface AB. An assumed trial circular failure surface with a center at O is given by points ABC. The soil mass above the failure surface has been divided into several slices. The forces acting on each slice are evaluated from a limit equilibrium of the slices. The equilibrium of the entire mass is determined by summing up the forces on each of the slices (Verruijt, 2001; Murthy, 2002). During the analysis, only a single slice is considered.

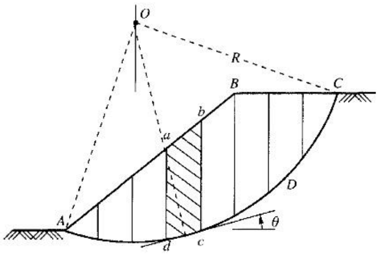

Figure 10 Limit equilibrium: Bishop method (Verruijt, 2001).

The forces acting on the single slice abcd are shown in Figure 11 and these are:

W = weight of the slice
N = total normal force on the failure surface cd
U = total pore water pressure
F_R = shear resistance acting on the base of the slice
E_1, E_2 = normal forces on the vertical faces be and ad
T_1, T_2 = shear forces on the vertical faces be and ad
θ = the inclination of the failure surface cd to the horizontal

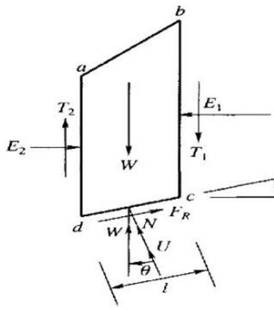

Figure 11 Forces acting on slice abcd in the Bishop method (Verruijt, 2001).

The system is statically indeterminate. An assumption is that the resultant of E_1 and T_1 are equal to E_2 and T_2, and their lines of action coincide. The method is as follows:

1. Define the normal and tangential components of weight

$$N = W\cos\theta$$
$$F_t = W\sin\theta \qquad (tangential\ component\ of\ W)$$

2. Define the unit stress on the failure surface (l), in this case:

$$\sigma_n = \frac{W\cos\theta}{l} \qquad \text{(normal stress)}$$
$$\tau_n = \frac{W\sin\theta}{l} \qquad \text{(shear stress)}$$

$$s = c' + \sigma' tan\phi' \qquad \text{(shear strength)}$$

Where

$c' = effective\ unit\ cohesion$
$\sigma' = effective\ normal\ stress\ on\ the\ potential\ surface\ of\ rupture$
$\phi' = effective\ angle\ of\ interanl\ friction$

3. With the shear strength, the total forces acting on the failure surface ADC

$$F_R = c'l + (\mathrm{W} \cos\theta - U) tan\phi' \qquad \text{(total resistance force)}$$
$$F_t = W\ sin\ \theta \qquad \text{(total actuating force)}$$

4. The main objective of the slope stability analysis is to determine the factor of safety. Bishop method uses the factor of safety concerning strength, which is used to compare the two shear forces acting on the slope. This way, this provides the rate of the interaction of both shears. A safety factor greater than 1.5 is needed to state that the slope stability is trustworthy, while a value lower or equal than 1 indicates that the slope stability is impending danger of failure due to the shear stress along the likely failure surface is greater than the limit shear strength of the soil. Its formula is:

$$F_S = \frac{F_R}{F_t}$$

Due to the found safety of factor presents a margin of error of 15 percentage, Bishop proposed the consideration of the resultant force E and T in the vertical faces of each slice to improve the accuracy of the analysis, Therefore,

5. Express all the forces acting on the vertical direction to maintain the equilibrium condition

$$\mathrm{N}' \cos\theta = W + \Delta T - U \cos\theta - F_R \sin\theta$$

Where

$$\mathrm{N}' = effective\ normal\ force\ on\ the\ failure\ surface\ cd \qquad (\mathrm{N}' = N - U)$$

If $F_S > 1$, then

$$F_R = \frac{c'l}{F_S} + \frac{N' * tan\phi'}{F_S}$$

6. Use the new total resistance force formula to figure out the effective normal force

$$\mathrm{N}' = \frac{W + \Delta T - U \cos\theta - \frac{c'l}{F_S} \sin\theta}{\cos\theta + \frac{tan\phi' * \sin\theta}{F_S}}$$

7. Take the moments about the center O of the trial circular failure surface to be used for the equilibrium of the mass above this surface

$$W \sin\theta\, R = F_R\, R$$

8. Use the total resistance force and the effective normal into the above formula to obtain the factor of safety.

$$F_S = \frac{\sum\{c'l\cos\theta + [(W - U\cos\theta) + \Delta T]tan\phi'\}\dfrac{1}{m_\theta}}{\sum W \sin\theta}$$

Where

$$m_\theta = \cos\theta + \frac{tan\phi' \sin\theta}{F_S} \qquad (Stability\ number)$$

F_S is presents in both sides of the equation, This way, a trial-and-error procedure needs be adopted to determine F_S. Moreover, the values assigned to $T\ and\ E$ need to satisfy the equilibrium of each slice as well as the conditions of

$$(E_1 - E_2 = 0)\ and\ (T_1 - T_2 = 0)$$

This method requires the analysis of many trial slip failure surfaces. This way, the failure surface with the lowest F_S is considered as the critical surface, which is prompt to suffer a failure. Moreover, this factor of safety reports a margin of error of about 1 percent.

4

Model set-up

This section describes more detailed the methodology to carry out the scenario analysis. Furthermore, the settings used for soil properties, dyke profiles, and water levels are described.

4.1.Methodology of the scenario analysis

The scenario analysis aims to provide a hypothetical output of a particular event based on the analysis of different scenarios. In this case, the analyzed event is the response of the outer slope in front of different water levels. For this purpose, the analysis uses 15 profiles from the regional flood defenses controlled by HHNK. Soil configuration was the main criteria for the selection of these profiles. Other factors such as dyke geometry and applied loads have also been used to find similarities between the pre-selected cross-sections.

Narvaez & Stichting Toegepast Onderzoek Waterbeheer (2020) argued that regional flood defenses in the Netherlands consist mainly of clay and peat, and usually, their reinforcement is made with clay. This occurs due to the defenses were made with the existing material in the area. However, the area of Noord Holland also has some sand dykes covered with a clayey covering layer. Due to these three soil materials are the most commonly employed in regional flood defenses in this area, the cross-sections for the modeling part will be selected according to the soil type and divided into three groups: clay, clay&peat, and clay&sand. Each group will be composed of five cross-sections, the dykes assigned to each group will take a generic name which consists of its group name (slope soil configuration) followed by a number from 1 to 5. For instance, a dyke with a slope of clay and sand is named "Clay&Sand 1".

The modeling part will evaluate a total of 90 scenarios. In this way, the analysis will use six scenarios for each of the 15 cross-sections. Each scenario contains a different water level, which will be defined according to a drawdown ratio L/H, where L indicates the height between the maximum external water level and the drop of external water level and H the maximum water level as shown in Figure 12. In this way, the water levels fluctuate between the two extreme cases: canal with full water level (L/H=0) and empty water level (L/H=1).

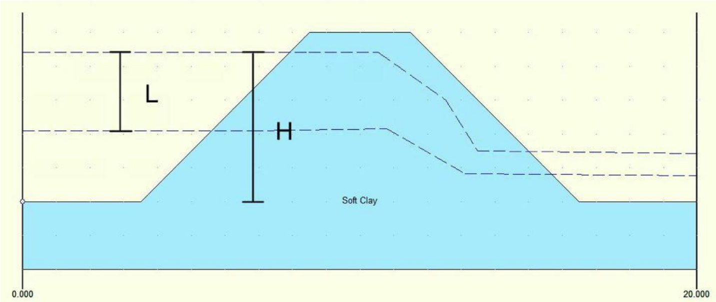

Figure 12 Representation of the drawdown ratios in a dyke with a maximum external water level H and a water drawdown L.

The inputs for the modeling are the selection of the method for the analysis, the soil parameters such as shear strength given by the friction angle, dilatancy, total unit weight and cohesion for each soil type, the external loads' values such as water levels and traffic loads, and the cross-section of the infrastructures. The values of these parameters employed in the different scenarios are described in the following paragraphs.

The output from the stability analysis will focus on two aspects, the development of the safety factor along with the different drawdown ratios and the relationship between the size of the slip circle and the drawdown ratio. Besides the numerical value of the factor of safety and the graphical result of the size of the slip plane, the different cross-sections will be compared between them based on similar features such as geometrical and soil configuration in order to see the effects of the different parameters influencing on the two main outputs of the analysis.

4.2. Set-up for the scenario analysis

4.2.1. Dike geometry

The dyke structures analyzed in the modeling are part of the regional flood defenses in Noord-Holland. HHNK provided the cross-sections of these structures. The geometrical dimensions of the modeling structures vary enormously. This is seen when the slope ratio (dyke height/dyke width) is compared between all the cross-sections. Figure 13 shows the dimensions used on the slope ratio.

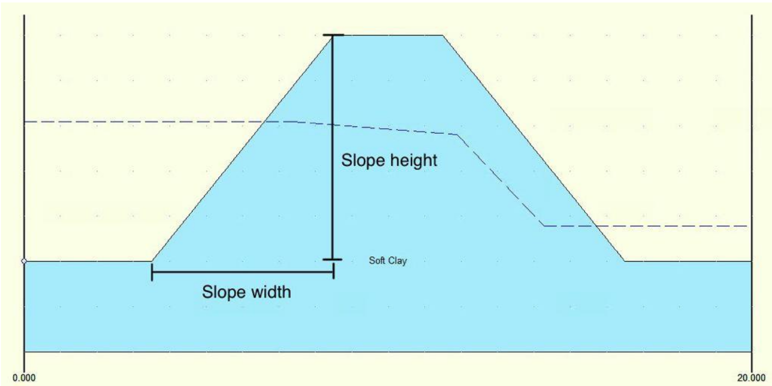

Figure 13 Representation of the slope ratio factors

There are steep slopes with ratios from 1:0.6 until very gradual slopes with ratios of 1:7. The most common slope ratio within the modeled defenses is 1:2. Table 2 shows a brief description of the dimension of the three groups of dykes. Furthermore, Figure 14 depicts the cross-section of the slopes with the extreme cases and the most common case. A complete description of each cross-section is shown in Appendix.

Table 2 Slope dimensions and ratio of 15 regional flood defences controlled by HHNK used in the modelling part.

Dyke	**Clay 1**	**Clay 2**	**Clay 3**	**Clay 4**	**Clay 5**
Slope height (m)	2,5	1,95	3,5	2,2	2,4
Slope width (m)	6,52	6,25	6	5,6	3,5
Slope ratio	1:2,5	1:3	1:2	1:2,5	1:1,5
Dyke	**Clay&Peat 1**	**Clay&Peat 2**	**Clay&Peat 3**	**Clay&Peat 4**	**Clay&Peat 5**
Slope height (m)	3,5	3,5	3,31	2,54	3,12
Slope width (m)	26,2	24	12,51	5,33	6,93
Slope ratio	1:7	1:6,5	1:4	1:2	1:2
Dyke	**Clay&Sand 1**	**Clay&Sand 2**	**Clay&Sand 3**	**Clay&Sand 4**	**Clay&Sand 5**
Slope height (m)	1,63	2,18	1,75	5,6	3,11
Slope width (m)	6,95	6,84	1,02	25,96	6,22
Slope ratio	1:4	1:3	1:0,6	1:4,5	1:2

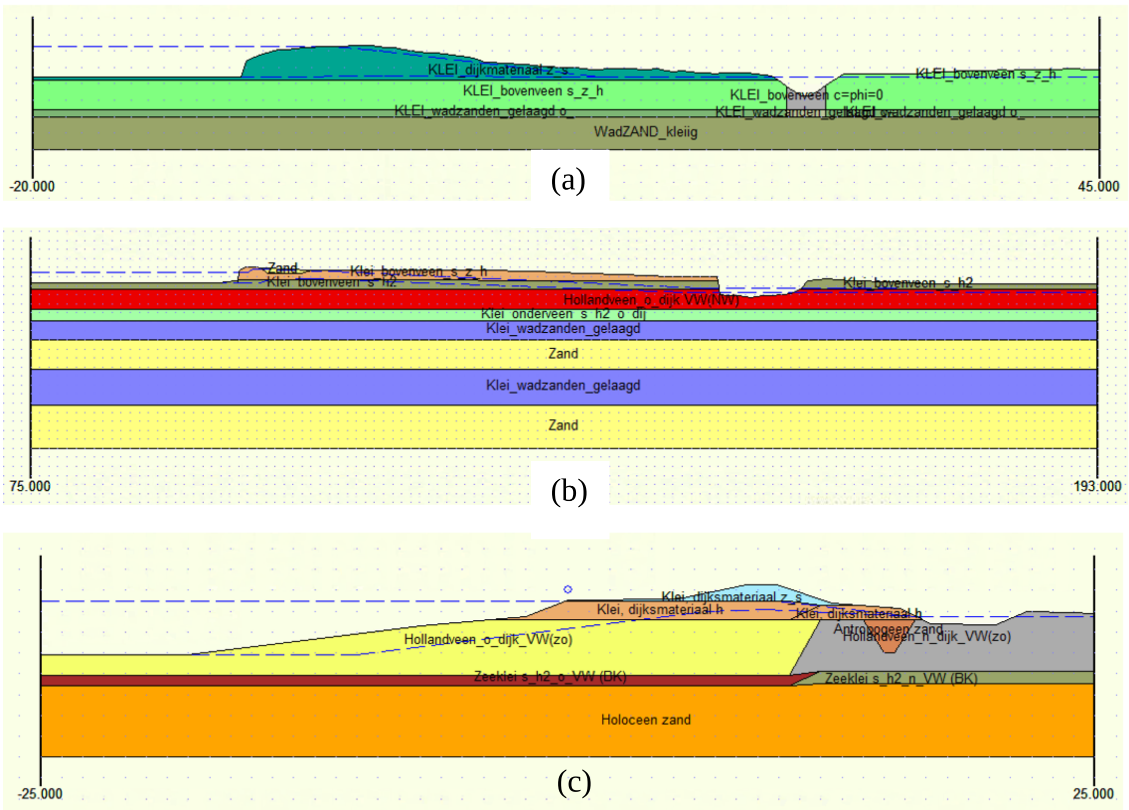

Figure 14 Geometrical profiles of three chosen regional flood defences controlled by HHNK with different slope ratios: (a) most common slope; (b) steepest slope; (c) flattest slope.

4.2.2. Soil parameters

The regional flood defenses have been traditionally constructed with materials of the same area. In the case of Noord Holland is concerned with clay and peat. Therefore, the soil configuration of a large part of the regional flood defenses has at least one type of clay and peat. However, there are also sand dykes covered with a clayey covering layer in this area. This way, three soil configurations have been identified to be used in the modeling part. These are dykes with homogeneous clay slopes, dykes with heterogeneous clay and peat slopes, and dykes with heterogeneous clay and sand slopes. Furthermore, the selected cross-sections were organized in groups according to these soil configurations.

Sixteen soil materials compose the soil configuration of the slopes of the 15 modeled regional flood defenses. These materials and their parameters are presented in Table 3. The C-Phi shear strength parameters were used in the modeling. Moreover, the total unit weight for the different types of clay and peat were taken from the report “ondergrenzen sterkteparameters” (Aracadis, 2019). Moreover, sand parameters were based on the Dutch norm NEN 9997-1+C2 (Royal Netherlands Standardization Institute, 2017). In the case of dilatancy, this parameter uses the exact value of the friction angle degree of each material. The description of the slope soil configuration of each modeled infrastructure is described in Appendix.

Table 3 Soil parameters of the slopes configuration of the 15 modelled regional flood defences.

Material	$\boldsymbol{Unit\,Weigt}$ $\boldsymbol{\gamma}$ $[\boldsymbol{kN/m^3}]$	$\boldsymbol{Cohesion}$ $\boldsymbol{c}$ $[\boldsymbol{kPa}]$	$\boldsymbol{Friction\ angle}$ $\boldsymbol{\phi}$ [°]	$\boldsymbol{Dilatancy}$ $\boldsymbol{\psi}$ [°]
Hollandveen_n_dijk	9,8/1,4	2,1	22,2	22,2
Hollandveen_o_dijk – vw (nw)	9,9/1,5	4,2	20,9	20,9
Hollandveen_o_dijk – vw (zo)	9,8/1,6	4,2	19,6	19,6
Klei_bovenveen s_z_h	15,4/9,3	4,2	32,8	32,8
Klei_dijkmateriaal h	13,9/6,9	0,8	27,3	27,3
Klei_dijkmateriaal z_s	16,7/11,5	4,2	34,5	34,5
Klei_groet_waardkanaal_oo	15,87/1,2	0	33,8	33,8
Klei_onderveen s_h2	14,1/7,7	0,8	18,0	18,0
Klei_onderveen s_h2_n_dijk	14/7,1	0,8	27,3	27,3
Klei_onderveen s_h2_o_dijk	13,9/6,9	0,8	28,5	28,5
Klei_onderveen s_z_h_n_dijk	15,3/9,0	4,2	26,2	26,2
Klei_onderveen s_z_h_o_dijk	15,4/9,0	4,2	28,2	28,2
Klei_wadzanden_gelaagd o_dijk	16,3/10,8	0,8	24,3	24,3
Zand	18,0/20,0	0	32,5	32,5
Zand_s_dijk	18,0/20,0	0	32,5	32,5
Zeeklei_ s_z_h_o_dijk	15,4/9,0	4,2	27,3	27,3

4.2.3. Water levels scenarios

The regional flood defenses protect the surrounding polder areas from the excess water draining out of the polder through pumps. In this way, the water level inside the canals is regulated by human intervention. Extreme rainfalls or breaches in the primary flood defenses can modify this water level. However, considerable modifications of water levels due to these events are rarely occurring. Therefore, the difference between average water levels and extreme water levels is limited to several decimetres.

The settlement of the scenarios is based on the gradual decrease of the water level in the canals. The scenarios will be defined according to the drawdown ratio L/H (where L indicates the height between the initial and the final drop of external water level, and H represents the maximum water level in the canal). There will be six scenarios for structure; the first presents a drawdown ratio L/H=1, representing a total water level in the canal, then the ratio decreased 20%, which means that the five following drawdown ratios analyzed are L/H=0.8, L/H=0.6, L/H=0.4, L/H=0.2, and L/H=0. This last ratio represents when the water level in the canal is parallel to the canal bed, i.e., an empty canal. Figure 15 shows an example of the schematization of the six scenarios analyzed in a cross-section.

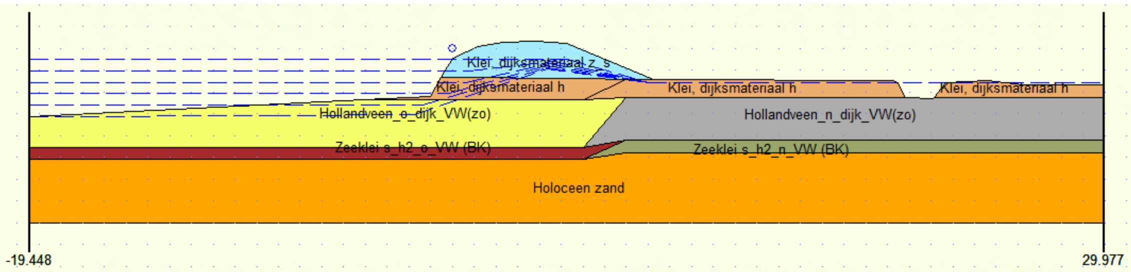

Figure 15 An example of the scenarios analysis for all the modelled flood defences and schematization of the phreatic lines for each scenario.

4.2.4. Schematization of the phreatic line

The phreatic line defines the soil state inside the slope. One of the factors that modified the location of the phreatic line is the pore water pressure. When a drawdown occurs, the phreatic surface decrease due to the pore water pressure in the slope decrease. During this process, the drainage of the inter-granular pores takes place, allowing air into them. In this way, the pore water pressure and the degree of saturation drop. Given that the pore pressure is a potentially destabilizing force in saturated soils, the schematization in the different scenarios is relevant.

According to their scenarios, the sets of phreatic lines for each cross-section were modelled as taking as reference the phreatic surface used by HHNK for high water level. Due to the D-Geo stability not allowing the dissipation process to model, the setting of these phreatic surfaces tried to mimic this process manually. In this way, the phreatic lines follow the same pattern as the phreatic line of the higher water level with a certain lower position. Following these patterns, the configuration of phreatic lines seeks to avoid extreme cases such as fully rapid drawdown or fully slow drawdown. These extreme cases provide higher or lower safety factors, either overestimating or underestimating the role of the phreatic surface under drawdown conditions. Figure 15 shows the schematization of the phreatic lines according to the different scenarios in one of the modeled Clay&Peat dykes

5

Model Results

This chapter shows the slope stability analysis performed on D-Geo Stability to the 15 chosen regional flood defenses. The output of the analysis aims to answer sub-question two and sub-question four. Firstly the development of the factor of safety during water drawdown is presented. Furthermore, in this part, the cross-sections will be compared to understand the influence of the different facto. Then, the relationship between the size of the slip surface and the drawdown ratio is presented.

5.1. Development of the factor of safety (FoS) under different drawdown scenarios

The stability analysis seeks to define a numerical form to evaluate if a structure is stable or impending danger of failure. One of the most used numerical forms to define the trustworthiness of the infrastructure regarding its stability is the factor of safety. A safety factor greater than 1 indicates that the shear strength of the soil is great enough to withstand the shear stress along the likely surface. In other words, the structure can support the applied loads and forces on it. On the other hand, a factor lower than 1 reveals that the shear stress cannot support the shear stress along the likely failure surface.

This way, the factor of safety of these cross-sections have been calculated with the Bishop method according to the parameters described in Set-up for the scenario analysis. Figure 16, Figure 17, and Figure 18 show the development of the safety factor of the cross-sections according to their group under drawdown conditions. The results reveal that the trends of safety factors on the groups Clay and Clay&Sand present similar patterns where most of the minimum factors of safety are reached at L/H=0.8 and L/H=1.0. On the other hand, the group of Clay&Peat dykes mainly present their minimum safety factors at L/H=0.6.

The three groups have at least one dyke that does not follow these trends, these dykes will be compared between dykes of the same group that presents similar characteristics such as slope ratio, applied loads, and drawdown size (the difference between the maximum and minimum water level in the canal) in order to determine the possible influencing factors in this disagreements. These factors will be presented for each dyke in tables.

5.1.1. Dykes with slopes of only clay

Fig XX shows the factor of safety of clay dykes under different drawdown ratios. It can be seen that in most of the cases, the drawdown ratio L/H=0 presents the highest factor of safety. Then, these values decrease until they reach their minimum values at drawdown ratio L/H=1 in 3 of 5 dykes. In the case of dykes Clay 1 and Clay 3, the minimum safety factor is reached at drawdown ratios L/H=0.6 and L/H=0.8, respectively. These dykes present a recovery after reached their minimum values at lower drawdown ratios. The analysis also shows that in the case of dykes Clay 2, Clay 4, and Clay 5, the reduction of the safety factor between the two extreme drawdown ratios is smaller than in the case of Clay 1 and Clay 3. Another aspect to consider is the increase of the factor of safety of Clay 5 at L/H=0.2. Furthermore, the parameters of the different dykes are shown in Table 4

Table 4 Special parameters of the group of Clay flood defences

Dyke	**Clay 1**	**Clay 2**	**Clay 3**	**Clay 4**	**Clay 5**
Lowest FoS	2.10	2.54	1.13	1.21	1.20
L/H at lowest FoS	0.6	1	0.8	1	1
Slope ratio	1:2,5	1:3,0	1:2,0	1:2,5	1:1,5
Applied load	5	13	5	5	13
Materials	2	2	4	2	1
Drawdown size	2.4	1.9	3.3	1.2	1.4

Clay 1 will be compared with Clay 4 due to both dykes presents similar profiles with a slope ratio of 1:2,5 and experience an applied load of 5 kN/m2. Moreover, both dykes have the same types of soil. In this way, the main difference between these dykes is the drawdown size, due to Clay 1 has a drawdown size of 2,37 m compared with a drawdown size of 1,2. It can be seen that the size of the drawdown, in this case, influences the time to respond of the slope. On the other hand, a larger drawdown size at high drawdown ratios also provides a higher safety factor, as can be seen in Clay 1 at L/H=0 with a FoS=2.84 compared with a FoS=1,72 of Clay 4 at the same drawdown ratio.

The other dyke to compare is Clay 3, which reaches its minimum safety factor earlier than most of the dykes in this group. In this case, Clay 3 will be compared with Clay 4. Both dykes have the same applied load, 5 kN/m2, and similar slope ratios, 2,5 and 2,0 respectability, The main difference between these dykes is the soil types and the drawdown size. The slope of Clay 3 is made of 4 types of Clay, while the slope of Clay 2 slopes consists of two types. Furthermore, the drawdown size of Clay 3 is almost three times the size of Clay 4. Here, the drawdown size also influences the prompt decrease of the factor of safety. Moreover, the soil parameters from the different types of material also impact the stability of the slope. For instance, Clay 3 has two types of Clay with low cohesion, while Clay in Clay 4 has higher cohesion values.

The analysis in dykes with slope clays shows that the slope stability under different drawdown levels does not represent a significant risk of failure because the stability factor has not reached values lower than 1. However, factors such as the drawdown size and the slope configuration with different types of materials influence the development of safety factors in these modeled defenses.

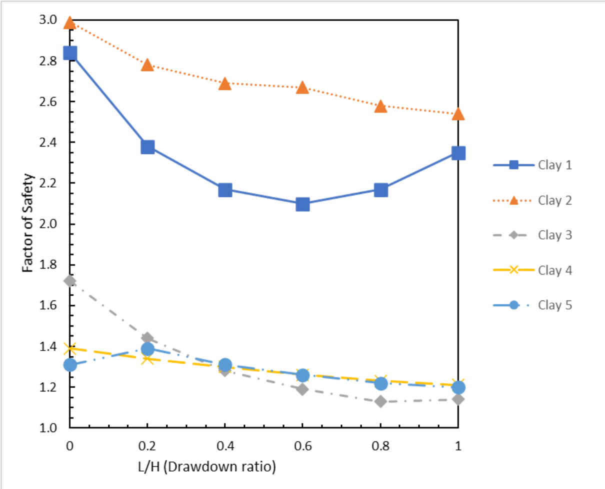

Figure 16 Development of factors of safety under different drawdown ratios of the group of clay dykes.

5.1.2. Dykes with slopes of clay and peat

Fig XX shows the development of the factor of safety of dykes with slopes of clay and peat. These types of slopes present a similar pattern in all the modeled cases, where the maximum factor of safety is located at drawdown ratio L/H=0, and the minimum value is reached at L/H=0.4 in dykes Clay&Peat 1 and Clay&Peat 5, and at L/H=0.6 in dykes Clay&Peat 2, Clay&Peat 3 and Clay&Peat 4. After reaching the minimum value, the trend of the factor of safety starts to recover slowly in the subsequent lower drawdown ratios. It can be seen that in the cases of dykes that reach the minimum factor of safety at L/H=0.4, the stability decrease is higher with a decrease of around 14% of its maximum value in comparison with the range of decrease of the other dykes, which present a decrease of about 9% of its maximum factor of safety. Table 5 shows the parameters to compare these dykes.

Table 5 Special parameters of the group of Clay&Peat flood defences

Dyke	**Clay&Peat 1**	**Clay&Peat 2**	**Clay&Peat 3**	**Clay&Peat 4**	**Clay&Peat 5**
Lowest FoS	1.69	1.14	0.74	1.08	1.36
L/H at lowest FoS	0.4	0.6	0.6	0.6	0.4//0.6
Slope ratio	1:7,0	1:6,5	1:4,0	1:2,0	1:2,0
Applied load	5	13	13	5	5
Materials	2	2	3	2	2
Drawdown size	2.6	3.2	2.6	2.4	2.3

Clay&Peat 1 will be compared with Clay&Peat 5, these two dykes reach its minimum at L/H=0.4, but also Clay&Peat 5 follows the trend of the group having its minimum also at L/H=0.6. The applied load on both dykes is the same, 5 kN/m2. Furthermore, their sizes of drawdown are almost the same. The main difference between these dykes is the slope ratio. Clay&Peat 1 has a very flat slope, while Clay&Peat 5 has a steep slope. Considering the vast difference in slope ratios, it can be argued that the influence of slope ratio is minor on slope stability. However, this is not the case. The similar response of these dykes can be explained by the analysis of the soil types of the slopes. The shear strength parameters of Clay&Peat 1 are smaller than soil parameters of Clay&Peat 5, especially cohesion. This way, it can be said that the effect of slope stability has been counteracted by the shear strength parameters of the soils of the slopes.

The other dyke that presents discrepancies is Clay&Peat 3. Although these dyke reach its minimum factor of safety at the same drawdown ratio as most of the dykes, the development of the factors of safety as drawdown occurs of Clay&Peat 3 shows that the infrastructure of this dyke cannot support the shearing shear stress along the likely failure surface. In this way, the infrastructure will not support drawdown ratios lower than 0.2, as shown in the graph. In this way, Cla&Peat 1 will be compared with Clay&Peat 3 to identify possible factors influencing this situation. Both show a similar geometry profile.
Furthermore, their soil configuration is the same as well as the drawdown size. This way, the only two factors that differ from these cases are the applied load and the slope ratio. In both cases, the values of these parameters are totally opposite. However, Clay&Peat 1 presents high factors of safety at all drawdown ratios. It can be argued that the possible factor creating this situation is the high applied load to Clay&Peat 3, which is almost triple a load of Clay&Peat 1.

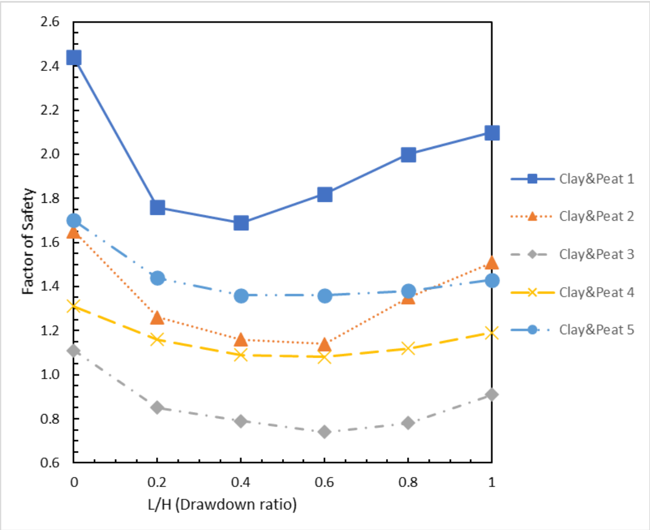

Figure 17 Development of factors of safety under different drawdown ratios of the group of clay and peat dykes.

5.1.3. Dykes with slopes of clay and sand

Fig shows the factors obtained from the analysis to dykes with slopes of clay and sand. There are four dykes that present similar development of safety factors: Clay&Sand 1, Clay&Sand 2, Clay&Sand 3, and Clay&Sand 5. In these dykes, the maximum safety factor is experienced at drawdown ratio L/H=0, while the minimum factor of safety is presented in drawdown ratios higher than L/H=0.8. All these dykes shows a relatively small range of change between the two extreme factors of safety, the more significant decrease of this factor present Clay&Sand 5, with around a decrease of 0.79 in the factor of safety. On the other hand, Clay&Sand 4 shows totally different behavior compared to the other dykes of the group. Its minimum factor safety is reached at L/H=0.2. Although the minimum values occur at a high drawdown ratio, the development shows that the slope recovers stability as the water levels fall. Table 6 describes the factors of the different structural parameters of these dykes.

Table 6 Special parameters of the group of Clay&Sand flood defences

Dyke	**Clay&Sand 1**	**Clay&Sand 2**	**Clay&Sand 3**	**Clay&Sand 4**	**Clay&Sand 5**

Lowest FoS	1.42	1.47	1.06	2.10	1.95
L/H at lowest FoS	1	0.8	0.8	0.2	1
Slope ratio	1:4,0	1:3,0	1:0,6	1:4,5	1:2,0
Applied load	5	13	8	5	0
Materials	2	2	3	2	3
Drawdown size	1.16	2.1	1.16	4.4	2.55

To understand the behaviour of Clay&Sand 4, this dyke will be compared with Clay&Sand 1. In this case, both dykes present the same soil configuration and applied load. Furthermore, the slope ratio is very similar. The drawdown size is the main difference between these dykes. Clay&Sand 4 has a size drawdown of 4.4 m. Instead, Clay&Sand 1 only presents a drawdown size of 1.16 m. Since this is the only considerable difference between these dyke, it can be argued that a high drawdown size influences the development of the factor of safety to reach its minimum values faster.

Nevertheless, it can be seen that the drawdown size also affects the slope stability positively. Clay&Sand 4 and Clay&Sand 5 present the largest drawdown sizes and the highest factor of safety values. On the other hand, Clay&Sand 1 and Clay&Sand 3 have the smallest drawdown size, and it is reflected in the lowest factors of safety between the dykes of the group.

Finally, according to the performance in this analysis, it can be said that the development of the factor of safety in dykes with slopes of clay and sand shows that this soil configuration provides enough safety under different water levels due to any dykes present an FoS lower than 1.

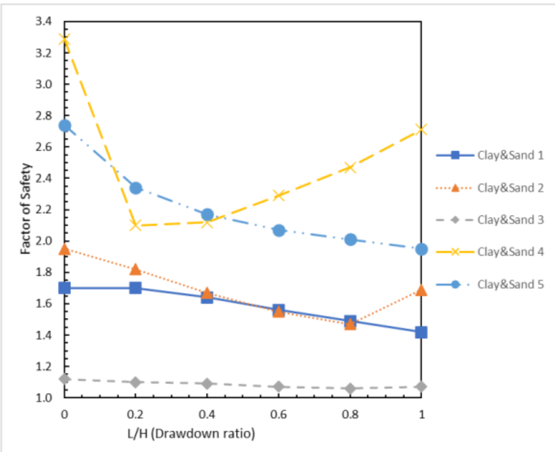

Figure 18 Development of factors of safety under different drawdown ratios of the group of clay and sand dykes.

5.2. Development of the size of the slip surface under drawdown conditions.

Research sub-question 4 seeks to determine the correlation between the size of the slip surface and the amount of drawdown. For this, the resulting slip surfaces obtained under the two extreme drawdown ratios will be presented graphically. Furthermore, the coordinates of the centre point and radius length will be also shown for each cross section of each group.

5.2.1. Dykes with slopes of only clay

Table 7 presents the coordinates of the center point and radius forming the slip surface on dykes with clay slopes. The coordinate x in all the cross-sections starts near the slope face at L/H=0. However, as the drawdown ratio increases, this coordinate tends to move away from the slope location. In the case of coordinate y, the points move upwards in most of the cases. However, only in one case, Clay 2, the coordinate y moves downward. Finally, it can be seen that the radius increase its length in most of the case, the radius only decreases its length on dykes where its y coordinates go downward.

Given the results of the modeling, it can be said that the slip surface is most likely to increase its size as the water level decrease, as can be seen in Figure 19, where dykes Clay 1, Clay 3, Clay 4, and Clay 5 presents a bigger slip surface at L/H=1.

Table 7 Characteristics of factors of the slip plane in the extreme scenarios of dykes with Clay slopes

Dyke	Clay 1		Clay 2		Clay 3		Clay 4		Clay 5	
Drawdown ratio	0.0	1.0	0.0	1.0	0.0	1.0	0.0	1.0	0.0	1.0
Centre point x coor.	-5.6	-7.2	-5.8	-7.3	-7.0	-7.8	-4.4	-5.2	29.3	31.4
Centre point y coor.	2.2	2.4	5.4	1.0	1.8	2.1	2.1	2.4	5.3	6.4
Radius (m)	4.4	5.9	7.6	3.0	6.7	7.2	4.6	5.9	7.0	8.4

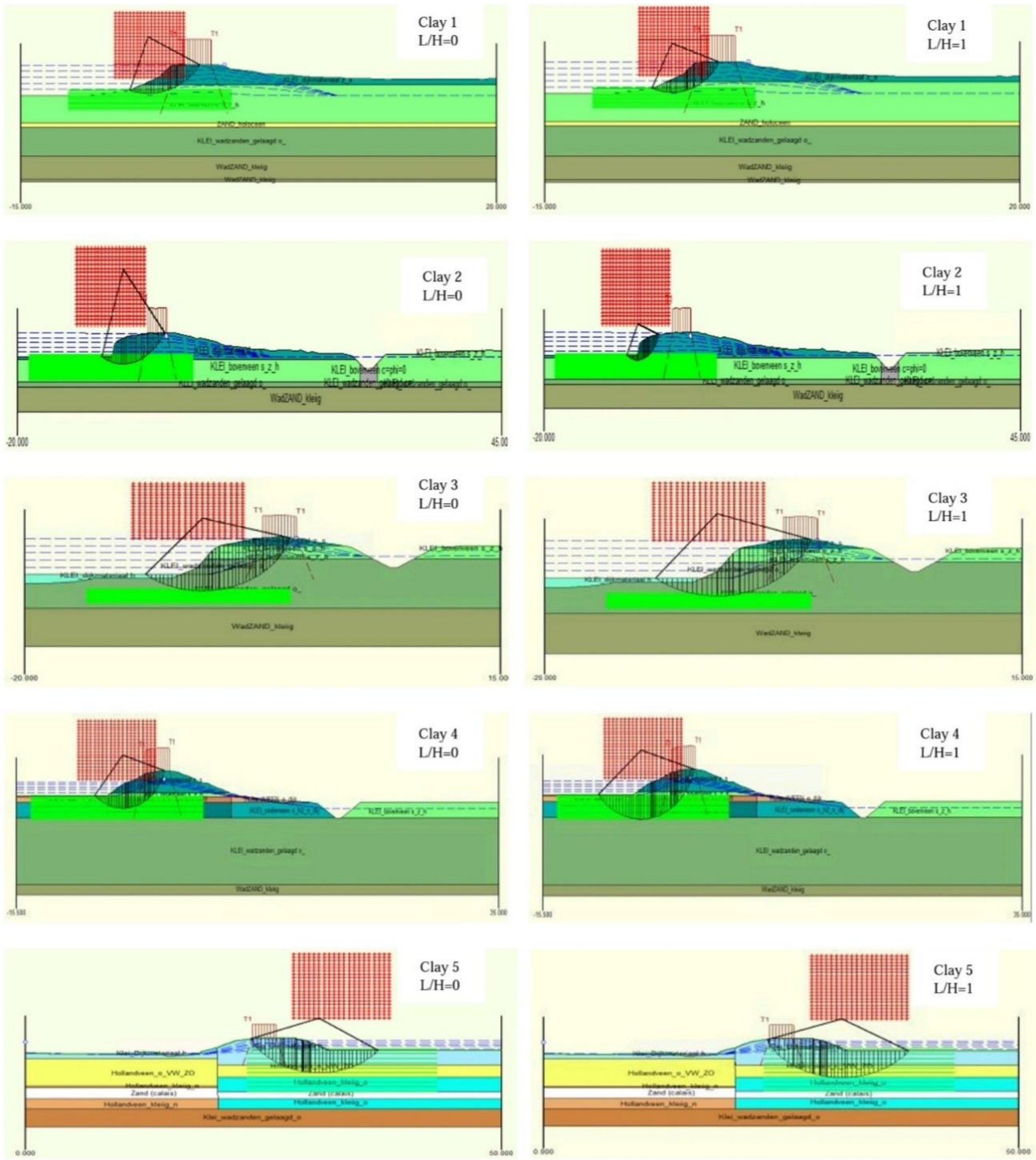

Figure 19 Graphical results of the slip plane in the extreme scenarios of dykes with Clay slope

5.2.2. Dykes with slopes of clay and peat

Table 7 shows the slip surface parameters of dykes with slopes of clay and peat. The coordinate x in these dykes is more away like a water level decreases. In this group, all the x coordinate moves to the left, as shown in Figure 20. A similar relationship as occurred in the previous group takes place in the clay and peat dykes. The centre points that their y coordinate moves upward present a larger radius at drawdown ratio L/H=1 compared to the radius length at L/H=0. On the other hand, the slip surface that their y coordinates move downwards experience the decrease of the radius length as water level decrease.

To sum up, dykes with slopes of clay and peat experience more extensive slip surfaces when the center points moved upwards as the water level decreases. The slip surfaces of dykes with slopes of clay and peat at the two extreme drawdown ratios are shown in Figure 20

Table 8 Characteristics of factors of the slip plane in the extreme scenarios of dykes with Clay&Peat slopes

Dyke	Clay&Peat 1		Clay&Peat 2		Clay&Peat 3		Clay&Peat 4		Clay&Peat 5	
Drawdown ratio	0.0	1.0	0.0	1.0	0.0	1.0	0.0	1.0	0.0	1.0
Centre point x coor.	2.6	1.2	2.2	0.9	-0.9	-1.2	5.4	3.6	94.8	94.2
Centre point y coor.	4.3	6.0	2.3	2.3	1.1	1.3	3.2	1.9	4.2	2.3
Radius (m)	9.0	10.7	5.3	6.6	6.0	6.4	6.3	5.0	8.4	7.3

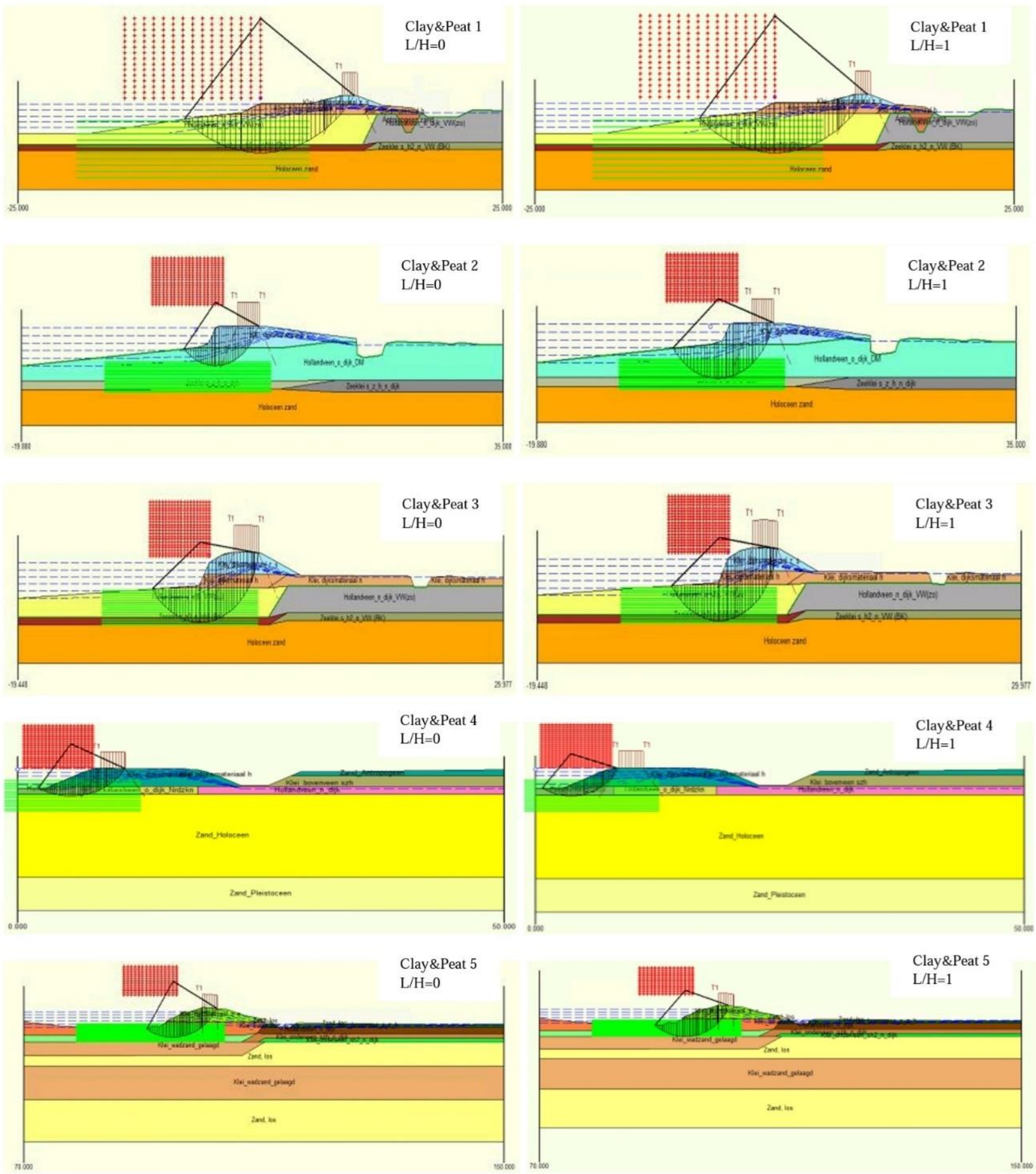

Figure 20 Graphical results of the slip plane in the extreme scenarios of dykes with Clay&Peat slopes

5.2.3. Dykes with slopes of clay and sand

Table 9 shows the center point coordinates and radius of the slip circle of dykes with slopes of clay and sand. As in the former cases, the coordinate x moves away from the slope surface as the water level decreases. In this group of dykes, some of the center points do not have to experience movements of their coordinates. For instance, dykes Clay&Sand 1 and Clay&Sand 2 presents the same coordinate x at L/H=0 and L/H=1. A similar event occurs on dykes Clay&Sand 4 and Clay&Sand 5, where their y coordinate keeps in the same place. Although some coordinates keep constant, the radius length either decrease or increase according to the movement of the x and y coordinates as shown in all the graphical representation in Figure 21.

In conclusion, the size of the slip surface will increase if their center points move away from the location of the slope surface. At the same time, the size of the slipe surface will decrease as the center point approaches the slope surface.

Table 9 Characteristics of factors of the slip plane in the extreme scenarios of dykes with Clay&Sand slopes

Dyke	Clay&Sand 1		Clay&Sand 2		Clay&Sand 3		Clay&Sand 4		Clay&Sand 5	
Drawdown ratio	0.0	1.0	0.0	1.0	0.0	1.0	0.0	1.0	0.0	1.0
Centre point x coor.(m)	47.0	47.0	54.1	54.1	98.1	97.0	-19.9	-21.5	0.7	-1.2
Centre point y coor.(m)	2.5	1.8	4.7	4.1	1.7	0.7	6.8	6.8	3.8	3.8
Radius (m)	5.7	5.6	9.7	9.1	4.1	3.1	9.3	9.5	7.2	7.6

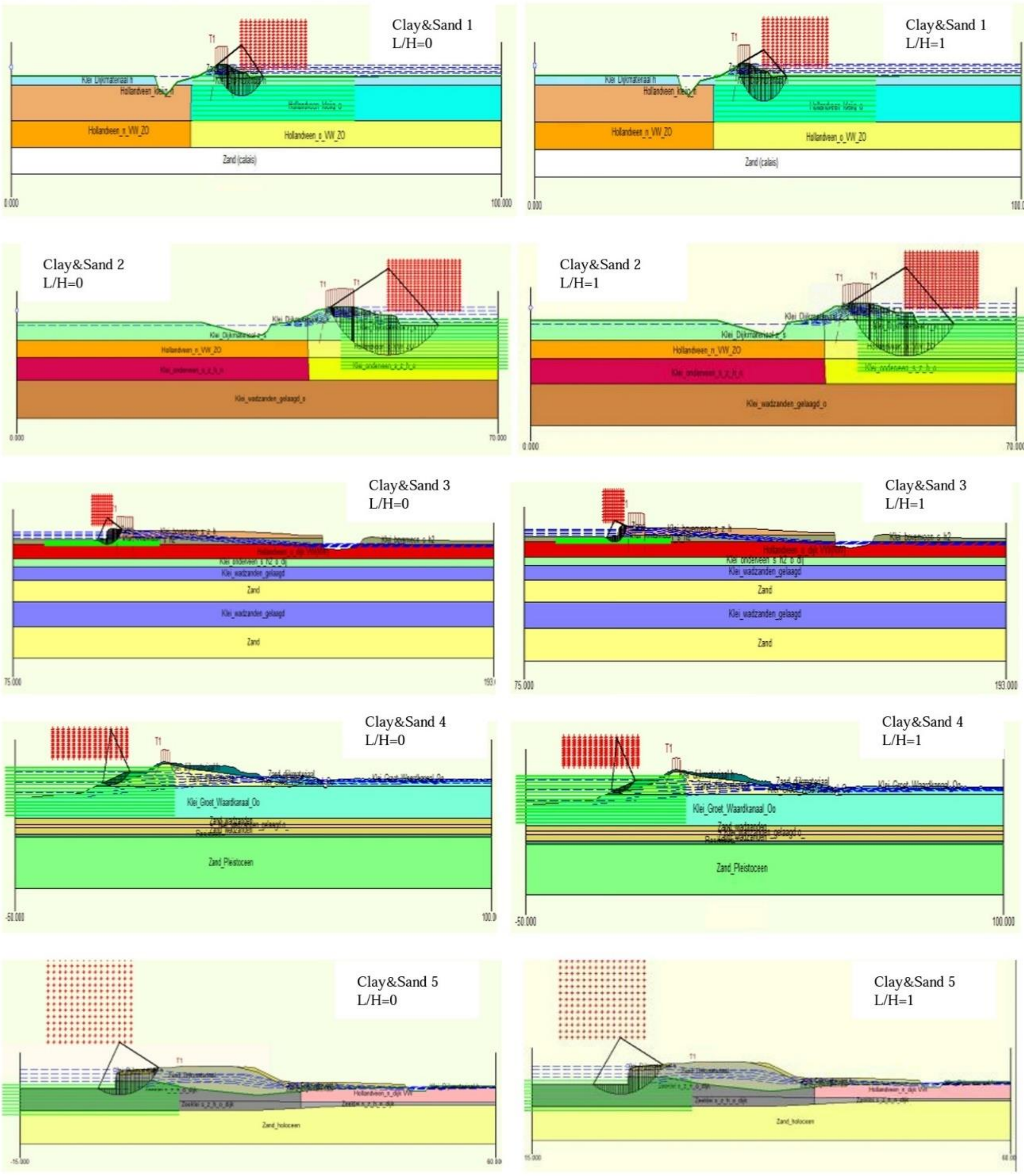

Figure 21 Graphical results of the slip plane in the extreme scenarios of dykes with Clay&Sand slopes

6
Discussion

In the first part of this chapter, the elements employed in the model setup will be discussed. In this way, the input values and considered assumptions can be reflected. The second part will focus on discussing the modeling results.

6.1.Model set up

The first limitation in the modeling part was calculating the pore water pressure during the drawdown condition. Since the Bishop method, the limit equilibrium method employed in D-Geo Stability for the stability analysis omits the calculation of pore pressure induced by seepage force, a realistic estimation of the resulting pore pressure inside the slope cannot be calculated. Research on the impact of this omission shows that the safety factors calculated without considering seepage-induced pore pressure can be overestimated by as much as 30 percent (Pyke, 2017). A transient seepage analysis can estimate this induced pore pressure. For example, Berilgel (2006) used the finite element method to conduct a coupled analysis on PLAXFLOW that considers the development of pore pressures induced by stress and seepage forces.

The cross-sections were selected and divided based on their slope soil configuration. Although the dykes within the same group contained the same materials on their slope. The material properties were not the same for all the soils due to clay, sand, and peat types. Furthermore, factors such as slope geometry and applied loads were not considered as primary selection criteria. In this way, a general conclusion regarding specific infrastructure characteristics has been difficult to draw.
Moreover, it is questionable whether the analyses based on similar soil configuration provide relevant insight on the influence of the factors such as slope geometry and applied loads on the stability analysis.

It can be argued how representative the schematization of the phreatic surface for the different scenarios is since the setting of the phreatic lines for the different scenarios were performed manually only based on the pattern of the maximum water. The phreatic line determines the state of soil inside the slope and the sign of pore water pressure. This way of schematization can lead overestimate or undertime the factor of safety encountered by the stability software.

6.2.Model results

The results from the development of safety factors under different drawdown conditions have provided relevant insight into the influence of geometrical factors and applied loads. Although the results showed marked trends in the three groups, relevant factors for more realistic modeling were not considered, such as drawdown rate and consolidation process. This occurs due to the limitations of the software D-Geo stability. Furthermore, the influence of setting the phreatic lines manually for the different scenarios cannot be determined. In this way, the results are highly dependent on the schematization of the phreatic lines.

The relationship between the size of the slip plane and the drawdown size provides limited information regarding the factors influencing this relationship. The software provides the slip circle most likely to fail based on the setting of the grid and tangent lines. In this way, the finding slip circle is dependent on the manual configuration of these factors.

7
Conclusions

This section seeks to answer the sub-questions and the main research question proposed in the introduction of the research.

The research aims to understand the failure mechanism outer slope instability under drawdown conditions and improve the methodology employed in assessing this mechanism conducted by Hoogheemraadschap Hollands Noorderkwartier in the regional flood defenses in North Holland. By understanding the current methods employed to analyze this failure mechanism, the factors influencing the slope stability, and their influence, the safety assessment process can be done more efficiently and confidently. For this, a summary of the state-of-the-art knowledge in slope stability under rapid drawdown conditions and an analysis of the relationship between the amount of drawdown and the size of the slip plane will be presented.

To answer this research objective, the main four subquestions has been answered:

1. **What are approaches currently used to analyze the outer slope response under drawdown conditions?**

The slope stability analysis have used three approaches to analyse the homogeneous and inhomogeneous slopes by considering the rapid drawdown condition. These are laboratory tests, limit equilibrium with the limit equilibrium method and numerical solutions with finite element analysis. The limit equilibrium methods has been commonly used to it straightforward process of calculation. However, its limitation regarding computational difficulties and numerical inconsistencies at locating the critical slip surface and establishing the factor of safety have revealed some the drawdbacks of this approach. On the other hand, the finite element method are currently more applied in the stability analysis due to it allows to find the critical slope surface and calculate the factor of safety without assuming any failure shape. In this way, the failure surface is determined as it occurs in reality. Furthermore, FEM also provides to monitor the progressive failure and to evaluate the stresses, deformation and pore pressures in the studied embankments.

2. **What factors determine if a slope becomes unstable during rapid drawdown conditions?**

When a water drawdown occurs, the slope suffers two effects: the reduction of the external hydrostatic pressure and the modification of the internal pore water pressure. These two changes affect directly to the slope stability of the infrastructure. In theory, these two factors can be considering as the parameters to define the slope stability. However, both the reduction of the hydrostatic pressure and the modification of the pore pressure depends on other factor to determine the dimensions of these changes. These elements controlling the two main effects on the slope, hydrostatic pressure and pore water pressure, are which indeed control the stability of the infrastructure.

In this way, these two effects are controlled by the hydraulic conductivity of the soil, the drawdown size, the drawdown rate, the slope ratio, the height of the slope, the applied loads and the soil strength parameters.

3. **What factors determine how fast a slope becomes unstable during rapid drawdown conditions?**

The parameters that determine the fastness of instability varies according the analysis employed to evaluate the modification of the pore water pressure and the factors that determine the change of the stabilizing hydrostatical external pressure. Given that the finite element method provides a more realistic approach to the real behaviour of slope under drawdown conditions. This approach will serve as reference. The main factor influencing the factor of safety in this approach is the hydraulic conductivity of soil. Then, the drawdown rate also plays an important role.

On the other hand, the limit equilibrium method was employed on the modelling part in this research. Although the parameter time could not be modelled due to software limitations, the development of the factor of safety alongside the decrease of the drawdown ratio provides good insight about the factors that influence to the early decrease of the factors of safety. In this way, it could seen that slope ratio, drawdown size and applied loads influence in the factors of safety to reach their minimum values at lower drawdown ratios, which means in less time.

4. **What correlation is there between the amount of water-level drawdown and the size of the slip plane?**

The relationship between the size of the slipe surface and the size of the drawdown can be described by considering the location of the centre point and the length of the radius that creates the circumference. In this way, at low drawdown ratios the centre point shows its nearest location to the slope surface, and a short radius length. As drawdown ratio starts to increase the centre point start to move away from the slip surface. However, it can follow a downward or upward movement, of this movement will depend the length of the radius and also the size of the slip plane. In general terms, based on the modelling defences on this report, it could be said that in most of the case the radius of the slipe circle increase as the drawdown ratio also increases. However, the centre points move away from its previous point. Therefore, although the size of the slip plane at low drawdown ratios were bigger, the entry slip surface inside the slope seems to keep constant in most of the cases.

8 Recommendations

Based on the results of this research, it can be recommended the following aspects:

- Although D-Geo Stability provides go insight regarding the stability of infrastructures. It is recommended to use other software such as Plaxis, where FEM can be employed. Furthermore, it is highly recommended that the software allows the employment of time factor in the analysis.

- The schematization of the phreatic line is of vital importance in the modeling part. Therefore, for future modeling approaches. It can be helpful to use software that determines the schematization of the phreatic lines according to the due configuration and the drawdown ratio and rate, such as PLAXFLOW.

- In further research, it is recommended to use a great number of cross-sections such that at least three to four cross-sections with the same characteristics can be compared. In this way, the main factors influencing these failure mechanisms can be detected more precisely and their influence grade.

- During the analysis, a maximum drawdown to the bottom level was considered as an extreme point. In reality, the drawdown is limited to the surface level in the polder that breaches. In this way, it is advisable to consider an upper limit value for further analysis.

References

Alonso, E. E., & Pinyol, N. M. (2016). Numerical analysis of rapid drawdown: Applications in real cases. *Water Science and Engineering*, *9*(3), 175–182. https://doi.org/10.1016/j.wse.2016.11.003

Alonso, E. & Puigmartí, N. (2009). Slope stability under rapid drawdown conditions. https://upcommons.upc.edu/bitstream/handle/2117/11200/01_IWL2009_Alonso-Pinyol.pdf

Aracadis. (2019, December). *Ondergrenzen sterkteparameters: Regionale proevenverzameling Noord-Nolland v7.04* (084039990 F). Arcadis Nederland B.V.

Berilgen, M. M. (2007). Investigation of stability of slopes under drawdown conditions. *Computers and Geotechnics*, *34*(2), 81–91. https://doi.org/10.1016/j.compgeo.2006.10.004

D-Geo Stability: Slope stability software for soil engineering (16.2). (2016). [User Manual]. Deltares systems. https://usermanual.wiki/Pdf/DGeoStabilityManual.202069651/view

Dutch Water Authorities. (2017). *Water governance the Dutch water authority model*. Den Haag; Dutch Water Authorities. https://dutchwaterauthorities.com/wp-content/uploads/2019/02/The-Dutch-water-authority-model-2017.pdf

Hammouri, N. A., Malkawi, A. I., & Yamin, M. M. (2008). Stability analysis of slopes using the finite element method and limiting equilibrium approach. *Bulletin of Engineering Geology and the Environment*, *67*(4), 471–478. https://doi.org/10.1007/s10064-008-0156-z

Hoogheemraadschap Hollands Noorderkwartier. (2019). *Visie op Waterveiligheid* [Slides]. Hoogheemraadschap Hollands Noorderkwartier. https://www.hhnk-visieopwaterveiligheid.nl/index2.html

Hoogheemraadschap Hollands Noorderkwartier. (2020a, June 29). *English*. Hoogheemraadschap Hollands Noorderkwartier. https://www.hhnk.nl/english.

Hoogheemraadschap Hollands Noorderkwartier. (2020b, July 17). *Veiligheid beoordelen*. Hoogheemraadschap Hollands Noorderkwartier. https://www.hhnk.nl/veiligheid-beoordelen

Hoogheemraadschap Hollands Noorderkwartier. (2020c, November 2). *Wat doet HHNK?* Hoogheemraadschap Hollands Noorderkwartier. https://www.hhnk.nl/wat-doet-hhnk.

Hoogheemraadschap Hollands Noorderkwartier. (2021, May). *Location of Hollands Noorderkwartier. Photo provided by: Jan-Willem Evers.*

Johansson, J. (2014). *Impact of water-level variations on slope stability*. Luleå University of Technology.

Jorissen, R., Kraaij, E., & Tromp, E. (2016). Dutch flood protection policy and measures based on risk assessment. E3S Web of Conferences, 7, 20016. https://doi.org/10.1051/e3sconf/20160720016

Lane, P. A., & Griffiths, D. V. (2000). Assessment of Stability of Slopes under Drawdown Conditions. *Journal of Geotechnical and Geoenvironmental Engineering*, *126*(5), 443–450. https://doi.org/10.1061/(asce)1090-0241(2000)126:5(443)

Murthy, V. N. S. (2002). Geotechnical Engineering: Principles and practices of Soil Mechanics and Foundation Engineering (1st Edition) (9/25/02). In *Geotechnical Engineering: Principles and Practices of Soil Mechanics and Foundation Engineering* (pp. 365–418). Taylor & Francis Inc. https://www.academia.edu/8914673/Principles_and_Practices_of_Soil_Mechanics_and_Foundation_Engineering

Narvaez, L. B. & Stichting Toegepast Onderzoek Waterbeheer. (2020). *Analyse berekening stabiliteit buitenwaarts van regionale keringen*. Stichting Toegepast Onderzoek Waterbeheer (STOWA). https://www.stowa.nl/sites/default/files/assets/PUBLICATIES/Publicaties%202020/STOWA%202020-15%20buitenwaartse%20stabiliteit.pdf

OECD (2014), *Water Governance in the Netherlands: Fit for the Future?*, OECD Studies on Water, OECD Publishing, Paris, https://doi.org/10.1787/9789264102637-en.

Slomp, R. (2012). *Flood Risk and Water Management in the Netherlands* (2012 updat ed.). Rijkswaterstaat/Ministry of Infrastructure and the Environment. https://edepot.wur.nl/241151.

Pinyol, N. M., Alonso, E. E., & Olivella, S. (2008). Rapid drawdown in slopes and embankments. *Water Resources Research*, *44*(5), 1–22. https://doi.org/10.1029/2007wr006525

Rocscience Inc. (2001) Application of the finite element method to slope stability, Toronto Royal Netherlands Standardization Institute (2017). Geotechnical design of structures - Part 1: General rules. Dutch norm NEN 9997-1+c2:2017. Standards ICS codes 91.080.01,93.020.

Verruijt, A. (2001). *Soil Mechanics*. Delft University of Technology. https://ocw.tudelft.nl/wp-content/uploads/SoilMechBook.pdf.

Zhang, J., Cao, J., Mu, L., Wang, L., & Li, J. (2019, January). *Buoyancy Force Acting on Underground Structures considering Seepage of Confined Water* (No. 7672930). Hindawi. https://doi.org/10.1155/2019/7672930

Appendix

A. Description regional flood defence “Clay 1”

Dyke geometry	
Crest height (m)	2.46
Crest width (m)	4.5
Base width (m)	15
Slope height (m)	2.5
Slope width (m)	6.52
Slope ratio	1:2,5

Soil configuration				
Material	$Unit\ Weigth$ γ $[kN/m^3]$	$Cohesion$ c $[kPa]$	$Friction$ $angle$ ϕ [°]	$Dilatancy$ ψ [°]
Klei_dijkmateriaal z_s	16,7/11,5	4,2	34,5	34,5
Klei_bovenveen s_z_h	15,4/9,3	4,2	32,8	32,8

Outputs slope stability						
Drawdown ratio	0.0	0.2	0.4	0.6	0.8	1.0
Centre point x coordinate	-5.63	-5.63	-5.63	-5.63	-6.16	-6.16
Centre point y coordinate	2.16	1.90	1.63	1.37	1.63	1.90
Radius	4.37	4.11	3.85	3.69	4.49	4.00
Factor of Safety	2.84	2.38	2.17	2.10	2.17	2.35
Beta	7.30	6.14	5.54	5.28	5.22	6.37
Probability of failure	1,4E-13	4,2E-10	1,5E-08	6,3E-08	9,0E-08	9,4E-11

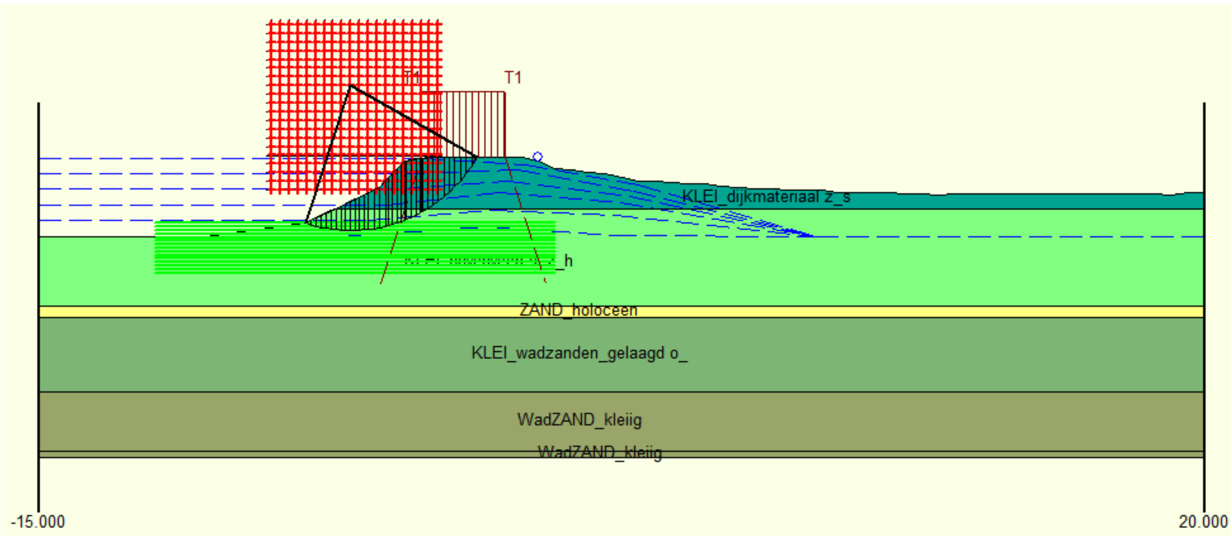

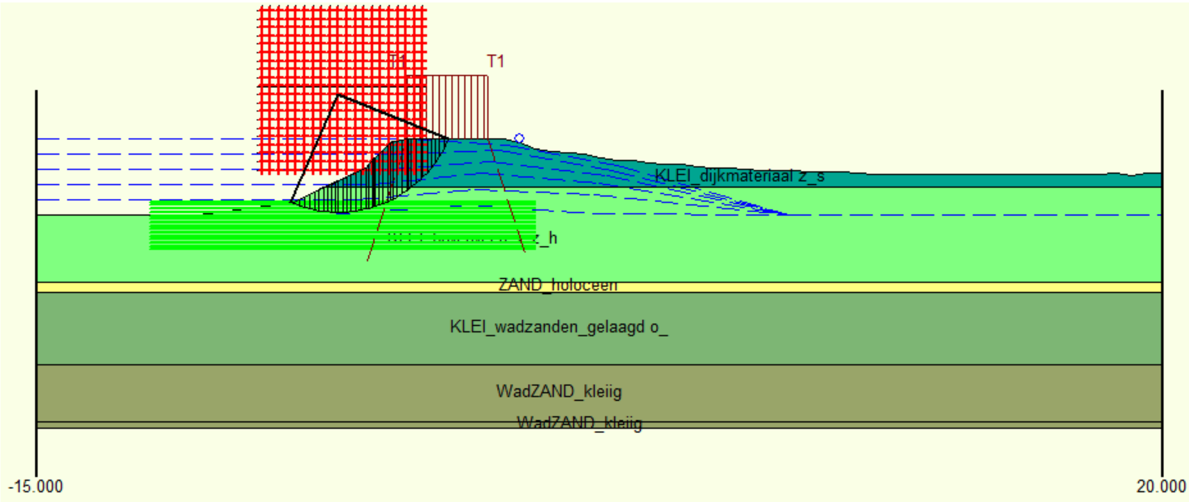
T1
T1
KLEI_dijkmateriaal z_s
ZAND_holoceen
KLEI_wadzanden_gelaagd o_
WadZAND_kleiig
WadZAND_kleiig
-15.000
20.000

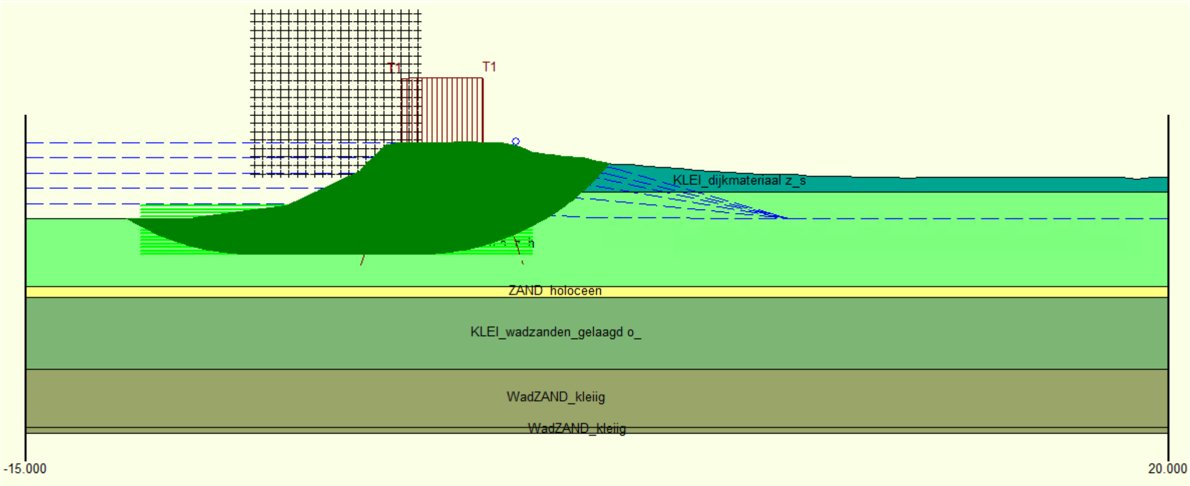
T1
T1
KLEI_dijkmateriaal z_s
ZAND_holoceen
KLEI_wadzanden_gelaagd o_
WadZAND_kleiig
WadZAND_kleiig
-15.000
20.000

B. Description regional flood defence “Clay 2”

Dyke geometry	
Crest height (m)	1.93
Crest width (m)	5
Base width (m)	14.25
Slope height (m)	1.95
Slope width (m)	6.25
Slope ratio	1:3

Soil configuration				
Material	*Unit Weigth* γ $[kN/m^3]$	*Cohesion* c $[kPa]$	*Friction angle* ϕ $[°]$	*Dilatancy* ψ $[°]$
Klei_dijkmateriaal z_s	16,7/11,5	4,2	34,5	34,5
Klei_bovenveen s_z_h	15,4/9,3	4,2	32,8	32,8

Outputs slope stability						
Drawdown ratio	0.0	0.2	0.4	0.6	0.8	1.0
Centre point x coordinate	-5.84	-5.84	-5.84	-6.32	-7.26	-7.26
Centre point y coordinate	5.42	4.79	4.16	4.47	1.00	1.00
Radius	7.59	7.04	6.91	7.47	3.00	3.00
Factor of Safety	2.99	2.78	2.69	2.67	2.58	2.54
Beta	8.26	7.73	7.25	7.12	7.04	6.99
Probability of failure	7,3E-17	5,4E-15	2,1E-13	5,3E-13	9,3E-13	1,3E-12

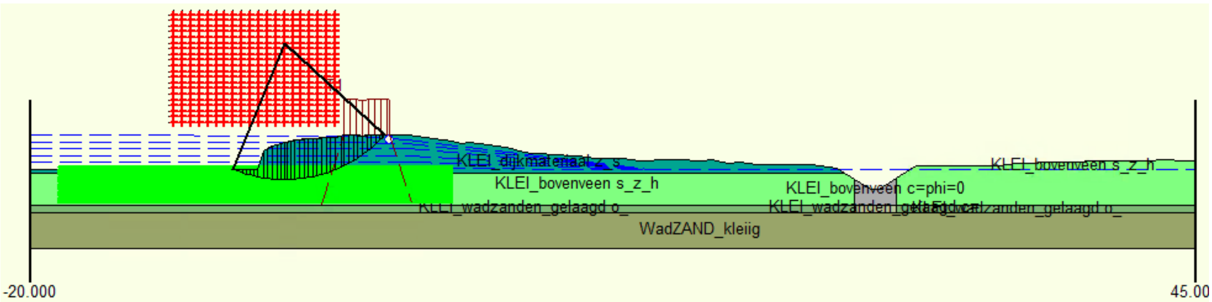

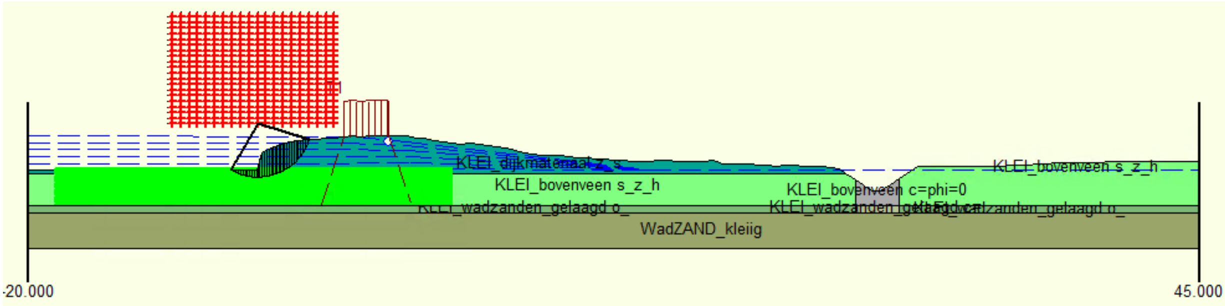

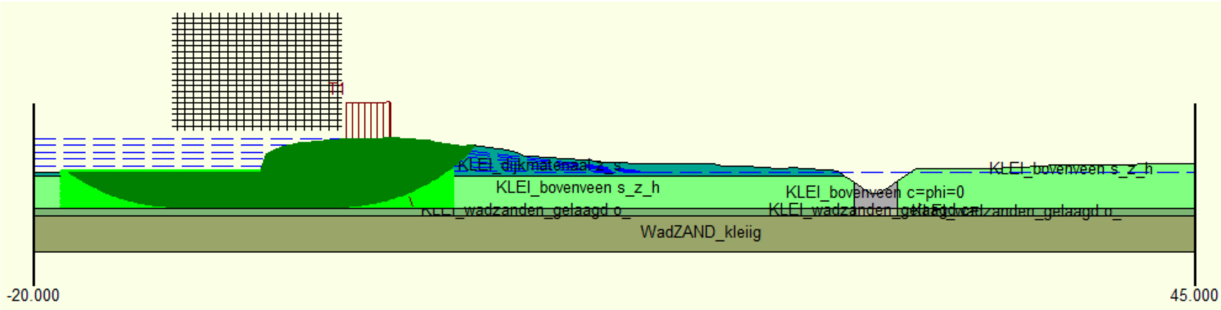

KLEI_dijkmateriaal z_s
KLEI_bovenveen s_z_h
KLEI_bovenveen c=phi=0
KLEI_bovenveen s_z_h
KLEI_wadzanden_gelaagd o_
KLEI_wadzanden_gelaagd o_
WadZAND_kleiig
-20.000
45.000

C. Description regional flood defence “Clay 3”

Dyke geometry	
Crest height (m)	3.5
Crest width (m)	9
Base width (m)	15.5
Slope height (m)	3.5
Slope width (m)	6
Slope ratio	1:2

Soil configuration				
Material	*Unit Weigth* γ $[kN/m^3]$	*Cohesion* c $[kPa]$	*Friction angle* ϕ [°]	*Dilatancy* ψ [°]
Klei_dijkmateriaal z_s	16,7/11,5	4,2	34,5	34,5
Klei_bovenveen s_z_h	15,4/9,3	4,2	32,8	32,8
Klei_wadzanden_gelaagd o_dijk	16,3/10,8	0,8	24,3	24,3
Klei_dijkmateriaal h	13,9/6,9	0,8	27,3	27,3

Outputs slope stability						
Drawdown ratio	0.0	0.2	0.4	0.6	0.8	1.0
Centre point x coordinate	-6.95	-6.95	-6.95	-7.37	-7.37	-7.79
Centre point y coordinate	1.84	2.37	2.37	2.63	2.37	2.10
Radius	6.68	7.21	7.21	7.54	7.27	7.15
Factor of Safety	1.72	1.44	1.28	1.19	1.13	1.14
Beta	3.47	2.24	1.45	1.01	0.69	0.71
Probability of failure	2,61E-04	1,25E-02	7,35E-02	1,55E-01	2,46E-01	2,38E-01

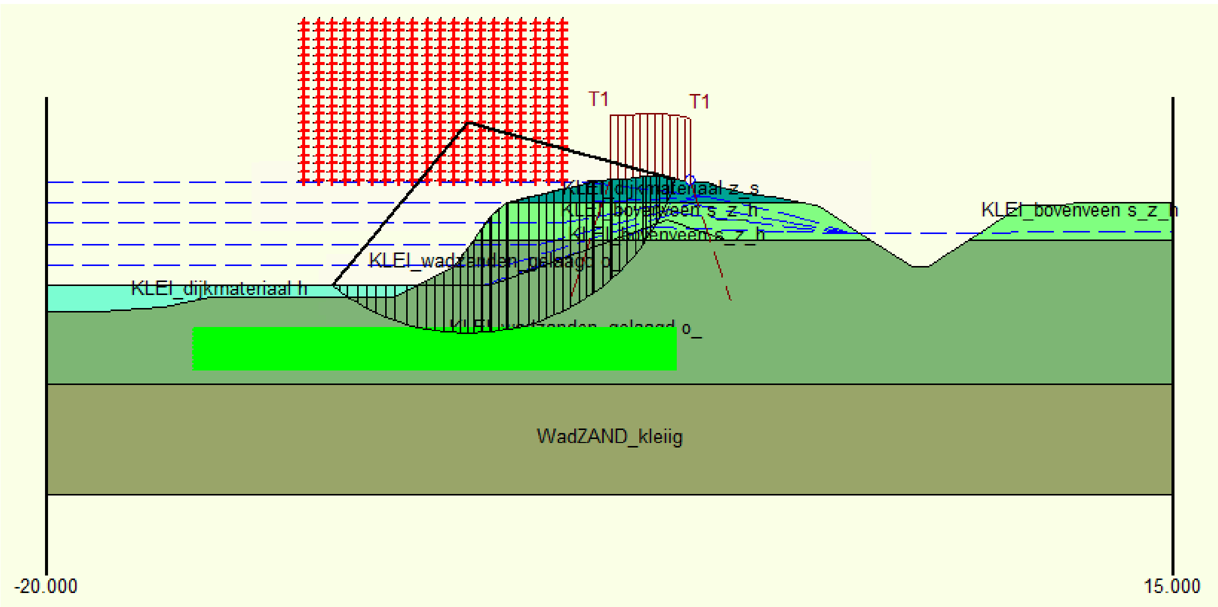

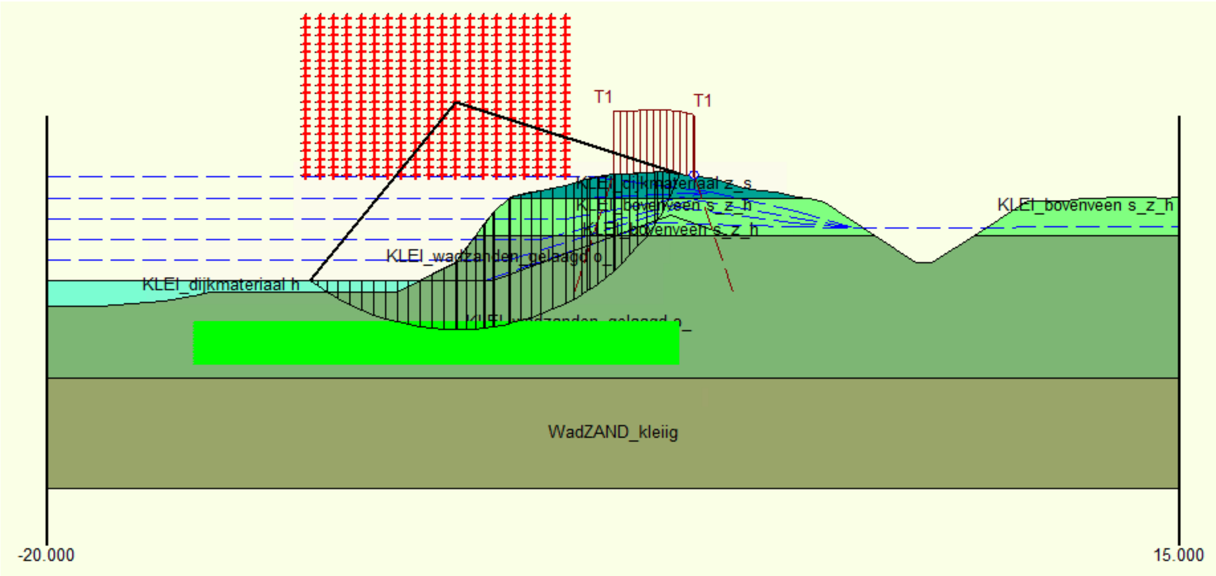

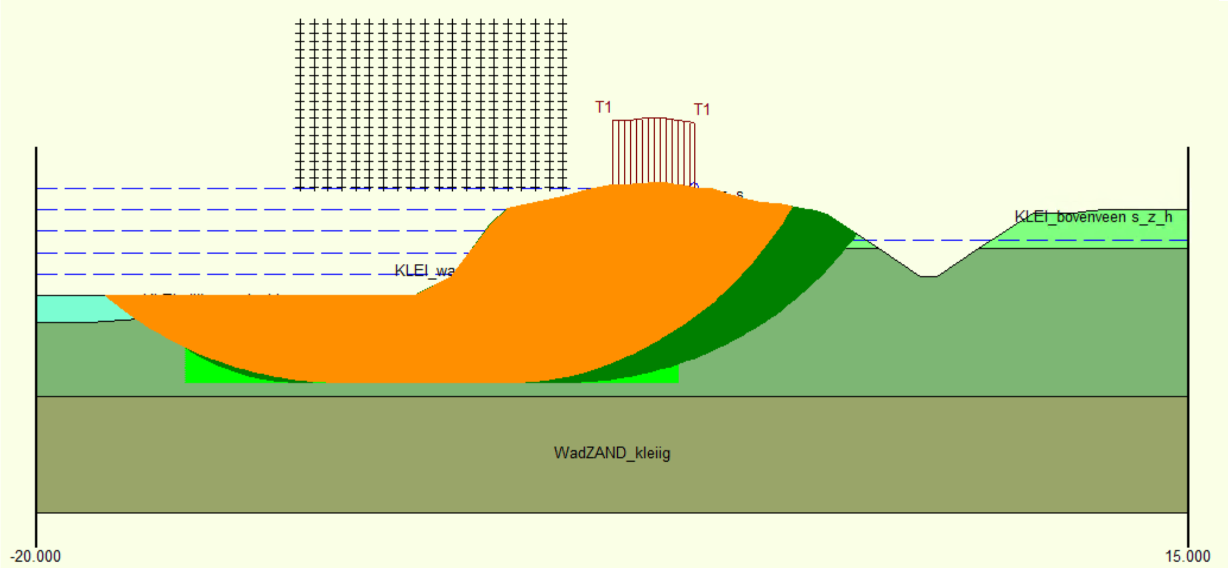

D. Description regional flood defence “Clay 4”

Dyke geometry	
Crest height (m)	2.2
Crest width (m)	5.1
Base width (m)	14
Slope height (m)	2.2
Slope width (m)	5.6
Slope ratio	1:2,5

Soil configuration				
Material	*Unit Weigth* γ $[kN/m^3]$	*Cohesion* c $[kPa]$	*Friction angle* ϕ [°]	*Dilatancy* ψ [°]
Klei_dijkmateriaal z_s	16,7/11,5	4,2	34,5	34,5
Klei_bovenveen s_z_h	15,4/9,3	4,2	32,8	32,8

Outputs slope stability						
Drawdown ratio	0.0	0.2	0.4	0.6	0.8	1.0
Centre point x coordinate	-4.37	-4.79	-4.79	-4.79	-4.79	-5.21
Centre point y coordinate	2.10	2.10	2.10	1.84	1.84	2.37
Radius	4.61	4.71	4.71	5.34	5.34	5.87
Factor of Safety	1.39	1.34	1.30	1.26	1.23	1.21
Beta	2.71	2.42	2.11	1.93	1.74	1.55
Probability of failure	3,3E-03	7,7E-03	1,7E-02	2,6E-02	4,1E-02	6,2E-02

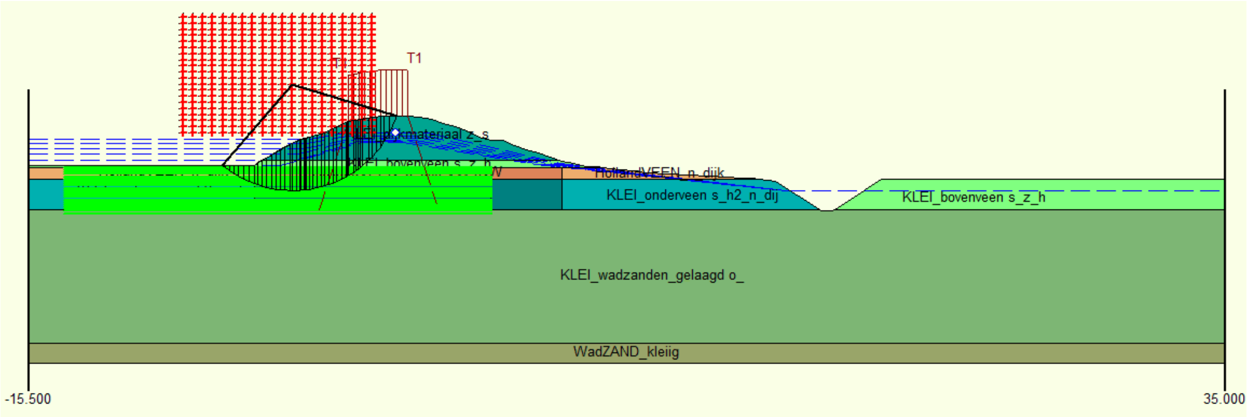

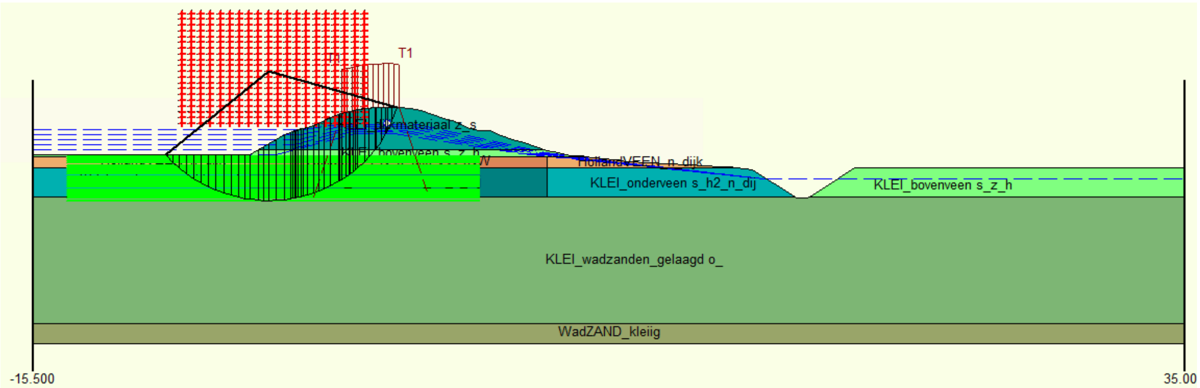

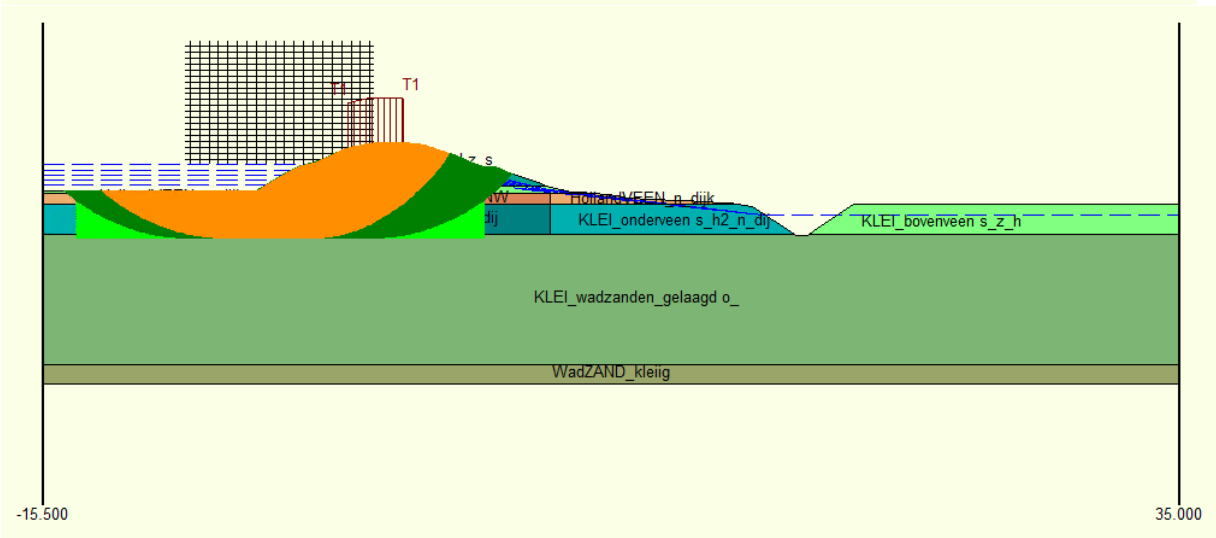

E. Description regional flood defence “Clay 5”

Dyke geometry	
Crest height (m)	2.4
Crest width (m)	4.6
Base width (m)	13.7
Slope height (m)	2.4
Slope width (m)	3.5
Slope ratio	1:1,5

Soil configuration				
Material	*Unit Weigth* γ $[kN/m^3]$	*Cohesion* c $[kPa]$	*Friction angle* ϕ [°]	*Dilatancy* ψ [°]
Klei_dijkmateriaal h	13,9/6,9	0,8	27,3	27,3

Outputs slope stability						
Drawdown ratio	0.0	0.2	0.4	0.6	0.8	1.0
Centre point x coordinate	29.25	30.83	31.36	31.36	31.36	31.36
Centre point y coordinate	5.29	3.39	3.39	3.39	3.39	3.39
Radius	6.96	7.73	8.39	8.39	8.39	8.39
Factor of Safety	1.31	1.39	1.31	1.26	1.22	1.20
Beta	1.46	2.38	1.95	1.66	1.43	1.27
Probability of failure	7,16E-02	8,57E-03	2,56E-02	4,86E-02	7,62E-02	1,02E-01

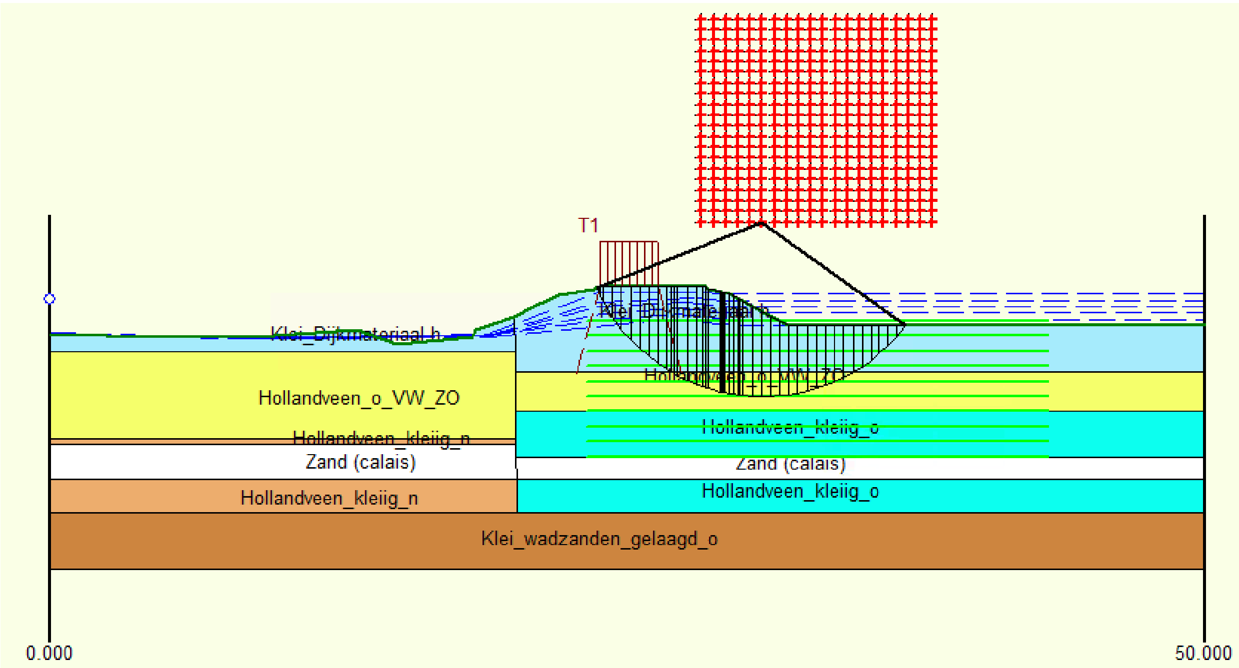

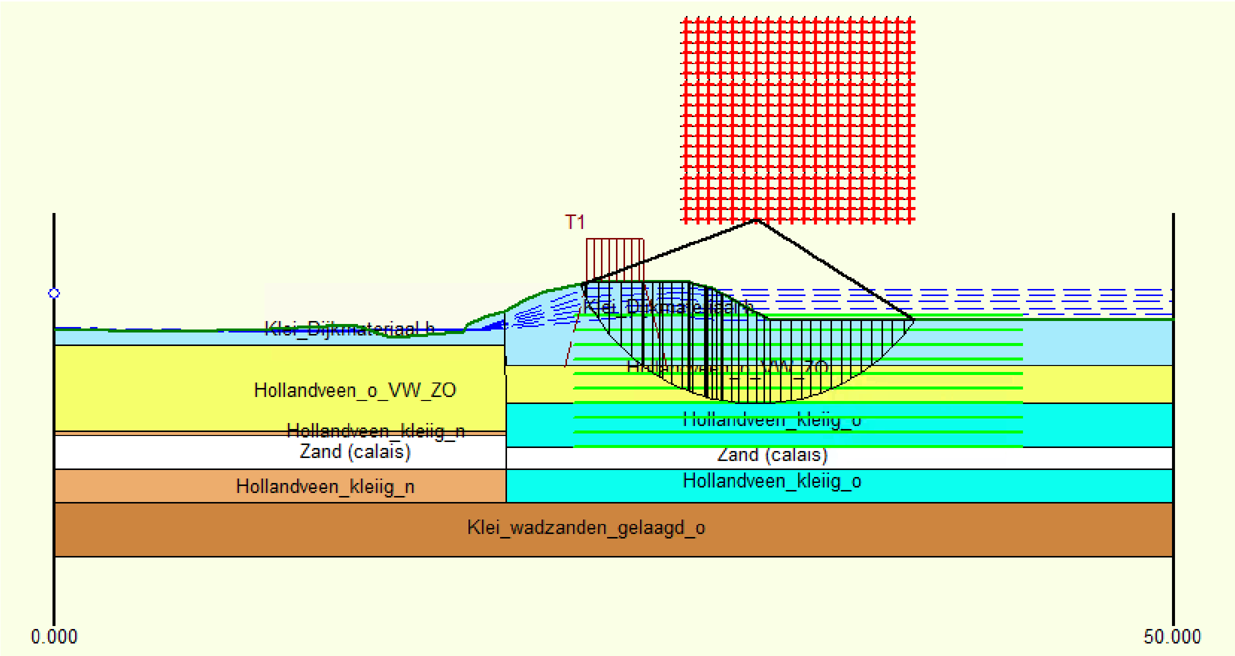
T1
Klei_Dijkmateriaal h
Klei_Dijkmateriaal h
Hollandveen_o_VW_ZO
Hollandveen_o_VW_ZO
Hollandveen_kleiig_n
Hollandveen_kleiig_o
Zand (calais)
Zand (calais)
Hollandveen_kleiig_n
Hollandveen_kleiig_o
Klei_wadzanden_gelaagd_o
0.000
50.000

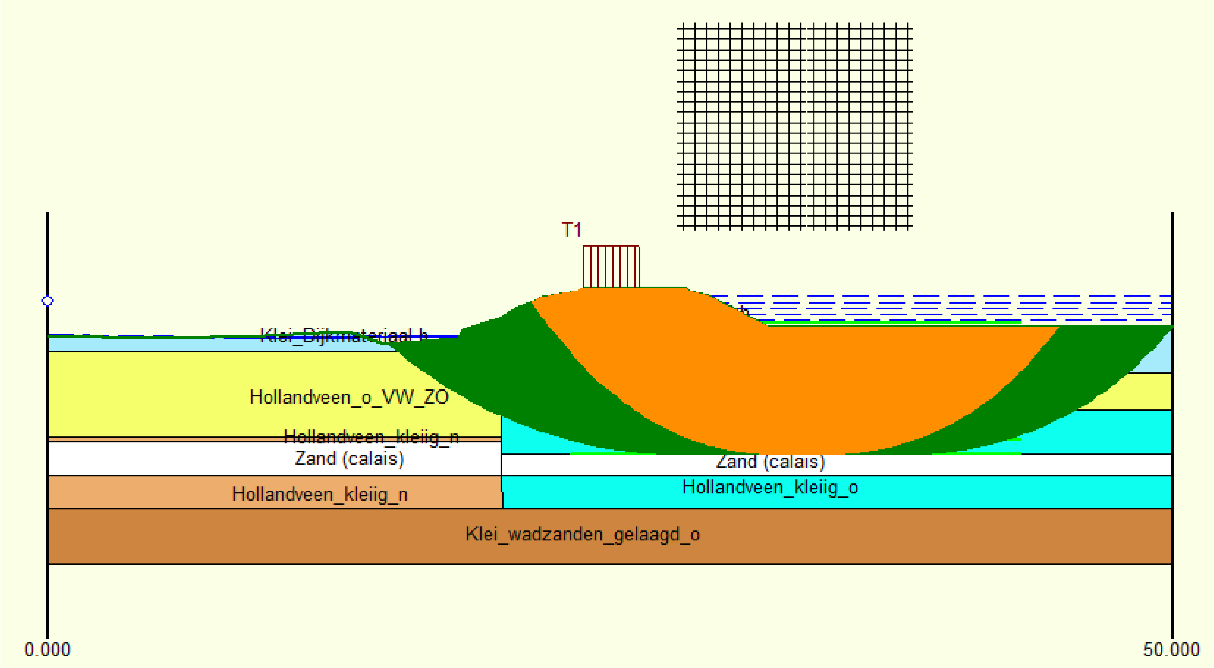
T1
Klei_Dijkmateriaal h
Hollandveen_o_VW_ZO
Hollandveen_kleiig_n
Zand (calais)
Zand (calais)
Hollandveen_kleiig_n
Hollandveen_kleiig_o
Klei_wadzanden_gelaagd_o
0.000
50.000

F. Description regional flood defence “Clay&Peat 1”

Dyke geometry	
Crest height (m)	3.5
Crest width (m)	1.66
Base width (m)	35
Slope height (m)	3.5
Slope width (m)	26.2
Slope ratio	1:7

Soil configuration				
Material	*Unit Weigth* γ $[kN/m^3]$	*Cohesion* c $[kPa]$	*Friction angle* ϕ [°]	*Dilatancy* ψ [°]
Klei_dijkmateriaal h	13,9/6,9	0,8	27,3	27,3
Hollandveen_o_dijk – VW (ZO)	9,8/1,6	4,2	19,6	19,6

Outputs slope stability						
Drawdown ratio	0.0	0.2	0.4	0.6	0.8	1.0
Centre point x coordinate	2.58	1.63	1.16	-4.53	1.16	1.16
Centre point y coordinate	4.32	6.00	6.00	6.00	6.00	6.00
Radius	8.96	10.65	10.65	10.65	10.65	10.65
Factor of Safety	2.44	1.76	1.69	1.82	2.00	2.10
Beta	6.86	4.11	3.97	4.24	5.63	6.07
Probability of failure	3,3E-12	1,9E-05	3,6E-05	1,1E-05	9,1E-09	6,3E-1

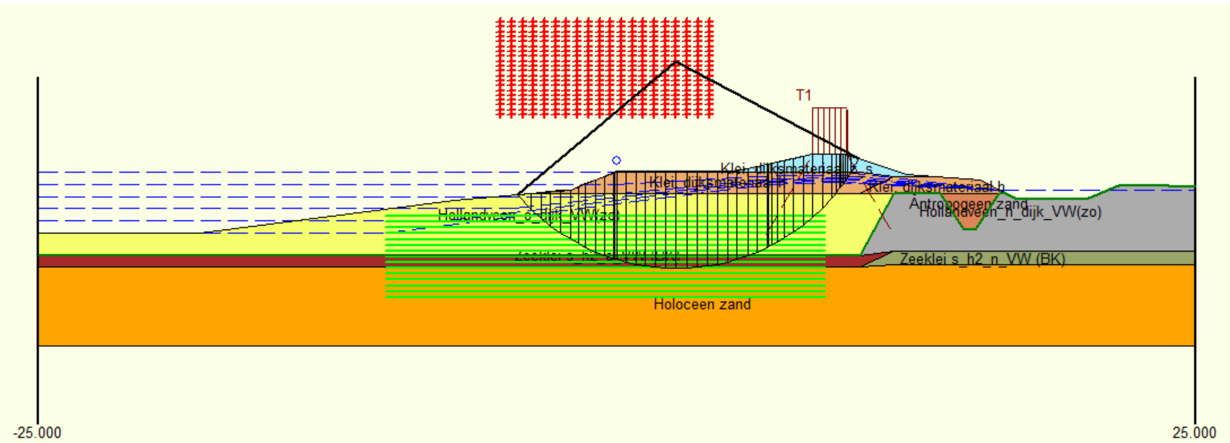

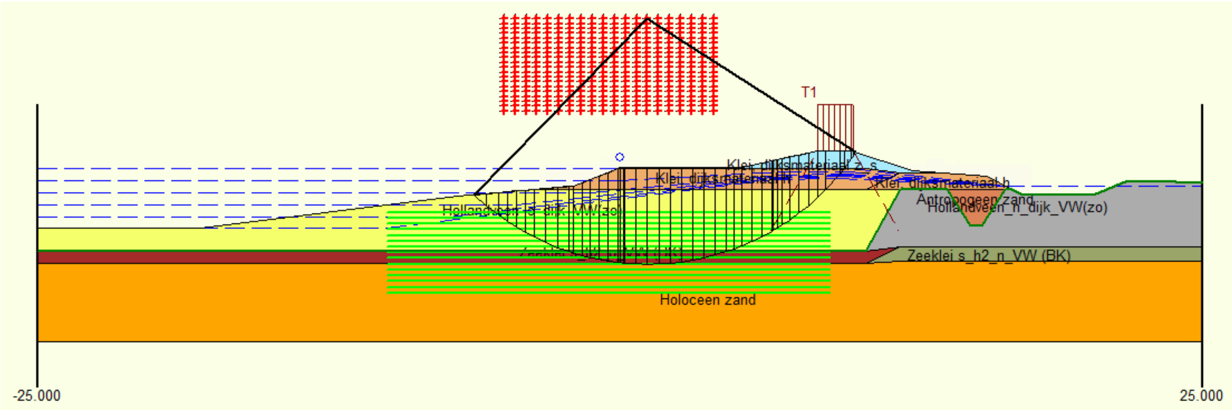
T1
Klei_dijksmateriaal_z_s
Klei_dijksmateriaal
Klei_dijksmateriaal_h
Antropogeen zand
Hollandveen_s_dijk_VW(zo)
Hollandveen_h_dijk_VW(zo)
Zeeklei s_h2_n_VW (BK)
Holoceen zand
-25.000
25.000

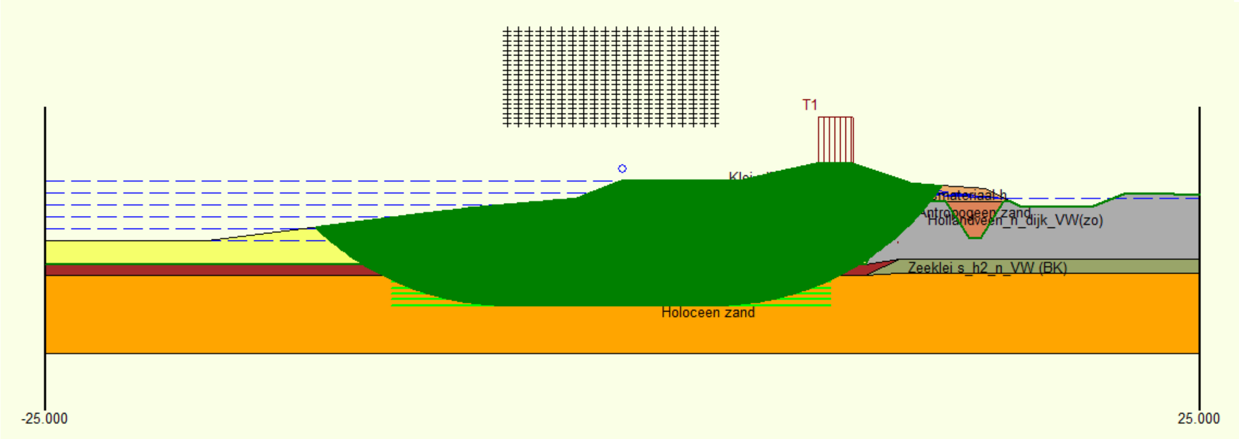
T1
Antropogeen zand
Hollandveen_h_dijk_VW(zo)
Zeeklei s_h2_n_VW (BK)
Holoceen zand
-25.000
25.000

G. Description regional flood defence “Clay&Peat 2”

Dyke geometry	
Crest height (m)	3.5
Crest width (m)	7.2
Base width (m)	30
Slope height (m)	3.5
Slope width (m)	24
Slope ratio	1:6,5

Soil configuration				
Material	*Unit Weigth* γ $[kN/m^3]$	*Cohesion* c $[kPa]$	*Friction angle* ϕ [°]	*Dilatancy* ψ [°]
Klei_dijkmateriaal z_s	16,7/11,5	4,2	34,5	34,5
Hollandveen_o_dijk – VW (NW)	9,9/1,5	4,2	20,9	20,9

Outputs slope stability						
Drawdown ratio	0.0	0.2	0.4	0.6	0.8	1.0
Centre point x coordinate	2.16	0.90	0.90	0.05	0.47	0.90
Centre point y coordinate	2.33	2.12	2.12	2.33	2.73	2.33
Radius	5.33	6.57	6.57	7.43	7.18	6.64
Factor of Safety	1.65	1.26	1.16	1.14	1.35	1.51
Beta	3.13	1.46	0.91	0.91	2.19	2.94
Probability of failure	8,8E-04	7,2E-02	1,8E-01	1,8E-01	1,4E-02	1,6E-03

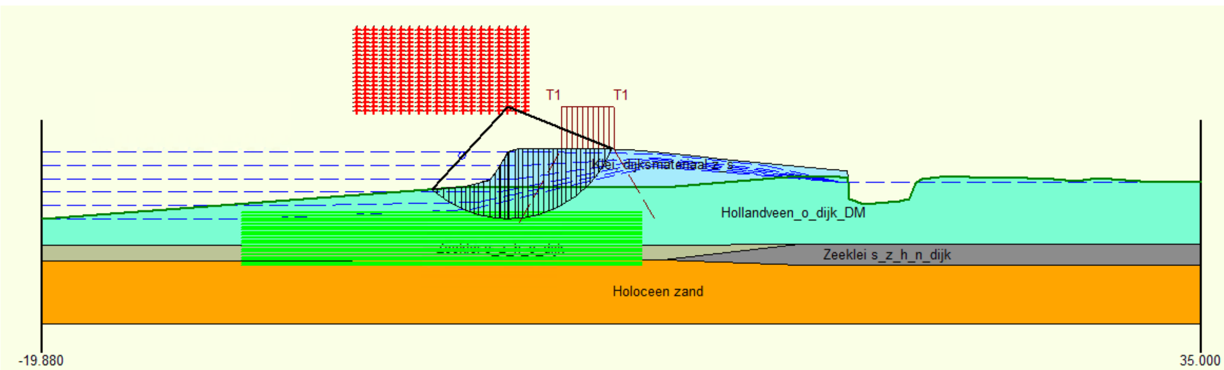

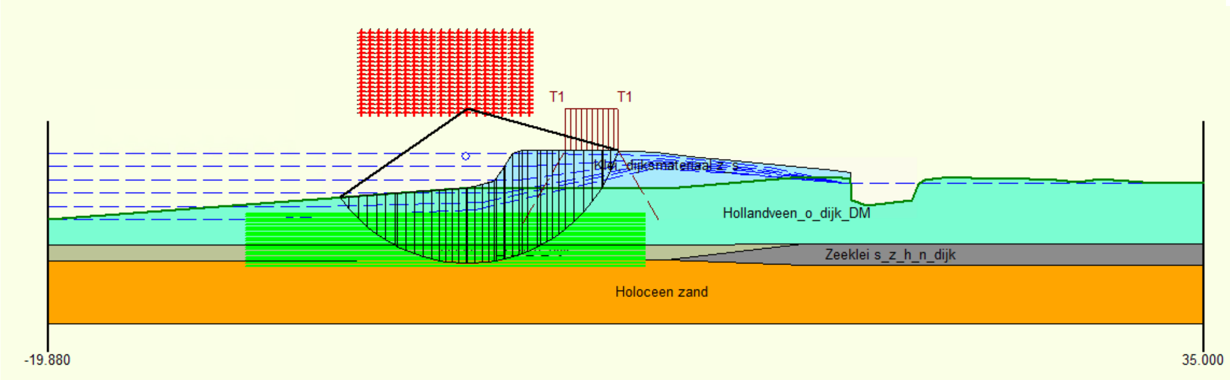

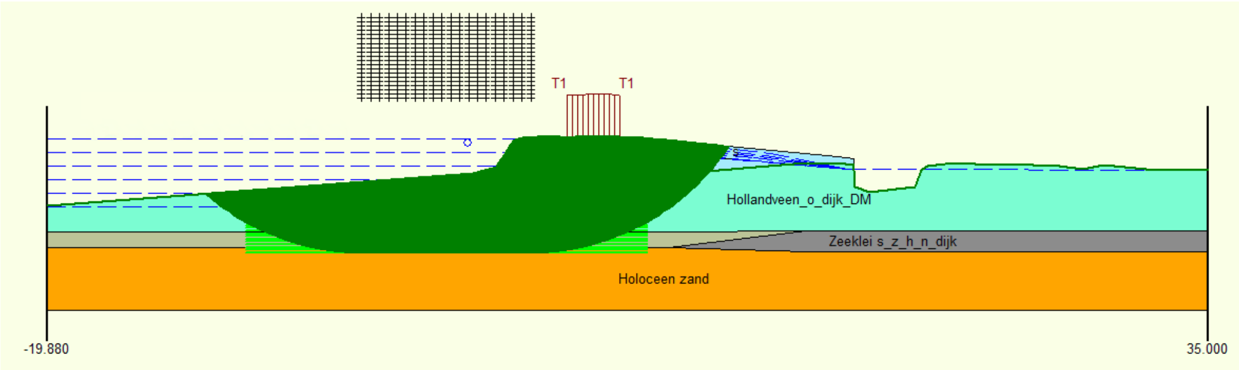
T1
T1
Hollandveen_o_dijk_DM
Zeeklei s_z_h_n_dijk
Holoceen zand
-19.880
35.000

H. Description regional flood defence “Clay&Peat 3”

Dyke geometry	
Crest height (m)	3.31
Crest width (m)	4
Base width (m)	18.45
Slope height (m)	3.31
Slope width (m)	12.51
Slope ratio	1:4

Soil configuration				
Material	*Unit Weigth* γ $[kN/m^3]$	*Cohesion* c $[kPa]$	*Friction angle* ϕ [°]	*Dilatancy* ψ [°]
Klei_dijkmateriaal z_s	16,7/11,5	4,2	34,5	34,5
Klei_dijkmateriaal h	13,9/6,9	0,8	27,3	27,3
Hollandveen_o_dijk – VW (ZO)	9,8/1,6	4,2	19,6	19,6

Outputs slope stability						
Drawdown ratio	0.0	0.2	0.4	0.6	0.8	1.0
Centre point x coordinate	-0.92	-0.92	-1.23	-1.23	-1.23	-1.23
Centre point y coordinate	1.05	0.84	1.26	1.26	1.26	1.26
Radius	5.99	5.95	6.38	6.38	6.38	6.38
Factor of Safety	1.11	0.85	0.79	0.74	0.78	0.91
Beta	0.67	-1.26	-1.79	-2.24	-1.99	-0.89
Probability of failure	2,5E-01	8,9E-01	9,6E-01	9,8E-01	9,7E-01	8,1E-01

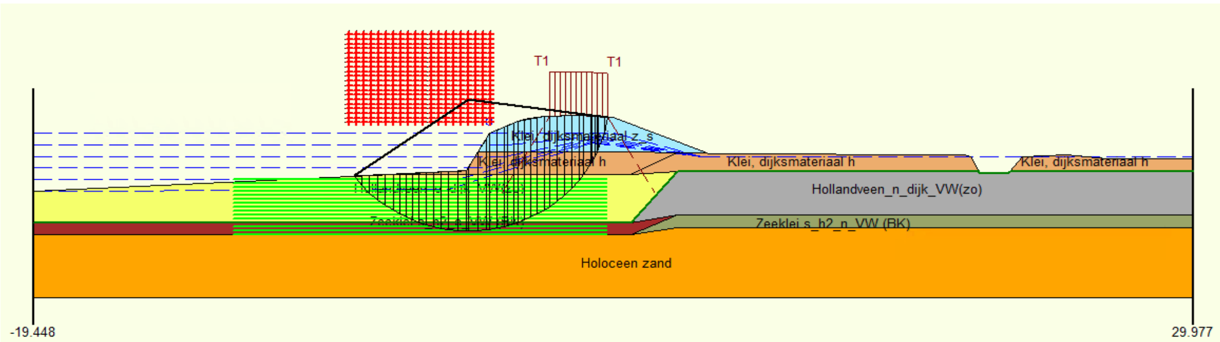

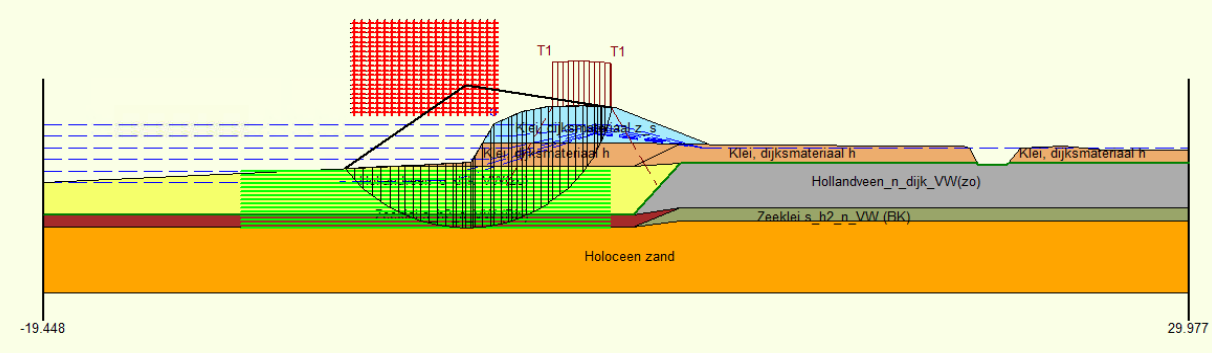

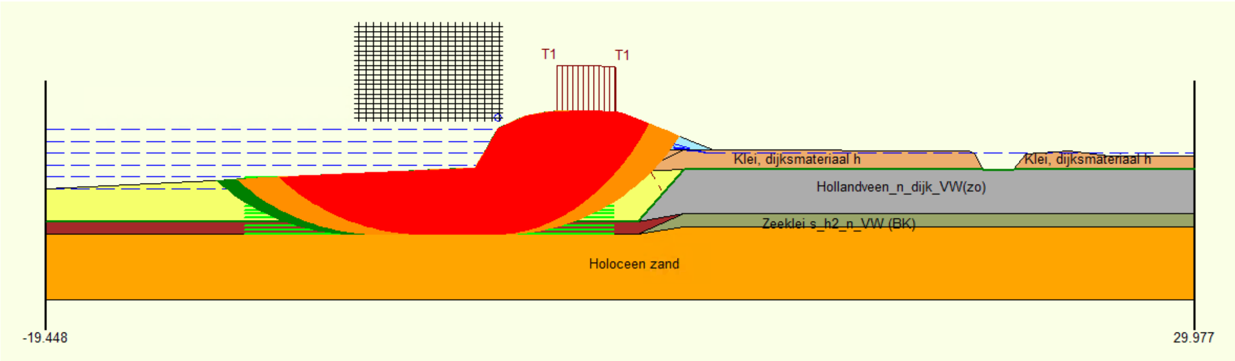

T1
T1
Klei, dijksmateriaal h
Klei, dijksmateriaal h
Hollandveen_n_dijk_VW(zo)
Zeeklei s_h2_n_VW (BK)
Holoceen zand
-19.448
29.977

I. Description regional flood defence “Clay&Peat 4”

Dyke geometry	
Crest height (m)	2.54
Crest width (m)	11.3
Base width (m)	20
Slope height (m)	2.54
Slope width (m)	5.33
Slope ratio	1:2

Soil configuration				
Material	$Unit\ Weigth$ γ $[kN/m^3]$	$Cohesion$ c $[kPa]$	$Friction$ $angle$ ϕ [°]	$Dilatancy$ ψ [°]
Klei_dijkmateriaal h	13,9/6,9	0,8	27,3	27,3
Hollandveen_n_dijk	9,8/1,4	2,1	22,2	22,2

Outputs slope stability						
Drawdown ratio	0.0	0.2	0.4	0.6	0.8	1.0
Centre point x coordinate	5.43	5.43	5.06	4.69	4.32	3.59
Centre point y coordinate	3.17	3.17	2.91	2.91	2.91	1.85
Radius	6.33	6.33	6.07	6.07	6.07	5.02
Factor of Safety	1.31	1.16	1.09	1.08	1.12	1.19
Beta	2.01	1.10	0.61	0.50	0.81	1.31
Probability of failure	2,2E-02	1,3E-01	2,7E-01	3,1E-01	2,1E-01	9,5E-02

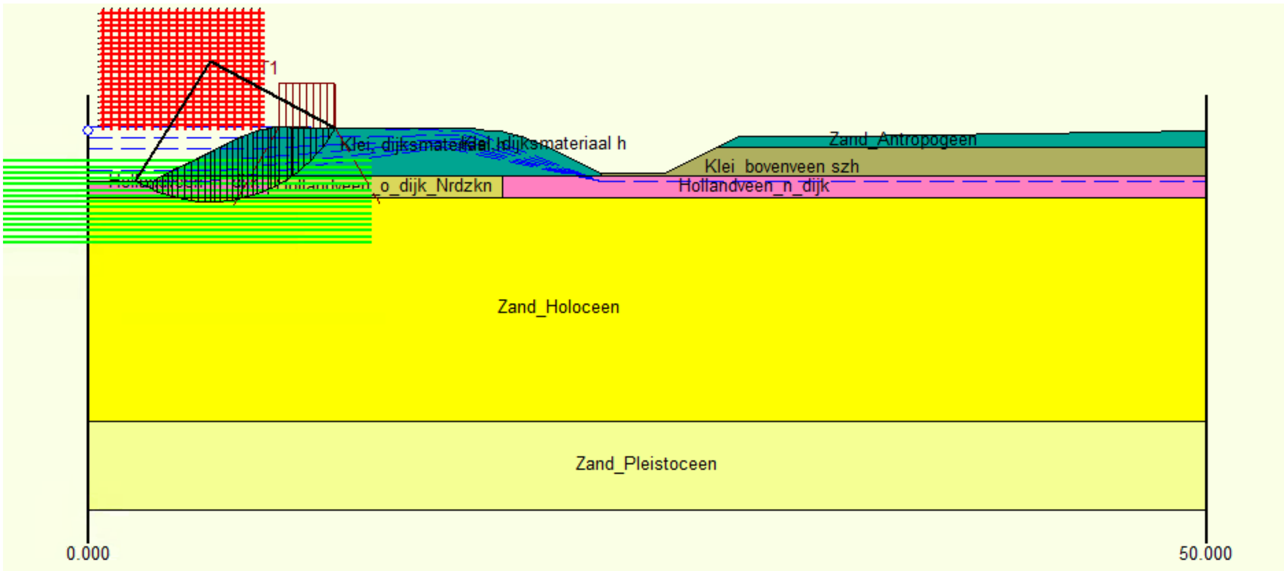

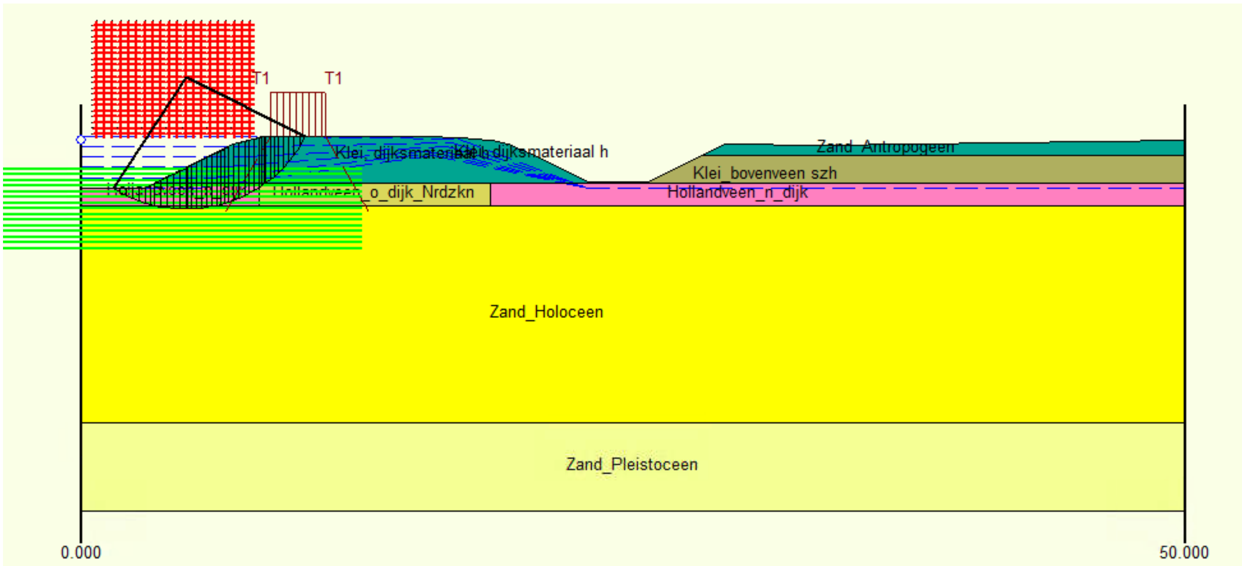

T1
T1
Klei_dijksmateriaal h
Zand_Antropogeen
Klei_bovenveen szh
Hollandveen_o_dijk_Nrdzkn
Hollandveen_n_dijk
Zand_Holoceen
Zand_Pleistoceen
0.000
50.000

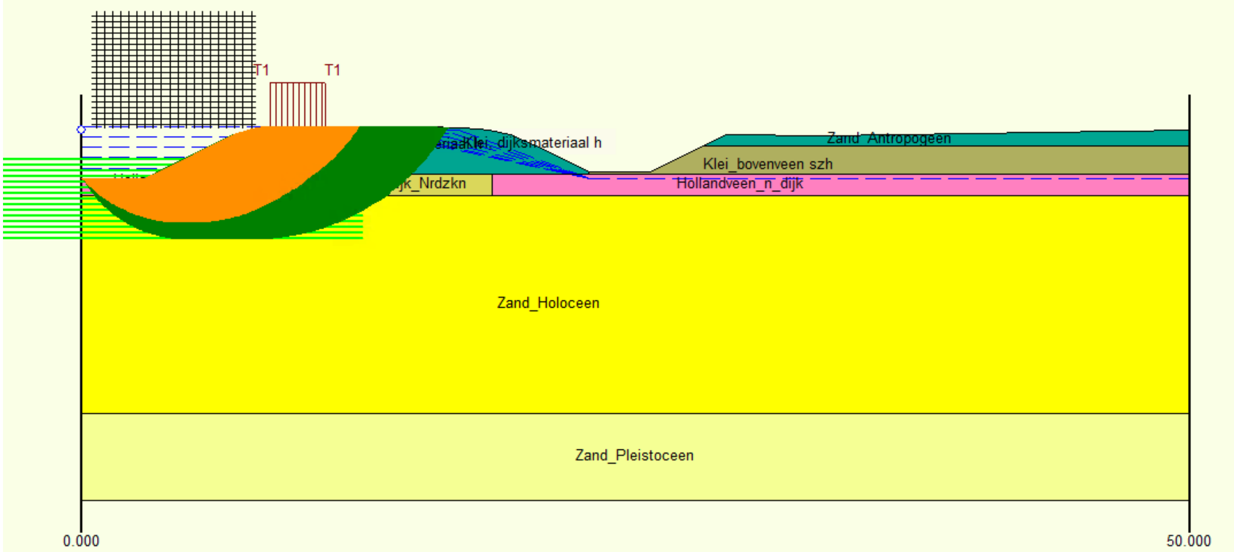

T1
T1
Klei_dijksmateriaal h
Zand_Antropogeen
Klei_bovenveen szh
Hollandveen_n_dijk
Zand_Holoceen
Zand_Pleistoceen
0.000
50.000

J. Description regional flood defence “Clay&Peat 5”

Dyke geometry	
Crest height (m)	3.12
Crest width (m)	4
Base width (m)	19.3
Slope height (m)	3.12
Slope width (m)	6.93
Slope ratio	1:2

Soil configuration				
Material	$Unit\ Weigth$ γ $[kN/m^3]$	$Cohesion$ c $[kPa]$	$Friction$ $angle$ ϕ [°]	$Dilatancy$ ψ [°]
Klei_dijkmateriaal z_s	16,7/11,5	4,2	34,5	34,5
Hollandveen_o_dijk – VW (NW)	9,9/1,5	4,2	20,9	20,9

Outputs slope stability						
Drawdown ratio	0.0	0.2	0.4	0.6	0.8	1.0
Centre point x coordinate	94.77	94.77	94.77	94.77	94.15	94.15
Centre point y coordinate	4.15	3.54	2.93	2.33	2.63	2.33
Radius	8.44	7.98	7.51	7.33	7.63	7.33
Factor of Safety	1.70	1.44	1.38	1.36	1.36	1.43
Beta	4.25	2.91	2.64	2.58	2.63	3.05
Probability of failure	1,1E-05	1,8E-03	4,1E-03	4,9E-03	4,2E-03	1,1E-03

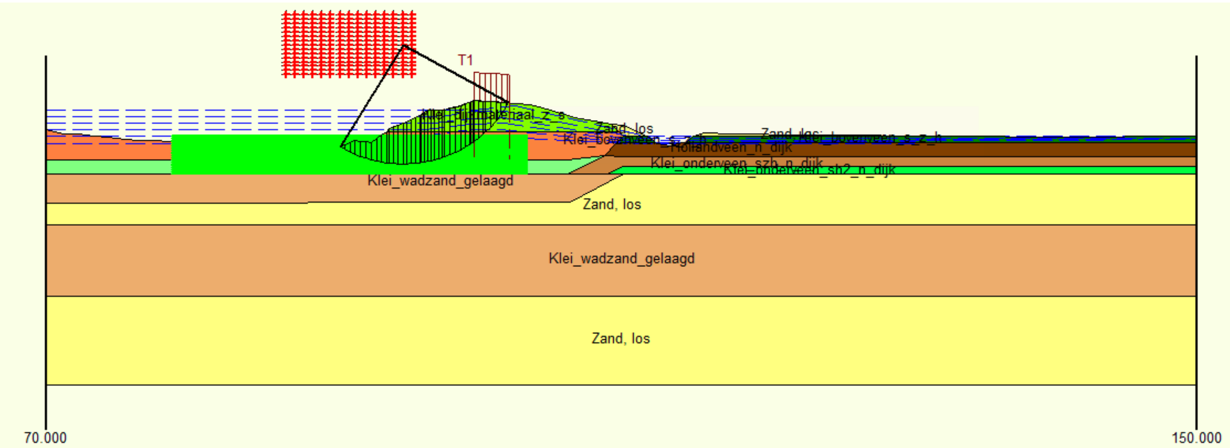

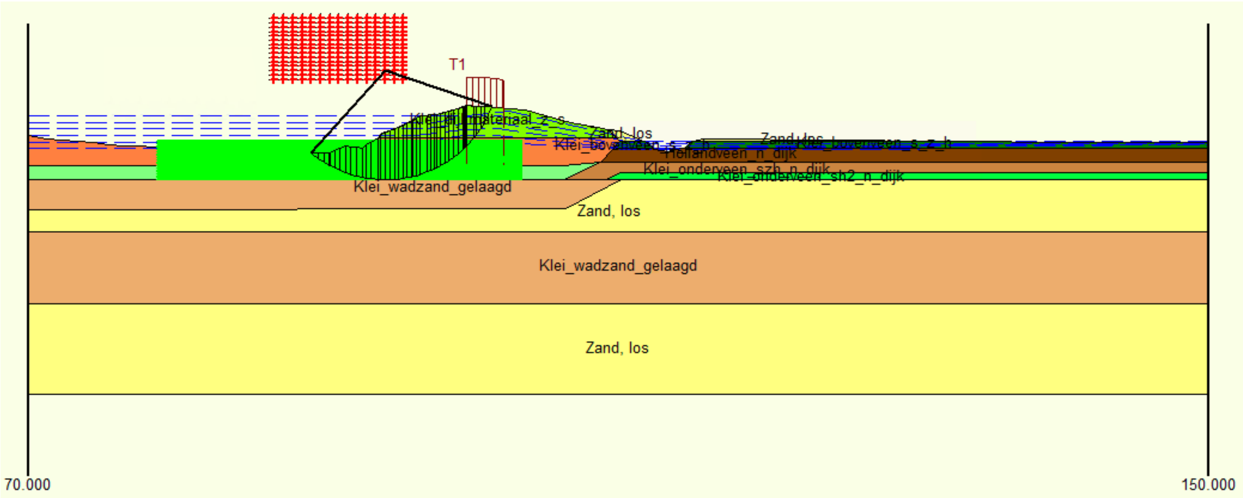
T1
Zand, los
Klei_wadzand_gelaagd
Zand, los
Klei_wadzand_gelaagd
Zand, los
70.000
150.000

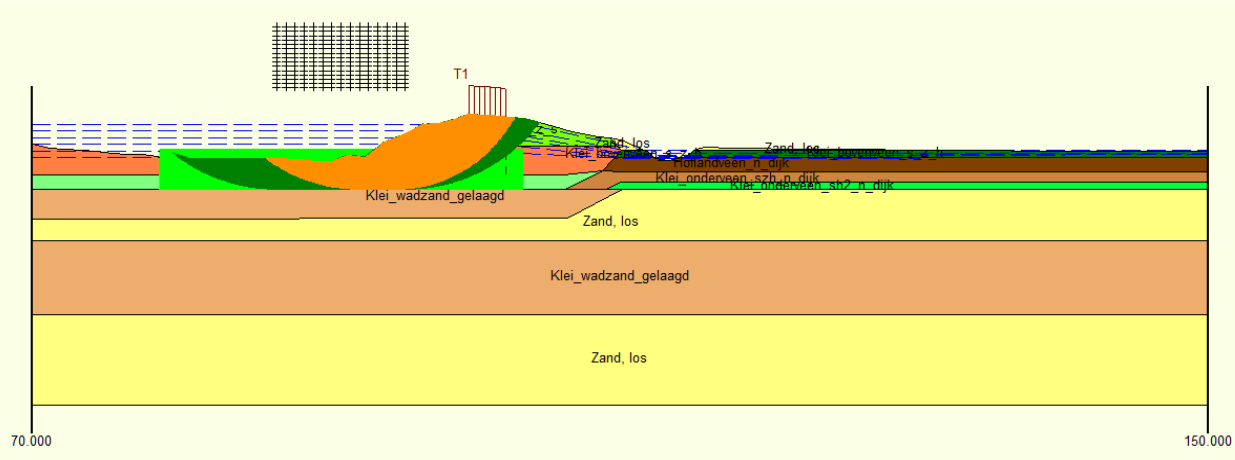
T1
Zand, los
Hollandveen_n_dijk
Klei_wadzand_gelaagd
Zand, los
Klei_wadzand_gelaagd
Zand, los
70.000
150.000

K. Description regional flood defence “Clay&Sand 1”

Dyke geometry	
Crest height (m)	1.96
Crest width (m)	2
Base width (m)	15.2
Slope height (m)	1.63
Slope width (m)	6.95
Slope ratio	1:4

Soil configuration				
Material	*Unit Weigth* γ $[kN/m^3]$	*Cohesion* c $[kPa]$	*Friction angle* ϕ [°]	*Dilatancy* ψ [°]
Zand_s_dijk	18,0/20,0	0	32,5	32,5
Klei_dijkmateriaal h	13,9/6,9	0,8	27,3	27,3

Outputs slope stability						
Drawdown ratio	0.0	0.2	0.4	0.6	0.8	1.0
Centre point x coordinate	47.00	47.00	47.00	47.00	47.00	47.00
Centre point y coordinate	2.50	2.14	2.50	2.50	1.79	1.79
Radius	5.72	5.37	5.72	5.72	5.56	5.56
Factor of Safety	1.70	1.70	1.64	1.56	1.49	1.42
Beta	4.01	4.04	3.79	3.42	2.86	2.48
Probability of failure	3,1E-05	2,6E-05	7,5E-05	3,1E-04	2,1E-03	6,5E-03

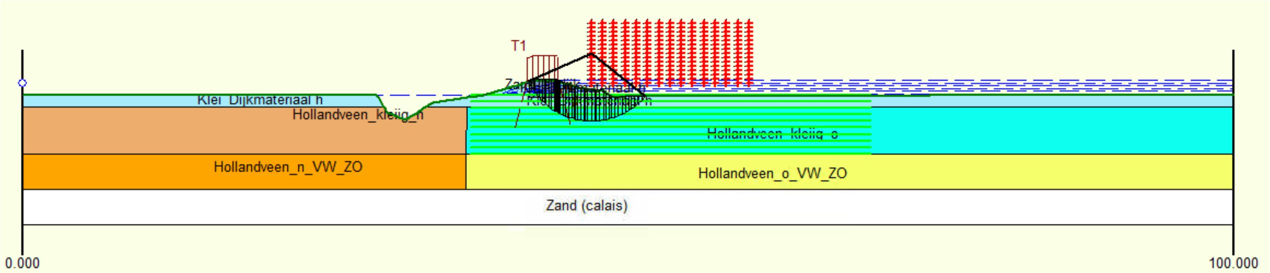

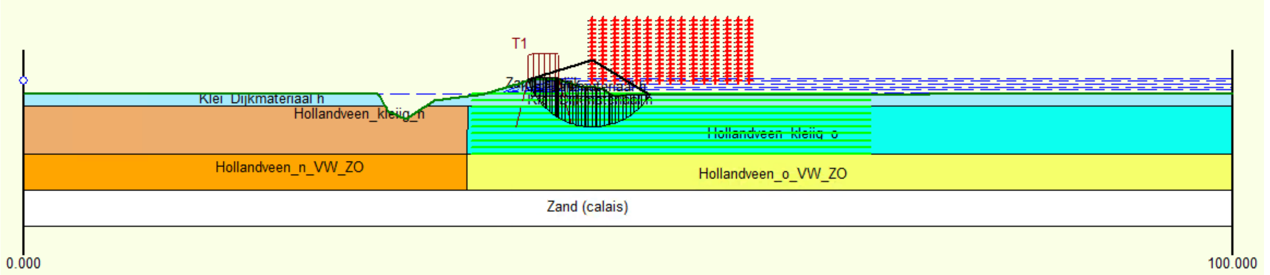

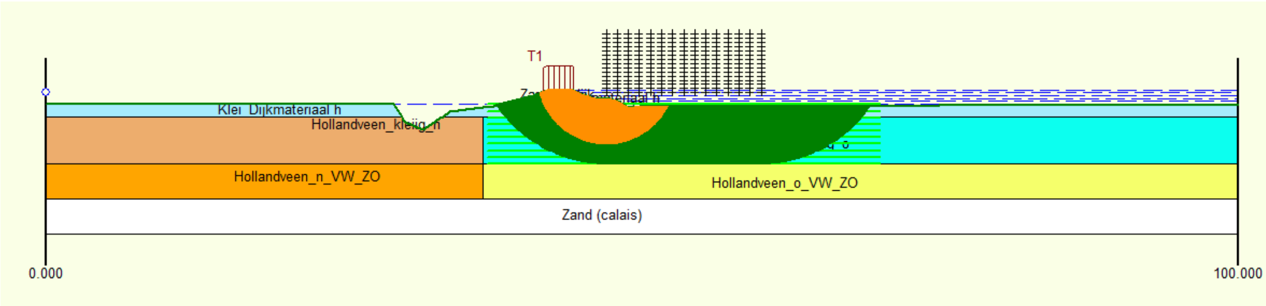

T1
Klei_Dijkmateriaal_h
Hollandveen_kleiig_h
Hollandveen_n_VW_ZO
Hollandveen_o_VW_ZO
Zand (calais)
0.000
100.000

L. Description regional flood defence “Clay&Sand 2”

Dyke geometry	
Crest height (m)	2.18
Crest width (m)	3.46
Base width (m)	18.81
Slope height (m)	2.18
Slope width (m)	6.84
Slope ratio	1:3

Soil configuration				
Material	*Unit Weigth* γ $[kN/m^3]$	*Cohesion* c $[kPa]$	*Friction angle* ϕ [°]	*Dilatancy* ψ [°]
Zand_s_dijk	18,0/20,0	0	32,5	32,5
Klei_dijkmateriaal z_s	16,7/11,5	4,2	34,5	34,5

Outputs slope stability						
Drawdown ratio	0.0	0.2	0.4	0.6	0.8	1.0
Centre point x coordinate	54.06	54.06	54.06	54.06	54.06	54.06
Centre point y coordinate	4.72	5.01	5.01	4.41	4.14	4.14
Radius	9.65	9.94	9.94	9.07	9.07	9.07
Factor of Safety	1.95	1.82	1.67	1.55	1.47	1.69
Beta	5.03	4.52	3.84	3.35	2.91	4.02
Probability of failure	2,4E-07	3,1E-06	6,2E-05	4,1E-04	1,8E-03	2,9E-05

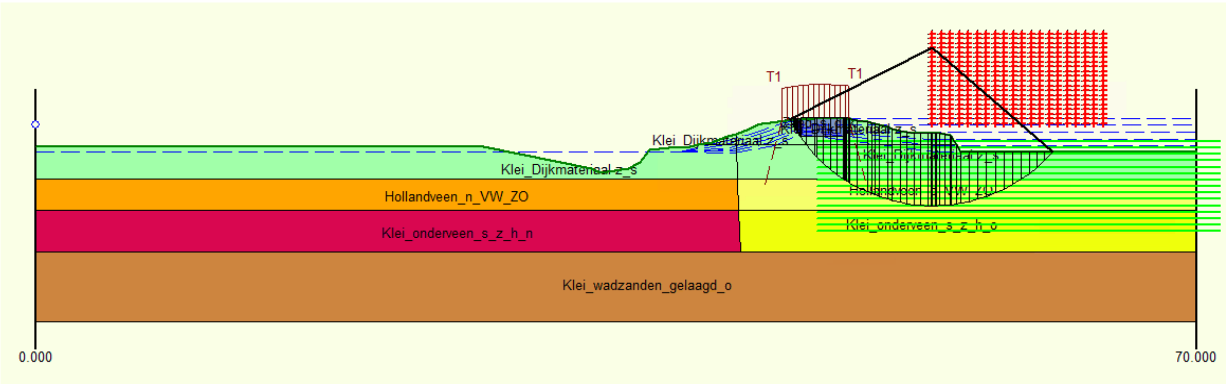

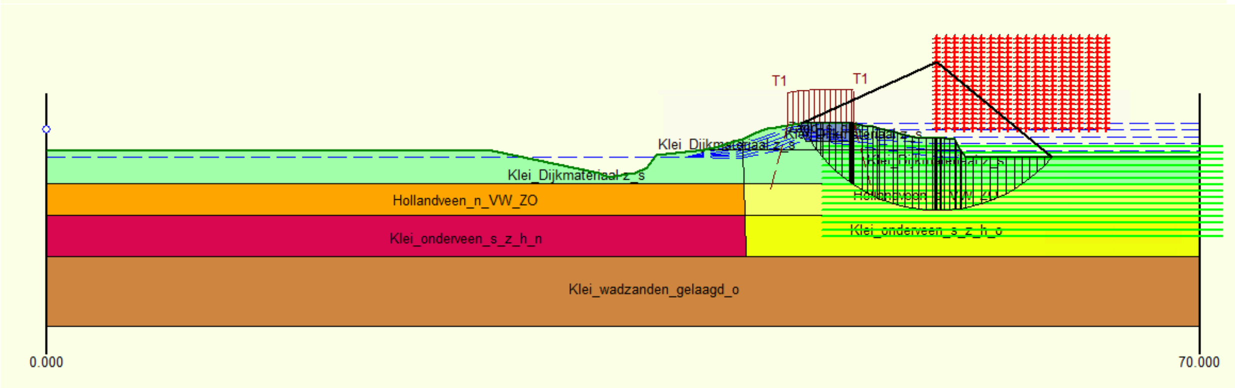

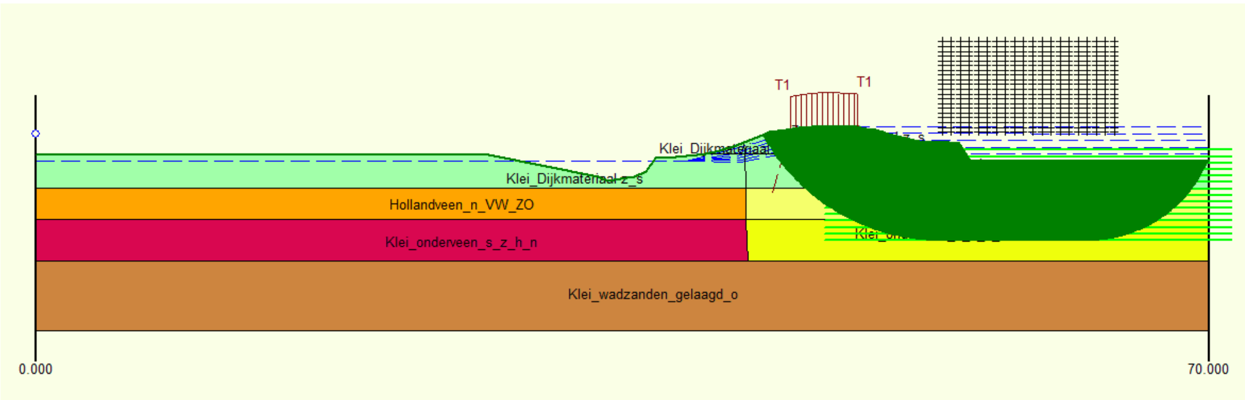
T1
T1
Klei_Dijkmateriaal
Klei_Dijkmateriaal-z_s
Hollandveen_n_VW_ZO
Klei_onderveen_s_z_h_n
Klei_wadzanden_gelaagd_o
0.000
70.000

M. Description regional flood defence “Clay&Sand 3”

Dyke geometry	
Crest height (m)	1.75
Crest width (m)	1.14
Base width (m)	54.26
Slope height (m)	1.6
Slope width (m)	0.93
Slope ratio	1:0,6

Soil configuration				
Material	$Unit\ Weigth$ γ $[kN/m^3]$	$Cohesion$ c $[kPa]$	$Friction\ angle$ ϕ $[°]$	$Dilatancy$ ψ $[°]$
Zand_s_dijk	18,0/20,0	0	32,5	32,5
Klei_bovenveen s_z_h	15,4/9,3	4,2	32,8	32,8
Klei_onderveen s_h2	14,1/7,7	0,8	18	18

Outputs slope stability						
Drawdown ratio	0.0	0.2	0.4	0.6	0.8	1.0
Centre point x coordinate	98.05	98.05	98.05	98.05	97.02	97.02
Centre point y coordinate	1.69	1.69	1.69	1.22	0.27	0.74
Radius	4.09	4.09	4.09	3.62	2.64	3.14
Factor of Safety	1.12	1.1	1.09	1.07	1.06	1.07
Beta	0.34	0.39	0.58	0.75	0.33	0.50
Probability of failure	3,6E-01	3,4E-01	2,8E-01	2,3E-01	3,7E-01	3,1E-01

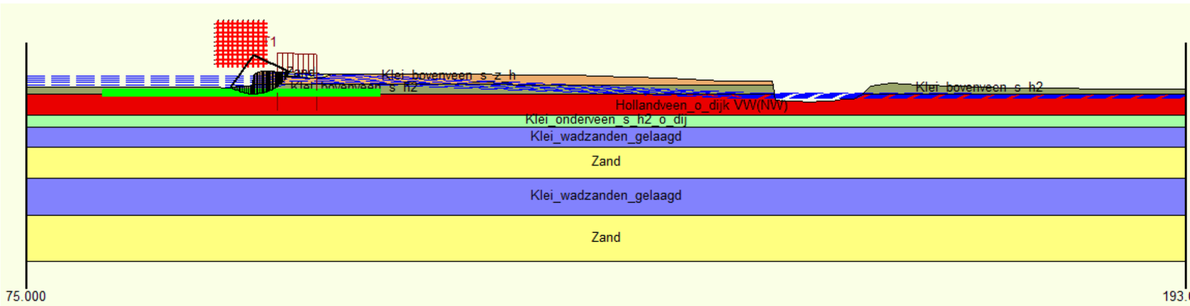

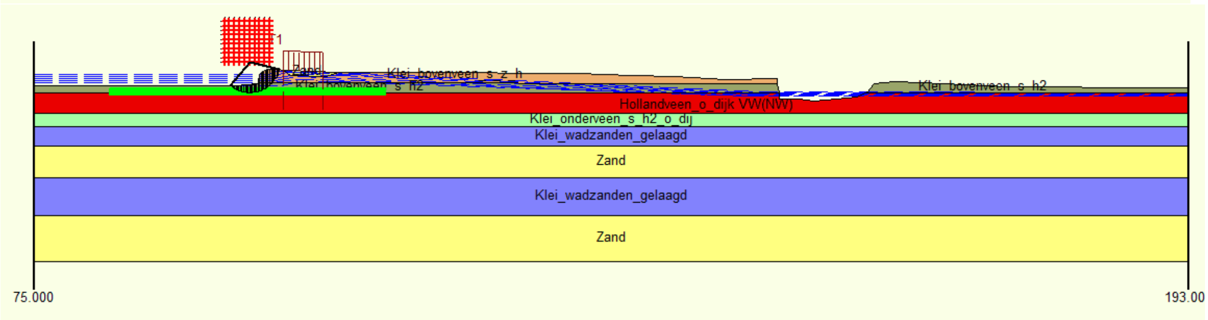

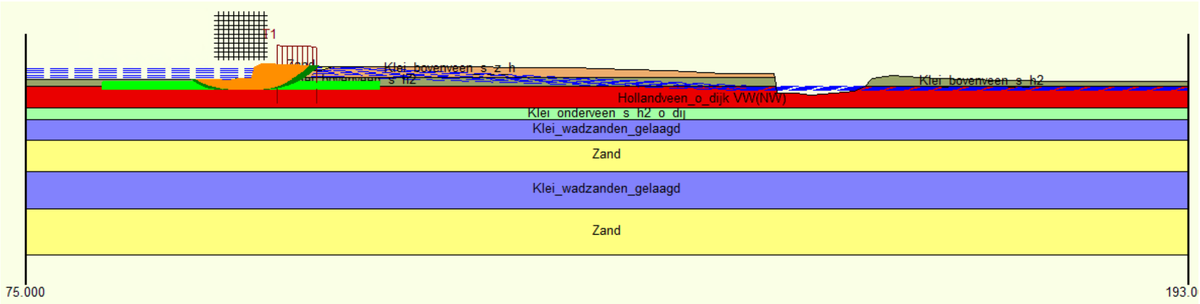

T1
Zand
Klei_bovenveen_s_z_h
Klei_bovenveen_s_h2
Hollandveen_o_dijk VW(NW)
Klei_onderveen_s_h2_o_dij
Klei_wadzanden_gelaagd
Zand
Klei_wadzanden_gelaagd
Zand
75.000
193.0

N. Description regional flood defence “Clay&Sand 4”

Dyke geometry	
Crest height (m)	5.6
Crest width (m)	25.23
Base width (m)	57.44
Slope height (m)	5.6
Slope width (m)	25.96
Slope ratio	1:4,5

Soil configuration				
Material	*Unit Weigth* γ $[kN/m^3]$	*Cohesion* c $[kPa]$	*Friction angle* ϕ [°]	*Dilatancy* ψ [°]
Klei_dijkmateriaal h	13,9/6,9	0,8	27,3	27,3
Zand_s_dijk	18,0/20,0	0	32,5	32,5
Klei_groet_waardkanaal_Oo	15,87/1,2	0.8	33,8	33,8

Outputs slope stability						
Drawdown ratio	0.0	0.2	0.4	0.6	0.8	1.0
Centre point x coordinate	-19.87	-19.87	-23.20	-26.54	-28.20	-21.54
Centre point y coordinate	6.77	5.07	6.77	6.77	2.00	6.77
Radius	9.32	7.62	9.89	11.03	6.84	9.32
Factor of Safety	3.29	2.10	2.12	2.29	2.47	2.71
Beta	7.18	4.80	5.17	4.75	4.60	5.79
Probability of failure	3,4E-13	7,8E-07	1,1E-07	1,0E-06	2,1E-06	3,5E-09

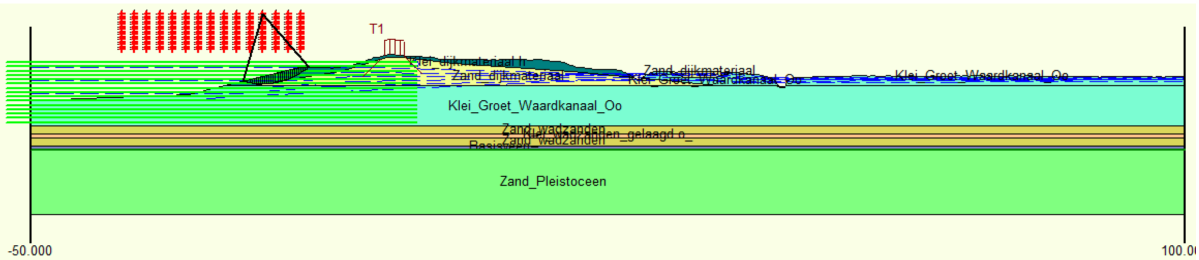

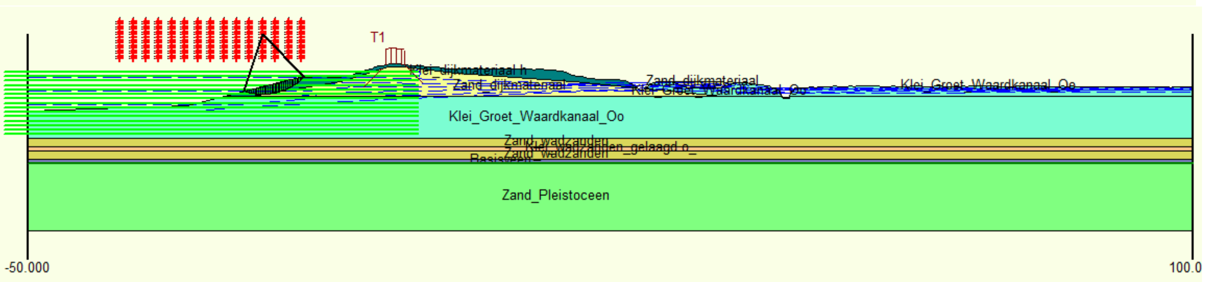

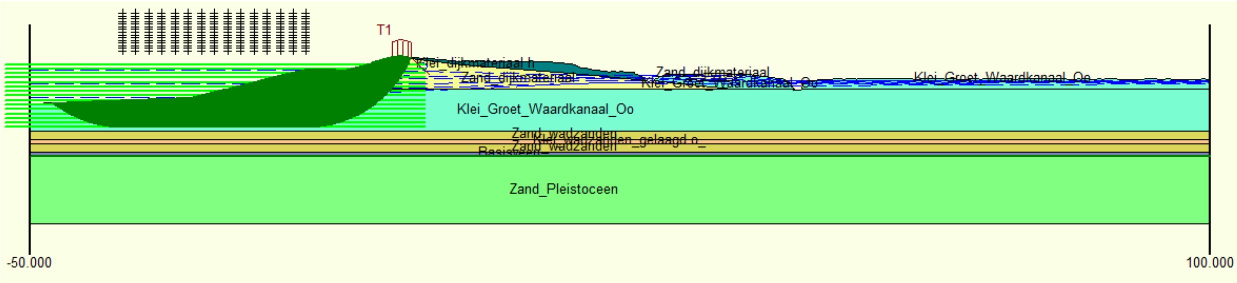
T1
Klei_dijkmateriaal_h
Zand_dijkmateriaal
Zand_dijkmateriaal
Klei_Groet_Waardkanaal_Oo
Klei_Groet_Waardkanaal_Oo
Klei_Groet_Waardkanaal_Oo
Zand_wadzanden
Zand_Klei_wadzanden_gelaagd_o_
Zand_wadzanden
Basisveen
Zand_Pleistoceen
-50.000
100.000

O. Description regional flood defence “Clay&Sand 5”

Dyke geometry	
Crest height (m)	3.11
Crest width (m)	11.90
Base width (m)	28.40
Slope height (m)	3.11
Slope width (m)	6.22
Slope ratio	1:2

Soil configuration				
Material	*Unit Weigth* γ $[kN/m^3]$	*Cohesion* c $[kPa]$	*Friction angle* ϕ [°]	*Dilatancy* ψ [°]
Klei_dijkmateriaal h	13,9/6,9	0,8	27,3	27,3
Zand_s_dijk	18,0/20,0	0	32,5	32,5
Zeeklei_ s_z_h_o_dijk	15,4/9,0	4,2	27,3	27,3

Outputs slope stability						
Drawdown ratio	0.0	0.2	0.4	0.6	0.8	1.0
Centre point x coordinate	0.67	-0.26	-0.26	-0.26	-0.26	-1.20
Centre point y coordinate	3.82	3.82	3.82	3.82	3.82	3.82
Radius	7.15	7.15	7.15	7.15	7.15	7.60
Factor of Safety	2.74	2.34	2.17	2.07	2.01	1.95
Beta	6.63	5.55	5.08	4.76	5.46	4.27
Probability of failure	1,6E-11	1,4E-08	1,8E-07	9,5E-07	2,6E-06	9,7E-06

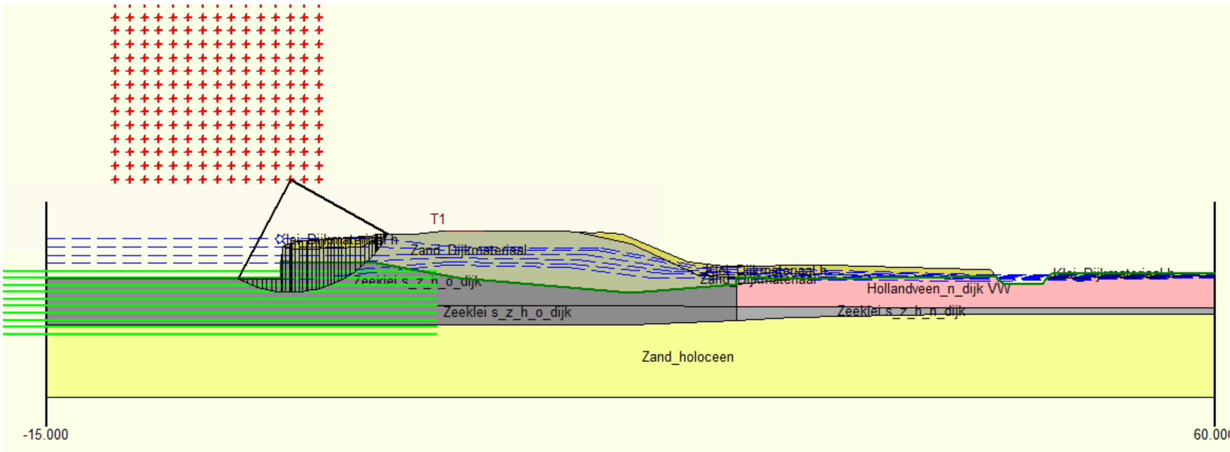

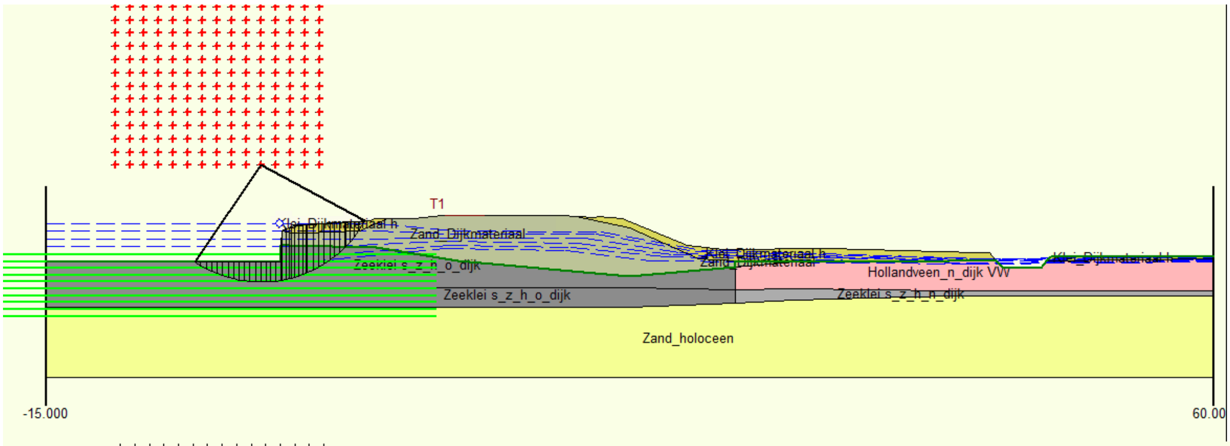
T1
Klei_Dijkmateriaal h
Zand_Dijkmateriaal
Zeeklei s_z_h_o_dijk
Zeeklei s_z_h_o_dijk
Klei_Dijkmateriaal h
Zand_Dijkmateriaal
Hollandveen_n_dijk VW
Klei_Dijkmateriaal H
Zeeklei s_z_h_n_dijk
Zand_holoceen
-15.000
60.00

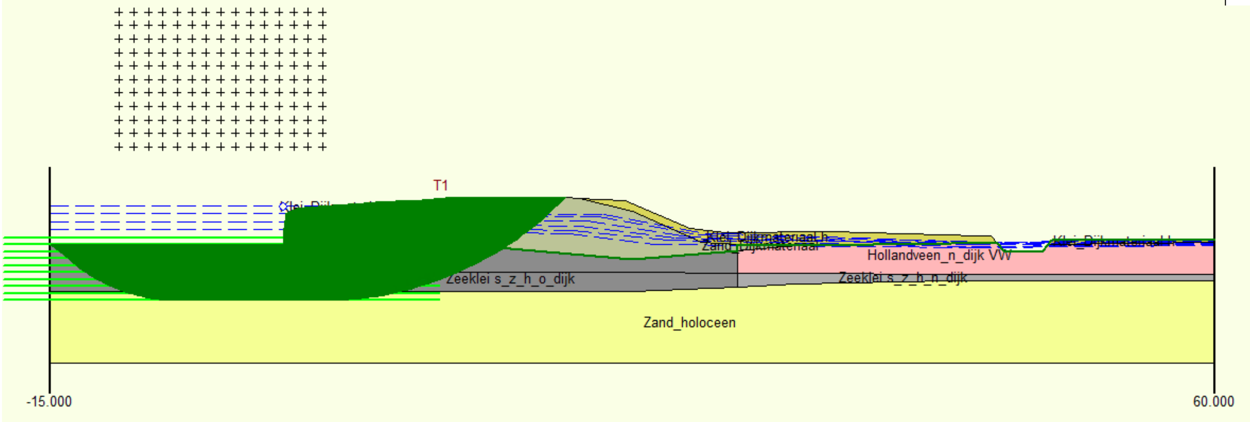
T1
Zeeklei s_z_h_o_dijk
Klei_Dijkmateriaal h
Zand_Dijkmateriaal
Hollandveen_n_dijk VW
Klei_Dijkmateriaal H
Zeeklei s_z_h_n_dijk
Zand_holoceen
-15.000
60.000